EARTHQUAKE HAZARD ASSOCIATED WITH DEEP WELL INJECTION

A Report to the
U.S. Environmental Protection Agency

Prepared by the
U.S. Geological Survey

Robert L. Wesson and Craig Nicholson

Open-file Report 87-331

Reston, Virginia
June, 1987

TABLE OF CONTENTS

I. EXECUTIVE SUMMARY 1

II. INTRODUCTION 6

III. SUMMARY OF EARTHQUAKES INDUCED BY DEEP WELL INJECTION 7

IV. CONDITIONS FOR EARTHQUAKE GENERATION 10

- Mohr–Coulomb failure criterion 10
- Description of the state of stress using Mohr circle 11
- Conditions for induced seismicity 12

V. STATE OF STRESS IN THE EARTH'S CRUST IN THE UNITED STATES 14

- Determining the magnitude and orientation of the local state of stress 15
- Stress orientation indicators 16
  - Earthquake focal mechanism solutions 16
  - Wellbore breakouts 16
  - Core-induced fractures 17
  - Fault offsets and other young geologic features 17
- Hydraulic fracture stress measurements in wells 18
  - Types of pressure-time records 20
- Comparison of fracture pressure and Mohr–Coulomb failure criterion 20
- Summary of stress measurements to date 21

VI. HYDROLOGIC FACTORS IN EARTHQUAKE TRIGGERING 22

(with assistance from Evelyn Roeloffs)

- Reservoir properties 24
- Fluid pressure changes resulting from injection 25
  - Infinite reservoir model (radial flow) 25
  - Infinite strip reservoir model 26

VII. UNRESOLVED ISSUES 27

- The problem of eastern and central U.S. seismicity 27
- Magnitudes of induced earthquakes 28

Potential for reactivation of old faults 29
Importance of small induced earthquakes 29
Spatial and temporal variability of tectonic stress 30
VIII. CONSIDERATIONS FOR FORMULATING REGULATIONS AND OPERATIONAL PROCEDURES 30
Site selection 31
Reservoir with high transmissivity and storativity 31
Stress estimate 31
Absence of faults 32
Regional seismicity 32
Well drilling and completion 33
Transmissivity and storativity 33
Stress measurement in reservoir rock 33
Pore pressure measurement 34
Faulting parameters 35
Well operation and monitoring 35
Determination of maximum allowable injection pressure 35
Comparison of actual and predicted pressure-time records 36
Seismic monitoring 36
Consideration of small earthquakes near bottom of well 37
APPENDIX A—EARTHQUAKES ASSOCIATED WITH DEEP WELL INJECTION 39
Denver, Colorado 39
Rangely, Colorado 40
Attica–Dale, New York 41
Texas oil fields 42
Permian Basin, West Texas 42
Cogdell oil field, West Texas 42
Atascosa County, South Texas 43
The Geysers, California 44

New Mexico 45
Nebraska 45
Southwestern Ontario, Canada 46
Matsushiro, Japan 46
Other less-well documented or possible cases 47
Western Alberta, Canada 47
Historical seismicity and solution mining in western New York 47
Historical seismicity and solution mining in northeastern Ohio 48
Recent seismicity and injection operations in northeastern Ohio 49
Los Angeles basin, California 50
Gulf Coast region: Louisiana and Mississippi 50
APPENDIX B—SUMMARY OF RESERVOIR INDUCED SEISMICIY 52
ACKNOWLEDGEMENTS 54
REFERENCES 55
TABLES 66
FIGURE CAPTIONS 68
FIGURES 73

I. EXECUTIVE SUMMARY

Injection of fluid into deep wells has triggered earthquakes in documented instances in Colorado, Texas, New York, New Mexico, Nebraska, Japan, Ontario, and possibly Alberta, Mississippi, Louisiana, and Ohio. Investigations of these cases have led to some understanding of the likely physical mechanism of the triggering, and criteria for predicting whether earthquakes will be triggered depending on the local state of stress in the earth's crust, the injection pressure, and the physical and hydrologic properties of the rocks into which the fluid is being injected. The aim of this report is to summarize the current state of understanding of this phenomenon, to describe the criteria for predicting whether earthquakes will be triggered by deep well injection, to identify remaining unanswered questions, and to indicate—from a seismological point of view—factors to be considered in developing regulations and operating procedures for deep well injection.

Of the well-documented cases of earthquakes related to fluid injection, most are associated with water-flooding operations for the purpose of secondary recovery of hydrocarbons. This is because secondary recovery operations often entail large arrays of wells injecting at high pressures into small, confined reservoirs with low permeabilities. In contrast, waste disposal wells typically inject at lower pressures into large, porous aquifers of high permeability. This explains in large part why, of the many hazardous and non-hazardous waste disposal wells in the United States, only one has ever been conclusively shown to be associated with triggering significant adjacent seismicity, and it is no longer in operation. This case involved a well at the Rocky Mountain Arsenal near Denver, Colorado, where fluid was injected into relatively impermeable, crystalline basement rock, causing the largest-known injection-induced earthquakes to date. The largest of these induced events was a magnitude 5.5, which caused an estimated $\$\frac{1}{2}$ million worth of damage in 1967. Although these earthquakes were by no means devastating, they did occasion extensive attention and concern in the Denver area.

In each of the well-documented examples, convincing arguments that the earthquakes were induced relied upon three principal characteristics of the earthquake activity. First, there was a very close geographic association between the zone of fluid injection and the locations of the earthquakes in the resulting sequence. Second, calculations based on

the measured or inferred state of stress in the earth's crust, and the measured injection pressure, indicated that the theoretical threshold for frictional sliding along favorably oriented, preexisting fractures, as indicated by the Mohr–Coulomb failure criterion, was likely exceeded. And third, a clear disparity between the previous seismicity and the subsequent earthquake activity was established, with the induced seismicity often characterized by large numbers of small earthquakes that persisted for as long as elevated pore pressures in the hypocentral region continued to exist.

Earthquakes are generated by slip on faults or fractures. A fault or fracture in close proximity to a high-pressure injection well thus becomes a potential location for induced earthquakes. The conditions for sliding on a fault are characterized by the Mohr–Coulomb failure criterion, which relates the shear stress required for fault slip to the inherent cohesion and coefficient of friction on the fault, the normal stress resolved across the fault, and the fluid pore pressure. This relationship, which depends on the orientation of the faults or fractures relative to that of the existing state of stress, as well as on the effect of changes in pore pressure resulting from fluid injection, is easily visualized using the Mohr circle description. As fluid pressure increases, the apparent strength of the fault decreases, increasing the potential for induced earthquakes.

Because the conditions for failure strongly depend on the state of stress in the earth's crust, measuring the *in situ* stress conditions is important to accurately assess the potential for inducing earthquakes. Several approaches are possible, but the most reliable method is the hydraulic fracture technique, in which the pressure required to create small fractures in the wellbore is precisely measured. This method is a variation of the standard hydrofracture technique to increase the transmissivity of a reservoir. Although pressures are monitored during commercial hydrofracture operations, these measurements generally do not constitute an adequate stress measurement. Sufficient measurements of stress are now available across the United States that regional stress patterns are beginning to emerge, and thus it is possible to predict the general orientation, and to some extent the magnitude, of the principal stresses at a given site. Supplemental measurements would be required, however, to provide accurate information relevant to the determination of maximum levels of injection pressure at a specific site.

The hydrologic properties of the reservoir also have a strong effect on the potential for inducing earthquakes by deep well injection. Transmissivity and storativity control the rate of increase in pore pressure throughout the formation as a result of fluid injection. For a given rate of injection, the higher the transmissivity and storativity, the lower the injection pressure required to attain the desired injection rate, and consequently, the lower the potential for triggering earthquakes. Transmissivity and storativity can be determined from tests made during well completion and verified by actual pressure-time records acquired during well operation. Estimates of pore pressure changes in the vicinity of a well, as a result of fluid injection, can then be predicted by analysis of the pressure history at the wellbore and by using variations of standard techniques from reservoir engineering or ground water hydrology.

Unresolved issues relating to the hazard associated with earthquakes induced by deep well injection include the generally poor understanding of the causes of natural earthquakes in the central and eastern United States, difficulties of estimating the maximum size of expected induced earthquakes, difficulties in assessing the potential for fault reactivation, the importance of small induced earthquakes—should they begin to occur near the bottom of an injection well, and quantifying the spatial and temporal variations in tectonic stress. An environmental concern, about which little is understood, is the potential for induced earthquakes to breach the confining layer of a waste-disposal reservoir, permitting upward migration of contaminated fluids. This possibility emphasizes the need for detailed seismic monitoring once adjacent seismicity is detected, to accurately determine the relative position of the earthquakes to the zone of fluid injection, and to assess the type and extent of the faulting involved.

Based on the present understanding of the phenomena of injection-induced earthquakes, several factors are recommended for consideration in the development of regulations and procedures for controlling deep well injection operations. These recommendations are made from a seismological point of view alone, and are not intended to supersede or replace alternative considerations made for other purposes. The recommended considerations include:

- **Site selection**

  - Reservoirs characterized by high transmissivity and storativity, and therefore capable of receiving fluid at low injection pressures, are less likely to be the site of induced earthquakes.

  - An estimate of the tectonic stress based on regional or surface measurements made prior to drilling, could serve as an early warning of potential earthquake problems and unanticipated low formation fracture pressures.

  - Since faults within the range of influence of an injection well are the potential loci for induced earthquakes, the absence of significant faults reduces the possibility of triggered seismicity. Geologic and geophysical surveys conducted to detect faults that may intersect the reservoir would also help in evaluating the integrity of the confining layer.

  - The existence of regional seismicity in the vicinity of a proposed site should be taken as evidence of sufficient levels of tectonic stress, and the existence of potential slip surfaces (faults), required for both natural and induced earthquakes.

- **Well drilling and completion**

  - Estimating the storativity and transmissivity of the reservoir based on measurements made at the time of well completion would provide an important means of predicting the build-up of injection pressure required to maintain a given injection rate.

  - If it can be accomplished without threatening the confining zone, a stress measurement by the hydrofracture technique in or below the reservoir rock is the key environmental measurement in predicting the potential for induced earthquakes, and the possibility of low formation fracture pressure.

  - Careful measurement of the initial formation pore pressure at the time of well completion, prior to injection, provides important information on the proximity to failure conditions in the unaltered natural state.

  - If anticipated injection pressures approach the levels expected to trigger the occurrence of earthquakes according to the Mohr–Coulomb failure criterion, assuming regional or generic values for the coefficient of friction and the cohesion of faults, then more precise local measurements of these values, if possible, would reduce the uncertainty in the specific level of injection pressure at which earthquakes would be expected.

- **Well operation and monitoring**

  - Given measurements of stress described above, it is possible to estimate the maximum injection pressure that can be used without fear of fracturing the formation or inducing earthquakes by allowing slip on a preexisting fault. These estimates can be made using the Mohr–Coulomb failure criterion.

  - Actual pressure-time curves measured at the wellhead can be compared with predicted curves to assure that the reservoir is behaving as assumed. Any increase in the apparent transmissivity should be scrutinized as possible evidence for the opening of fractures, or the occurrence of faulting.

  - If the maximum injection pressure at a site approaches the critical level anticipated to trigger the occurrence of earthquakes, then it would be prudent to monitor the injection operation with at least one high-sensitivity seismograph station. Monitoring should continue as long as significant levels of elevated fluid pressure are maintained in the reservoir.

  - The occurrence of any earthquakes near the bottom of an injection well should be reviewed carefully to assess the possibility that potentially damaging earthquakes might be induced, and to assess the potential for fracturing or faulting through the containment zone. Additional monitoring stations would then be recommended to accurately locate and analyze subsequent earthquake activity that may be expected.

II. INTRODUCTION

The injection of waste into deep isolated aquifers has been increasingly utilized for the disposal of certain types of hazardous fluid materials [EPA, 1974; 1985]. Other deep well injection operations are routinely carried out for the disposal of non-hazardous waste (*e.g.*, excess oil-field brine), for solution mining, and for the secondary recovery of hydrocarbons. Secondary recovery is by far the most common use of deep well injection. Although most deep well injection operations have no impact on earthquake activity, it has been conclusively shown that under some conditions the increase of fluid pressure in the reservoir associated with deep well injection can trigger or induce earthquakes. The first and best known instance of this phenomena—including the largest earthquakes—occurred during the 1960's in association with the waste injection well at the Rocky Mountain Arsenal near Denver. Since this discovery, additional examples of earthquakes induced by deep well injection have been documented (see Table 1 and Figure 1). It is conceivable, if not likely, that other examples of earthquakes induced by deep well injection may have gone unnoticed because the induced earthquakes were small and there were no nearby seismograph stations to record them.

Investigations of several of the earthquakes associated with deep well injection have led to some understanding of the likely physical mechanism of the triggering, and criteria for predicting whether earthquakes will be triggered depending on the local state of stress in the earth's crust, the injection pressure, and the physical and hydrologic properties of the rocks into which the fluid is being injected. The aim of this report is to summarize the current state of understanding of this phenomenon, to describe the criteria for predicting whether earthquakes will be triggered by deep well injection, to identify remaining unanswered questions, and to indicate—from a seismological point of view—factors to be considered in developing regulations and operating procedures for deep well injection.

This report is organized in the following way. General characteristics of the earthquakes induced by deep well injection are summarized in Chapter III. More detailed accounts of the individual case histories are included in Appendix A. Current understanding of the mechanism by which the earthquakes are induced is reviewed in Chapter IV. A review of tectonic stress is presented in Chapter V. Tectonic stress is one

of the key environmental factors contributing to the conditions for induced earthquakes. Current understanding of tectonic stress, why it is important, how it is measured, and how it varies across the United States are all discussed. The hydrologic factors involved in inducing earthquakes and the methods for calculating the change in the pressure field around an injection well are reviewed in Chapter VI. Unresolved issues and the limitations of current knowledge and understanding of the phenomena are discussed in Chapter VII.

Although several research issues remain unresolved, considerable information is currently available that may be of use in developing regulations and operating procedures for deep injection wells to minimize the possibility of problems associated with induced earthquakes. These considerations are discussed in Chapter VIII. Fortunately, favorable conditions for siting a deep injection well, namely the desirability of high permeability and porosity in the injection zone and a site situated away from known fault structures, also tend to be conditions for which the occurrence of induced earthquakes is less likely. Thus, implementation of these recommendations would likely have minimal adverse impact on site selection or operational procedures for injection wells located at otherwise favorable sites.

III. SUMMARY OF EARTHQUAKES INDUCED BY DEEP WELL INJECTION

Well-documented examples of seismic activity induced by fluid injection include: earthquakes triggered by waste injection near Denver [Healy *et al.*, 1968; Hsieh and Bredehoeft, 1981]; by secondary recovery of oil in Colorado [Raleigh *et al.*, 1972], southern Nebraska [Rothe and Lui, 1983], West Texas [Davis, 1985], western Alberta [Milne, 1970] and southwestern Ontario [Mereu *et al.*, 1986]; by solution mining for salt in western New York [Fletcher and Sykes, 1977]; and by fluid stimulation to enhance geothermal energy extraction at Fenton Hill, New Mexico [*e.g.*, House and McFarland, 1985]. In two specific cases, near Rangely, Colorado [Raleigh *et al.*, 1976] and in Matsushiro, Japan [Ohtake, 1974], experiments to directly control the behavior of large numbers of small earthquakes by manipulation of fluid injection pressure were successfully conducted. Table 1 gives a brief listing of each of the cases in which seismicity is clearly associated with adjacent injection well activities. A more complete summary is provided in Appendix A. Other

cases of induced seismicity, owing to either fluid injection or reservoir impoundment were recently reviewed and discussed by Simpson [1986].

In each of the well-documented examples, convincing arguments that the earthquakes were induced relied upon three principal characteristics of the earthquake activity. First, there is a very close geographic association between the bottom of the injection wells and the locations of the subsequent earthquakes. Second, calculations based on the measured or inferred state of stress in the earth's crust, and the measured injection pressure, indicate that the theoretical threshold for frictional sliding along favorably oriented, preexisting fractures, as indicated by the Mohr–Coulomb failure criterion, was likely exceeded. And third, a clear disparity between the previous seismicity and the subsequent earthquake activity could be established, with the induced seismicity often characterized by large numbers of small earthquakes that may persist for as long as elevated pore pressures in the hypocentral region continue to exist.

Most of the earthquakes induced by fluid injection are associated with water flooding operations to enhance secondary recovery of hydrocarbons (Table 1). This is not surprising, since the conditions for failure are much more favorable in injection operations of this type. Fluid injection for the purpose of secondary recovery typically involves high fluid pressures into confined reservoirs of limited extent and low permeability. Often, the producing field is a structural trap, perhaps defined by fault controlled boundaries. In contrast, waste disposal operations prefer to inject into large, porous aquifers with high permeabilities away from known fault structures. Furthermore, waste disposal operations typically involve only one to a few wells at any one location; whereas, with secondary recovery, the technique often involves large arrays comprising tens of wells over the entire extent of the producing field. These differences between the two types of operation make injection well activities for the purpose of secondary recovery much more conducive to triggering adjacent seismicity.

As indicated by a review of Table 1, many of the sites where earthquakes have occurred operate at injection pressures well above 100 bars ambient. The exceptions tend to be sites characterized by a close proximity to recognized surface or subsurface faults. In the Rangely and Sleepy Hollow oil field cases, faults are located within the pressurized reservoir, and were identified on the basis of subsurface structure contours. The Dale and

Matsushiro cases both occurred close to prominent fault zones exposed at the surface, the Clarenden-Linden and Matsushiro fault systems, respectively. In the one conclusive case of seismicity induced by waste-disposal operations, the Rocky Mountain Arsenal well near Denver, fluid injection inadvertently occurred directly into a major subsurface fault structure, later identified on the basis of the subsequent induced seismicity [Healy *et al.*, 1968] and the properties of the reservoir into which fluid was injected, as reflected in the pressure-time record [Hsieh and Bredehoeft, 1981].

The Rocky Mountain Arsenal well near Denver is thus the classic example of earthquakes induced by deep well injection. Prior to this episode, the seismic hazard associated with deep well injection had not been fully appreciated. Injection into the 3700 m-deep disposal well began in 1962, and was quickly followed by a series of small earthquakes, many of which were felt in Denver (Figure 2). It was not until 1966, however, that the correlation was noticed between the frequency of earthquakes and the volume of fluid injected (Figure 3). Pumping ceased in late 1966 specifically because of the possible hazard associated with the induced earthquakes, after which earthquakes near the bottom of the well stopped. However, earthquakes continued to occur, migrating up to 6 km away from the well over the next two years as the anomalous pressure front, established around the well during injection, continued to migrate outward from the injection point. The largest earthquakes in the sequence (between magnitude 5.0 and 5.5) occurred in 1967, after injection had stopped and well away from the injection well itself.

These results imply that fluid pressure effects of injection operations can extend well beyond the expected range of actual fluid migration. There are indications, however, that the risk posed by triggered earthquakes can be mitigated by careful control of the activity responsible for the induced seismicity. As shown by a number of cases detailed in Appendix A, seismicity can eventually be stopped either by ceasing the injection or by using lower pumping pressures. The occurrence of the largest earthquakes involved in the Rocky Mountain Arsenal case a year after pumping had stopped, however, indicates that the process, once started, may not be completely or easily controlled.

IV. CONDITIONS FOR EARTHQUAKE GENERATION

The case histories of injection-induced seismicity documented in Appendix A demonstrate that in sufficiently pre-stressed regions, elevating formation pore pressure by several tens of bars can cause a previously quiescent area to become seismically active. However, not all high-pressure injection wells trigger earthquakes. The reasons why depend on the characteristics of the earthquake faulting process, the local hydrologic and geologic properties of the zone of injection, the *in situ* stress field, and the specific conditions for earthquake triggering, many of which have only recently been understood and appreciated. A fundamental distinction exists, however, between factors that *cause* earthquakes versus mechanisms that may *trigger* earthquakes. Earthquakes result from the sudden release of stored elastic strain energy by frictional sliding along preexisting faults. The underlying cause of earthquakes is therefore the forces that are responsible for the accumulation of elastic strain energy in the rock and that raise the existing state of stress to near critical stress levels. Consequently, the hazard associated with fluid injection is not that it can generate sufficient strain energy for release in earthquakes, but that it may act to locally reduce the effective frictional strength of faults, and thereby trigger earthquakes in areas where the state of stress and the accumulated elastic strain energy are already near critical levels as a result of natural geologic and tectonic processes.

Mohr–Coulomb failure criterion

Since the shear strength of intact rock is considerably greater than the frictional strength between rock surfaces, slip during an earthquake typically occurs along preexisting faults, and will occur when the shear stress resolved across the fault exceeds the inherent shear strength and frictional stress on the plane of slip. Quantitatively, this condition is termed the Mohr–Coulomb failure criterion, and is expressed by the linear relation:

$$\tau_{crit} = \tau_0 + \mu\sigma_n,$$

where τ_{crit} is the critical shear stress required to cause slip on a fault, τ_0 is the inherent shear strength (cohesion) of the slip surface, μ is the coefficient of friction, and σ_n is the normal stress acting across the fault [*c.f.*, Jaeger and Cook, 1976]. For weak fault zones

with little cohesion, τ_0 is nearly zero and slip will occur when the shear stress is greater than or equal to an amount that is simply the product of the coefficient of friction and the stress normal to the plane of slip, *i.e.*, the frictional strength of the fault:

$$\tau_{crit} = \mu\sigma_n.$$

Figure 4 shows values of maximum shear stress (τ) as a function of effective normal stress for a variety of rock types [Byerlee, 1978]. The data indicate that the coefficient of friction (μ) for most rock types ranges between 0.6 and 1.0.

When fluid is present in the rocks, the effective normal stress is reduced by an amount equal to the pore pressure (p), and the shear stress required to cause sliding is reduced to:

$$\tau_{crit} = \mu(\sigma_n - p).$$

This reduction in the effective strength of crustal faults is the essential mechanism of induced seismicity. That is, for a constant state of tectonic stress, the effective strength of crustal faults can be reduced below the critical threshold by increasing the fluid pressure contained within the rocks, leading to a sudden slip and the occurrence of an earthquake.

Description of the state of stress using the Mohr circle

A simple graphical method for describing the state of stress and how it is altered by the introduction of fluids under pressure is given by the Mohr circle diagram (Figure 5) [Jaeger and Cook, 1976; Simpson, 1986]. The stresses acting on a given fault plane can be specified with respect to an orthogonal coordinate system, referred to as the principal stress axes, along which stresses are purely compressional. The stress components relative to these principal axes are called the principal stresses and are usually designated σ_1 (maximum), σ_2 (intermediate), and σ_3 (minimum). Shear and normal stress along and across fractures of various orientations are linear combinations of the maximum and minimum compressive stresses, and are defined by the locus of points around the Mohr circle, whose center is the average between the maximum and minimum principal stresses (*right*, Figure 5*b*). Thus, for a specific fault plane oriented at an angle α with respect to the minimum compressive stress direction, the shear and normal stresses acting along and across that plane will be

determined by a specific point on the Mohr circle (identified by an angle 2α drawn from the middle, *right,* Figure 5*b*). Larger stress differences between the maximum and minimum principal stresses (*i.e.,* the deviatoric stress) result in larger Mohr circles and thus, larger available shear stresses for causing slip along favorably oriented fractures.

The failure criterion is represented by a line with a slope equal to μ and an intercept equal to τ_0 (Figure 5*a*). Relative effective values of σ_1 and σ_3 necessary for failure define a circle tangent to the failure envelope. In other words, fault planes whose orientations with respect to a given stress field (σ_1 and σ_3) define values along the Mohr circle that intersect the failure envelope for a given τ_0 and μ will be most likely (*i.e.,* most favorably oriented) to slip (Figure 5*c*).

Figure 6 shows how an initial stress state (right circle) determined at the bottom of a well near Perry, Ohio is modified by changes in pore pressure (see Appendix A for details). As previously indicated, in the presence of a fluid, compressive stresses are opposed by the hydrostatic fluid pressure. This reduces the effective stress levels by an amount equal to the formation pore pressure, and moves the Mohr circle to the left (middle circle, Figure 6). In this example, the state of stress under hydrostatic conditions is close to, but does not exceed, the failure criterion for a fracture with no cohesion. Increasing the pore pressure by an amount equal to a nominal injection pressure of 110 bars moves the Mohr circle even further towards the failure envelope (left circle, Figure 6), and in fact, for the example shown, indicates a critical stress level is reached for fractures with cohesive strengths of as much as 40 bars and frictional coefficients of 0.6. Fractures with less cohesion or lower coefficients of friction would also be susceptible to failure.

Conditions for Induced Seismicity

Using the Mohr–Coulomb failure criterion, it is now possible to specify the conditions under which seismicity is most likely to be triggered by fluid injection. First, the existing regional stress field needs to be characterized by high deviatoric stress, *i.e.,* the difference between the maximum and minimum compressive stress is large, resulting in large Mohr circles. This does not require that the state of stress itself be large, only that large stress differences exist for different orientations. In fact, many areas identified as close to

incipient failure are characterized by relatively low states of stress. This is because low stress states may correspond with low normal stresses acting across potential slip surfaces. Low normal stress implies low frictional strength, *i.e.*, faults are weak and easily induced to slip. The Rocky Mountain Arsenal case near Denver occurred in a region of normal faulting, characterized by a relatively low state of stress, and as a consequence, relatively low effective normal stress and high shear stress across the fault that slipped [Zoback and Healy, 1984].

Second, there must be available for slip favorably oriented, preexisting faults or fractures. The earth's crust, for the most part, has numerous fractures of different size and orientation. However, many of these fractures are small, capable of generating only small earthquakes of little consequence, and many may not have the proper orientation relative to the existing regional tectonic stress field such that the conditions for failure are met. Thus, for fluid injection to trigger substantial numbers of significant earthquakes, a fault or faults of substantial size must be present, with proper orientation relative to the existing state of stress, characterized by relatively low effective shear strengths, and sufficiently close in proximity to well operations to experience a net pore pressure increase. As discussed in more detail below, the effects of fluid injection dissipate rather quickly with increasing distance from the well, such that for most typical values of hydrologic properties of aquifers of large spatial extent, the pore pressure effect beyond about 10 km is minimal.

Third, injection pressures at which well operations are conducted are relatively high. For example, the Cogdell field in West Texas (Table 1), which triggered the largest earthquake known to be associated with secondary recovery operations in the United States [Davis, 1985], operates at fluid injection pressures of nearly 200 bars above ambient. Other extensive well operations in the same tectonic province, and in fact operating within the same pay zone (the Canyon Reef formation), are not inducing adjacent seismicity, but they typically operate at injection pressures of 150 bars or less. Similarly, the Calhio waste disposal wells in northeastern Ohio (Table 1) may have triggered several small earthquakes in close proximity (< 5 km) to the injection site [Nicholson *et al.*, 1987], yet a number of other injection wells that utilize the same basal sandstone layer (the Mt. Simon formation) for the disposal of both hazardous and non-hazardous waste, have not done the same.

However, these other wells typically operate at half the pressure utilized by Calhio.

The hydrologic properties of a reservoir that are responsible for how rapidly fluid is accepted, and that in turn control the injection pressure for a constant fluid injection rate, also control how rapidly the pressure effect in the reservoir dissipates with distance from the point of fluid injection. Aquifers of large spatial extent, which require low injection pressures for high injection rates, also dissipate the pressure effect most rapidly, insuring that unless fluid is injected directly into a fault zone (as in the Rocky Mountain Arsenal case), the net pore pressure change from fluid injection will not extend any appreciable distance from the well. Thus, the distance between a favorably oriented fault, or fracture, capable of slip and an operating injection well is a critical factor in determining the potential for induced seismicity. Assessing the proximity of favorably oriented, preexisting fractures to a potential waste disposal site is difficult in the eastern and central United States, because many of the fault structures responsible for earthquakes in the past, and presumably the most likely ones responsible for earthquakes in the future, are not easily identified. Historical earthquakes in the east, unlike those in the western United States, have yet to produce any primary surface manifestation, making identification of active faults (or potentially active faults) uncertain. Reducing the risk of siting an injection well near a major fault may thus require extensive subsurface geologic mapping to assess the proximity of potential fault structures. In contrast, substantial progress has been made in the ability to assess the local state of stress, and thus ascertain the degree to which any potential faults or fractures in the vicinity of the well may be close to failure.

V. STATE OF STRESS IN THE EARTH'S CRUST IN THE UNITED STATES

Estimating the state of stress throughout the continental United States has become a very active research area over the last several years. Its determination is extremely important to both a further understanding of regional patterns of crustal deformation, as well as any accurate assessment of the local seismic hazard. The amount of energy available to be released in an earthquake is determined by the amount of elastic strain energy stored in the rocks of the earth's crust. The amount of strain energy available for release depends, in turn, on the state of stress. It is the state of stress that determines how close to failure

a preexisting fault may be and, as shown below, how much fluid pressure is required to trigger fault slip or to hydrofracture intact rock. Because of its importance, the variation in time and space of both its magnitude and direction has become the subject of several recent research projects. In many cases, the techniques developed to determine the state of stress actually measure secondary effects (like strain), rather than stress directly. The greatest difficulty, however, is measuring the necessary quantities at depths where earthquakes actually occur; otherwise questionable extrapolations must be used from measurements made at shallow depths. The advantage in assessing the potential for an existing injection well to trigger earthquakes is that, since any earthquakes induced by the well are likely to be shallow and in close proximity to the well itself, the presence of the well provides reasonable access to the hypocentral region where any potential induced events are likely to occur.

Determining the magnitude and orientation of the local state of stress

Measurements of the state of stress can be accomplished through a variety of techniques. In general, it is somewhat easier to determine the orientation of the principal stresses than it is to determine their magnitude. Nevertheless, orientations alone are still important, especially in the eastern United States where seismicity is relatively low, because the current stress regime may be substantially different from that which existed when major faults in the area were produced. Thus, the orientation of the principal stresses determined from actual *in situ* measurements (see Figure 7) can aid in identifying those faults that have orientations conducive to failure in the current tectonic stress field. Orientations and to some extent relative magnitudes of the principal stresses can be determined from earthquake focal mechanisms [*e.g.*, Zoback and Zoback, 1980; Michael, 1987], borehole elongations [Gough and Bell, 1981; Plumb and Hickman, 1985], core-induced drilling fractures [Evans, 1979; Plumb and Cox, 1987], and in some cases from the orientation of young geologic features, such as dikes, volcanic vent alignments, or recent fault offsets. Reliable determination of the absolute magnitude of the principal stresses typically requires measurements made using the hydraulic fracturing stress method.

Stress orientation indicators

Earthquake focal mechanism solutions

Earthquake focal mechanisms are some of the most commonly utilized indicators of principal stress directions. Focal mechanism solutions define two alternative planes of slip, as well as two stress axes, one of compression and one of tension (see Figure A1). A discussion of the possible orientations that these particular stress axes may have relative to the principal stress directions is given in McKenzie [1969].

The principal contribution of focal mechanism solutions is that they readily identify the specific type of faulting, and the orientation of actual planes of slip (faults) in the local area. By inference, the relative magnitude of the state of stress can then be derived, if one of the three principal stresses (σ_1, σ_2, or σ_3) is assumed to correspond with the vertical stress (S_v) induced by the weight of the overburden. Thus, in areas dominated by normal faulting, S_v corresponds with σ_1, implying that the magnitude of the other two orthogonal stresses (S_H and S_h, corresponding to the maximum and minimum *horizontal* compressive stress, respectively) are less than the overburden pressure. In regions of strike-slip faulting, S_v is intermediate, and in regions of thrust faulting, S_v is less than either S_H or S_h [Anderson, 1951]. If the orientation of the principal stresses are known from other data in the same stress province, focal mechanisms can be used to predict the orientation of available planes of slip, and the degree to which such planes are close to the plane of maximum shear.

Wellbore breakouts

Wellbore breakouts, also known as borehole elongations, are a phenomenon of wellbore deformation induced by inhomogeneous stresses in the crust (see Figure 7*c*). When a well is drilled into a medium, the presence of the cavity creates stress concentrations around the borehole wall [Hubbert and Willis, 1957]. These stress concentrations are greatest in the section of the wall parallel to the S_h direction. Bell and Gough [1979] interpreted the elongation of the borehole as spalling of weak material off the wellbore wall caused by localized compressive shear failure in the region where the compressive stress concentration was largest. Subsequent data [*e.g.*, Plumb and Hickman, 1985; Plumb and Cox, 1987] has

confirmed that wellbore breakouts are indeed the result of stress-induced shear failure under compression, and that the orientations of the borehole elongations consistently reflect the orientation of S_h. Measurement of the shape of the borehole wall with depth, using standard logging techniques (dipmeter or televiewer), can then assess the consistency of the orientations of S_H and S_h as a function of depth, as well as their spatial variation between wells (Figure 7*a*).

Core-induced fractures

A recently identified stress orientation indicator, similar to wellbore breakouts, is the observation of core-induced drilling fractures. This phenomenon, also called petal centerline fractures, typically consists of near-vertical or steeply dipping planar fractures observed in oriented rock cores (see Figure 7*c*), and are believed to represent extensional fractures formed in advance of a downcutting drill bit [Kulander *et al.*, 1977; GangaRao *et al.*, 1979]. Thus, unlike wellbore breakouts, which are compressional features (and therefore form parallel to the minimum horizontal compressive stress direction, S_h), the orientation of these fractures is thought to parallel the maximum horizontal compressive stress, S_H. Evans [1979] examined oriented cores from 13 natural gas wells in Pennsylvania, Ohio, West Virginia, Kentucky, and Virginia and determined petal centerline fracture orientations for hundreds of meters of core in most of the wells. Plumb and Cox [1987] also compiled regional data sets of core-induced fracture orientations. The inferred maximum horizontal stress directions derived from these measurements are generally consistent within wells, between nearby wells, and with adjacent hydraulic fracturing results, borehole elongations, and focal mechanism solutions (Figure 7).

Fault offsets and other young geologic features

In the presence of an inhomogeneous stress field, young geologic features such as dikes, or volcanic vent alignments are most likely to propagate in a direction parallel to the maximum horizontal compressive stress field. This assumes, however, the absence of any preexisting fabric, or other structural features such as faults to preferentially control dike or vent-alignment formation. Fault offset data can be used like focal mechanism solutions to constrain the orientation and relative magnitudes of the existing stress field

[*e.g.*, Angelier, 1979; Michael, 1984], with the added constraint that the fault plane is known. The stress orientations derived, however, are only valid for the time period during which fault slip occurred, and so are not necessarily valid for the current tectonic stress field.

Hydraulic fracture stress measurements in wells

The most reliable measurements of both the magnitude and the orientation of *in situ* stresses are made by the hydrofracture technique. The principle involved with this technique is similar to that for wellbore breakouts, except that failure results from tension rather than compression. In the hydraulic fracturing technique, one principal stress is assumed parallel to the borehole, and equal in magnitude to the overburden pressure (*i.e.*, S_v). If the pore pressure in the borehole exceeds at any point the strength of the intact rock and the stress concentration around the wellbore, a hydraulic fracture is produced (see Figure 7*c*). Since the points at which the borehole wall is weakest correspond with a vertical plane perpendicular to the minimum horizontal compressive stress (S_h), the hydraulic fracture will most likely propagate in that plane. The magnitude of S_h, therefore, can be determined from the pressure in the hydraulic fracture immediately after pumping into the well is stopped and the well is shut in. This is called the "instantaneous shut-in pressure" or ISIP. The magnitude of the maximum horizontal principal stress, S_H, can then be determined, providing that the assumption of elastic stress concentration around a circular borehole is valid. In some cases, however, the material around the wellbore clearly cannot support the concentration of stresses and fails in compression, resulting in borehole elongation mentioned above [Bell and Gough, 1982]. When this happens the assumption of elastic behavior near the wellbore is clearly not valid and S_H cannot be determined in the intervals exhibiting wellbore breakouts.

Basically, the method of hydraulic fracture stress measurement is to pack off an unfractured section of the wellbore, and then increase the fluid pressure in the packed off section until a fracture occurs in the borehole wall. Since the section is isolated (*i.e.*, packed off), the pressure is carefully monitored, and only a small volume of fluid is used, a small controlled fracture is produced, not a massive hydraulic fracture as in the case of

well stimulation to enhance circulation [*e.g.*, Pearson, 1981]. The fluid pressure required to cause the fracture is called the "breakdown pressure" (P_b) or "fracture pressure". The fluid pressure is then repeatedly cycled to determine the pressure required to reopen the fracture, pumping small volumes at constant flow rate, and permitting "flow-backs" to occur following each injection cycle to allow for the drainage of excess fluid pressure. The pressure and flow records produced under these controlled conditions will reflect both the procedures used during hydraulic fracturing as well as the *in situ* stress field. Thus, careful analysis of the pressure-time histories recorded during hydrofracturing can be used to estimate the magnitude of the principal stress components. Stress orientation is determined by using a borehole televiewer or impression-packer to ascertain the orientation of the hydraulic fracture created. Figure 8 shows an example of a typical hydraulic fracturing pressure-time record from a well drilled in crystalline rock near the San Andreas fault in central California at a depth of 185 m. In the case of a waste-disposal well, this measurement would be made ideally in the anticipated zone of injection, or if possible, in the basement rock below the waste-disposal aquifer.

From the results of Hubbert and Rubey [1957], Haimson and Fairhurst [1967] derived the equation:

$$P_b = 3S_h - S_H - p + T$$

relating the breakdown pressure, or the presumed pressure of fracture formation (P_b), to the horizontal principal stresses (S_h and S_H), the formation pore pressure (p), and the formation tensile strength (T). S_h can be determined from the ISIP. Determination of the magnitude of S_H requires knowledge of T, the effective tensile strength of the rock being fractured. A good *in situ* measure of T can be inferred from the difference between the fluid pressure required to fracture the rock (P_b), and the pressure needed to just barely open the newly-created fracture (*top,* Figure 9). In practice, several successive cycles of fluid injection may be required to accurately measure this quantity (*bottom,* Figure 9). It was then recognized that, if the initial formation pore pressure p and the ISIP were known, then S_H could be determined directly from the fracture-opening pressure (P_{fo}):

$$P_{fo} = 3S_h - S_H - p$$

[Bredehoeft *et al.*, 1976]. Figure 8 shows how each of the three values (Breakdown – P_b, Frac Open – P_{fo}, and ISIP) are reflected in the pressure-time history.

Types of pressure-time records

Using the equations above for P_b and P_{fo}, three types of pressure-time histories can be identified, depending on the relative values of P_b, P_{fo} and S_h. Figure 10 shows examples of these three types of pressure records and how each can be distinguished.

Comparison of fracture pressure and Mohr–Coulomb failure criterion

The increase in formation pore pressure by fluid injection in a well can thus induce either an hydraulic fracture or slip on a preexisting fault. In both cases, the critical pressure necessary for failure is dependent on the *in situ* stress field. Pressure limitations of maximum allowable injection pressures established for various waste-disposal operations are typically set below the estimated value of P_b to prevent an uncontrolled fracture of the confining layer above the aquifer used for waste-disposal, and the potential contamination of potable water supplies. Although the concept of "fracture pressure" (*i.e.*, the fluid pressure needed to cause a hydraulic fracture in the borehole wall) is well recognized in the drilling and well-operations industry, its dependence on the regional tectonic stress field, as well as on the tensile strength of the rock, is often not fully appreciated. Thus, before reasonable levels of injection pressure are set, accurate knowledge of the existing state of stress is extremely important.

In terms of the relative magnitudes of fluid pressure needed to induce slip on a preexisting fault *versus* the fluid pressure necessary to cause an hydraulic fracture, the pressure needed to cause slip is typically much lower. For example, suppose the state of stress can be characterized by a regime in which the vertical stress (S_v) is close to the maximum horizontal compressive stress (S_H), and the stress ratio (α) of the minimum to the maximum compressive stress is 0.65. It can be easily shown that the breakdown pressure (P_b) required to hydrofracture intact rock is given by:

$$P_b = S_v(3\alpha - 1) - p + T.$$

At a nominal depth of 2 km and for a rock density of 2.6 g/cm^3, S_v = 510 bars. If the tensile strength (T) is taken to be 40 bars, and the pore pressure is near hydrostatic (p = 200 bars), then P_b = 325 bars or 125 bars above ambient. Fracture-opening pressure (P_{fo}) would then be 285 bars or 85 bars above ambient. However, the critical fluid pressure (P_{crit}) necessary to induce sliding on a favorably oriented preexisting fracture with no cohesion is equal to:

$$P_{crit} = (K\sigma_3 - \sigma_1)/(K - 1)$$

where $K = [(\mu^2 + 1)^{\frac{1}{2}} + \mu]^2$, and μ is the coefficient of friction [Jaeger and Cook, 1976]. For a μ of 0.6, and a stress regime given above, this reduces to:

$$P_{crit} = S_v(3\alpha - 1)/2$$

which for the values of α and S_v given above, P_{crit} = 242 bars or only 42 bars above ambient. If the fault exhibits cohesion (τ_0), then the critical fluid pressure required to induce slip is proportionately greater. Nevertheless, under the conditions assumed above, an increase in fluid pressure of 42 bars would be sufficient to induce slip on planes with no cohesion that contain σ_2 and are oriented about 30° relative to σ_1; 85 bars would be sufficient to open preexisting fractures (increase transmissivity) oriented parallel to σ_1; and 125 bars would be sufficient to hydraulically fracture the intact rock of the borehole wall.

Setting maximum injection levels at pressures below that required to fracture the intact borehole wall will thus not guarantee the prevention of induced seismicity if favorably oriented, preexisting faults are present near the well. Conducting a controlled hydraulic fracture stress measurement will, however, determine both the safe fluid injection pressure to prevent an uncontrolled hydrofracture, as well as how close to failure any potential slip surface may be.

Summary of stress measurements to date

Compilations of various stress measurements have been made by several investigators [Sbar and Sykes, 1973; Lindner and Halpern, 1978; Zoback and Zoback, 1980; 1987]. These

summaries suggest that the continental Unites States can be divided into distinct stress provinces, within which the stress field is fairly uniform in both magnitude and direction. Figures 7 and 11 show some of the most recent compilations of stress orientations within the conterminous United States [Plumb and Cox, 1987; Zoback and Zoback, 1987]. Both sets identify the type of stress indicator used at each site. A more generalized stress map showing average principal stress orientations, the stress regime, and delineating the stress provinces is shown in Figure 12. In some cases, the boundary between various provinces is sharp, whereas in others it is broad and transitional.

Much of the central and eastern United States, where a large number of waste-disposal wells are concentrated, is characterized by a compressive stress regime. Reverse (thrust) and strike-slip faulting would be most likely to occur in this part of the country, with the vertical stress (S_v) less than one or both of the horizontal stresses. Since the maximum principal compressive stress is horizontal and oriented northeast to east, planes striking 30 to 45 degrees relative to S_H would typically be most favorably oriented for slip. Magnitudes of the principal stresses indicate that for large parts of the central United States, the state of stress is such that only small increases in pore pressure along such favorably oriented fractures are required to induce slip.

VI. HYDROLOGIC FACTORS IN EARTHQUAKE TRIGGERING

As described above, the increase of fluid pore pressure resulting from injection is the key perturbation to the natural environment responsible for inducing or triggering earthquakes. A well developed body of theory and computational techniques exists for the estimation of the temporal and spatial distribution of the pressure field from an injection well. Relatively straightforward analytic techniques are available for simple geometries, such as radial flow in a confined aquifer. Numerical modelling techniques are also available for more complicated geometries. The most complete analyses of the hydrologic factors involved in earthquake triggering were conducted in association with the Denver and Rangely earthquake sequences [Hsieh and Bredehoeft, 1982; Raleigh *et al.*, 1976]. In the Denver case, the pressure field was dominated by a fault or fracture zone of finite width with high permeability relative to the country rock. At Rangely, although the reservoir

geometry was less complex, the pressure field also seemed to be affected by the presence of a zone of high permeability that coincided with a mapped subsurface fault (see Figure A2). For most cases of Class I injection wells, sites are chosen to avoid faults where possible, and in such cases, estimating the development of the pressure field established around the well by fluid injection can rely on using relatively simple methods. However, if after the completion of the well, evidence comes to light suggesting that a more complex model of reservoir geometry is appropriate, it would then be necessary to reassess the net effect of fluid injection by utilizing more precise and sophisticated techniques for analysis.

Most of the common methods available for calculation of the pressure field from an injection well are adaptations of standard techniques used in ground water modelling [*c.f.*, Davis and DeWiest, 1966; Freeze and Cherry, 1979; Fetter, 1980]. However, as discussed above, changes in the standard techniques are required in the presence of faults, fractures, or other possible pathways for anisotropic fluid flow. In addition, if fluid is being injected into an extremely low permeability rock, typical of the crystalline basement were most earthquakes occur, other factors of importance may also come into play. Methods of calculating groundwater flow in such low-permeability environments are discussed by Neuzil [1986].

The critical reservoir characteristics for predicting the pressure field around an injection well are the transmissivity and storativity of the rocks. The lower the transmissivity, the more confined is the "pressure bulb" around the bottom of the well, and the more likely the buildup of high pore fluid pressure will be, increasing the concern for earthquake triggering. In as much as earthquakes occur on faults, and these same faults can, in some cases, act as zones of high permeability (or transmissivity), determining the presence of faults or fractures is important to the question of predicting the occurrence of induced seismicity.

In many cases where potentially active faults occur at some distance from the injection well, accurate fluid pressure changes are difficult to anticipate because detailed information about the hydrologic properties of the reservoir away for the injection well are lacking. For instance, waste may be injected into a basal sedimentary unit overlying basement. Although much may be known about the zone of injection, little may be known about the

hydrologic characteristics of the basement, where the potential for earthquakes—owing to the presence of faults and fractures—may well be significant. As shown below, some estimate of the average characteristics of the reservoir in the vicinity of a well can be inferred from measurements made during well completion and detailed monitoring of the well's pressure-time history.

Reservoir properties

For a given reservoir geometry, the fluid pressure field generated by injection is governed by the reservoir's transmissivity and storativity, which are functions of the porosity, permeability, and elastic constants of the aquifer. These parameters can be determined from laboratory tests on well cores, from piezometer tests, or from pumping tests. Pumping tests have the desirable characteristic that they average over a large volume of the aquifer, and therefore represent the most realistic estimates. The storativity, which gives the amount of fluid released per unit column of aquifer for a unit decline in head, can be calculated from the expression:

$$S = \rho g h(\alpha + n\beta)$$

where ρ is fluid density, g is the acceleration of gravity, h is the aquifer thickness, α is the vertical compressibility of the aquifer, n is the porosity, and β is the fluid compressibility. The transmissivity T is defined as:

$$T = Kb$$

where K is the saturated hydraulic conductivity, $K = k\rho g/\eta$, and k is the specific or intrinsic permeability, ρ is the density of the fluid, η is the dynamic viscosity of the fluid, and b is the thickness of the aquifer [Freeze and Cherry, 1979]. The storativity and transmissivity can be estimated from pumping tests, using curve matching techniques with type curves such as the Theis log-log plot curve, or the Jacob semi-log plot method [Freeze and Cherry, 1979].

Fluid Pressure Changes Resulting from Injection

For purposes of illustration, two types of reservoir models are presented. The first type of model is an infinite isotropic reservoir; the second involves reservoirs of finite width (*i.e.*, rectangular cross section), but of infinite length. These models are for the purpose of studying how fluid pressure propagates horizontally away from an injection well and do not address the question of how fluid pressure effects might migrate downward from the injection horizon towards potential earthquake producing structures in the basement.

Infinite reservoir model (radial flow)

The simplest model for estimating the development of a pressure field around an injection well is for radial flow in a single, infinite, isotropic aquifer of constant thickness. The pressure $p(r,t)$ at distance r and time t as a result of a constant flow rate Q into a reservoir that extends uniformly in all directions is given by the equation:

$$p(r,t) = \frac{\rho g Q}{4\pi T} \int_u^\infty \frac{e^{-\xi}}{\xi} d\xi$$

in which $u = r^2 S/4Tt$ [*e.g.*, Freeze and Cherry, 1979]. Figures 13 and 14 show example calculations for the pressure field around an injection well in Ohio. The values of storativity (5.4×10^{-5}) and transmissivity (2.0×10^{-5} m^2/sec) are rather low compared to those for optimal waste disposal operations, thus, the pressure at the wellbore required to achieve the desired rate of injection is rather high. Figure 13 shows the pressure change versus time curve at the wellbore for a well of radius 12 cm assuming a constant injection rate of 6.7×10^6 liters/month. Figure 13 also shows how the change in shape of the reservoir geometry can affect the pressure-time history at the wellbore. In the radial flow model, the pressure rises relatively rapidly at the wellbore in the first few years, then continues to rise but at an ever-decreasing rate. The attenuation of the pressure field with distance away from the well is shown in Figure 14. With increasing time, the pressure "bulb" around the well continues to grow. After 10 years of injection the pressure increase at a distance of 5 km from the well is about 15% of the value at the wellbore.

Infinite strip reservoir model

If fluid flow is confined to a narrow reservoir of finite width, then the pressure at a given distance from the well will be higher than for the radial flow models. This type of model was used by Hsieh and Bredehoeft [1981] to calculate the pressure distribution around the Rocky Mountain Arsenal well implicated in the Denver earthquake sequence. Even if there is no specific evidence to suggest that such a similar linear zone of high permeability is characteristic of a particular reservoir geometry, such calculations may still be useful to illustrate how large a pressure buildup is possible at any given distance, and to show how diagnostic the pressure history at the wellbore is of the shape of the reservoir into which fluid is being injected.

For injection into the center of a strip of width w and infinite extent in the x direction, a constant injection rate Q produces a pressure given by:

$$p(x,y,t) = \frac{\rho g Q}{4\pi T} \sum_{m=-\infty}^{\infty} \int_{u_m}^{\infty} \frac{e^{-\xi}}{\xi} d\xi$$

where $u_m = (x^2 + (y + mw)^2)S/4Tt$ and y is the distance from the center of the strip. Figure 13 shows how the pressure at the wellbore will increase with time for various widths of reservoirs with infinite length. Figures 15 and 16 show the attenuation of the pressure field with distance away form the well for the same two models. Two strip widths are considered, 1 km with a transmissivity of 2.0×10^{-5} m^2/sec, and 7.5 km width with a transmissivity of 4.5×10^{-6} m^2/sec. The transmissivities are selected to make the pressure-time curves comparable to the pressure-time curve for the radial flow case discussed above. Two points are clear. First, for a constant fluid injection rate, the pressure required at the wellbore initially rises more gradually for either of the two finite width reservoir models than for the case of radial flow, but continues to rise at a more rapid rate at later time intervals. Secondly, the narrower the postulated reservoir, the higher the formation fluid pressures that will be achieved at large distances from the wellbore. It is also evident that because reservoir geometry has such a significant effect on the pressure-time curves, these figures illustrate how analysis of the history of injection pressure can be used to discriminate the shape of the reservoir into which fluid is being injected.

VI. UNRESOLVED ISSUES

Although much is known about how earthquakes are induced by deep well injection, full understanding of the earthquake process is far from complete. Many issues remain unresolved, and as such, produce large uncertainties in the confidence with which adequate and appropriate regulations can be formulated. The following issues are considered some of the principal unresolved questions that bear directly on the issue of accurate seismic risk assessment.

The problem of eastern and central U.S. seismicity

From a seismic hazard point of view, the contiguous United States can be divided along a boundary roughly corresponding to the eastern front of the Rocky Mountains. Most of the earthquakes in the area to the west (Figure 1) are associated with active, well-defined geologic processes. In contrast, the cause of many of the earthquakes in the central and eastern United States is still poorly understood. In the west, the association of earthquakes, particularly large ones, with geologic faults is well established. In many cases these faults are visible at the surface, and it is possible, using geologic techniques, to demonstrate that displacement has occurred along these faults during the geologically recent past. With the exception of evidence for subsurface faulting in the vicinity of the 1811-1812 New Madrid, Missouri earthquakes, the relationship between faults and earthquakes in the central and eastern United States has been much more elusive. The discovery of the Meers fault in the Wichita Mountains of Oklahoma, along which large, relatively-recent movement has occurred, yet with which no current or historical seismicity has been associated, clouds the issue even further. The Charleston, South Carolina earthquake of 1886 provides perhaps the best example of some of the difficulties involved. Despite the continuing occurrence of small earthquakes in the Charleston area, and extensive geologic and geophysical investigations in the area, there is as yet no commonly agreed upon fault or faults judged to be responsible for the large historic earthquake there. Consequently, the primary basis for estimating future locations of earthquakes in the central and eastern United States remains the historic earthquake catalog.

Magnitudes of induced earthquakes

Although it seems extremely unlikely that deep well injection alone could induce a truly large earthquake in the central or eastern United States, there is currently no satisfactory method for estimating the maximum size earthquake that might be produced. Indeed, there is no method for estimating the increased probability for triggering earthquakes of any magnitude as the result of raising the pore fluid pressure through deep well injection.

Observations indicate that the magnitude of an earthquake increases roughly as the logarithm of the length of fault along which displacement occurs (Figure 17). Slip is also proportional to fault length. Thus, a magnitude 8 earthquake typically involves faulting along hundreds of kilometers of fault and meters of slip; whereas, a magnitude 3 earthquake might involve faulting over a surface with a dimension of a few tens of meters and a slip of a few centimeters. The largest earthquake associated with deep well injection was between magnitude 5 and 5.5 (Table 1: RMA, 1967; Snipe Lake, 1970). Although none of the induced earthquakes recorded so far would be considered devastating, the potential for damage from such earthquakes could be larger than for earthquakes in more tectonically active regions, because many of these events are shallow, occur in areas of low expected seismic hazard, and in regions of low attenuation of seismic waves (*c.f.*, Attica, New York, 1929, in Appendix A). Earthquakes in the eastern and central United States typically cause damage over larger areas as compared to earthquakes of the same size in the western United States. This is primarily the result of the lower attenuation of seismic waves in the east *versus* the west, but other factors may also be involved.

One of these factors which may affect damage potential, and which seems to distinguish earthquakes in the central and eastern United States from those in the west, is a tendency for eastern earthquakes to be associated with relatively smaller fault surfaces for a given magnitude earthquake. If true, this would imply that eastern earthquakes exhibit more slip per unit fault area than western earthquakes, and suggests that eastern earthquakes reflect higher stress drops. This would be coincident with the thinking that the crust of the earth beneath the central and eastern United States is cooler and, therefore, stronger than that beneath the western United States. The importance of this apparent difference

with respect to the seismic hazard associated with deep well injection is that, if correct, smaller faults in the vicinity of a well located in the eastern United States could produce larger earthquakes than might be anticipated based on relationships derived from more seismically active areas in the west.

Potential for reactivation of old faults

It is sometimes suggested that earthquakes in the central and eastern United States occur on reactivated, geologically old faults. Currently, the phenomenon of reactivation is poorly understood. Because of the large uncertainties in the inherent shear strength and time-dependent nature of friction with slip on faults, there are as yet no criteria for predicting whether an old fault might be reactivated, other than the determination of how close in orientation an existing fault may be relative to preferred planes of slip, as predicted by the Mohr–Coulomb failure criterion, in the current regional tectonic stress field.

Importance of small induced earthquakes

It may occur that a deep well injection operation induces small earthquakes in the immediate vicinity of the bottom of the well, as has been the case in several of the secondary oil recovery and solution mining cases described above. If these earthquakes are below the threshold for damage, or perhaps even below the threshold for non-instrumental detection, then it is not unreasonable to ask whether these earthquakes constitute a risk. Two questions arise. Do these small earthquakes indicate the potential for large, potentially damaging earthquakes? Do these small earthquakes indicate the possibility of breaching the confining horizon?

Obviously, the occurrence of small earthquakes indicates that, at least locally, the conditions for seismic slip are satisfied. In the western United States, the association of small natural earthquakes with a geologically recognizable fault is taken as evidence that the entire fault is active, and consequently, that a potentially larger earthquake, controlled by the dimension of the fault, is possible. In the central and eastern United States, our lack of knowledge concerning the size and distribution of buried faults prevents a similar line of reasoning.

The second question is more directly pertinent to the containment of hazardous wastes. The occurrence of small earthquakes near the bottom of a deep injection well may indicate faulting or fracturing processes that could conceivably lead to a breach in the overlying confining zone, and therefore conceivably permit hazardous materials to migrate upward toward potential drinking water supplies.

Neither of these questions can be answered at present. However, until such time as answers are forthcoming, it would seem prudent to regard the occurrence of small earthquakes near the bottom of a deep injection well with concern.

Spatial and temporal variability of tectonic stress

As described above, the key environmental parameter related to the potential for inducing earthquakes through deep well injection is the preexisting tectonic stress. The measurements available to date suggest that over wide regions of the country the orientations, and possibly the magnitudes, of the principal horizontal stresses are relatively constant, or at least slowly varying. Insufficient measurements exist, however, to indicate how rapidly in time and space the stress field may actually vary. In the central and eastern United States, there is at present little indication that the tectonic stress field changes rapidly with time. In the western United States, geodetic measurements suggest that small, but significant stress changes can occur over time scales of months to years. In particular, the occurrence of a nearby major earthquake could dramatically affect the local stress field on a time scale of seconds. Assessing the spatial variation in stress is almost as troublesome. For instance, some areas in the central and eastern United States tend to have more frequent small earthquakes than others. Whether this is related to the spatial variation in the tectonic stress field, or alternatively, to the spatial distribution and orientation of potential planes of slip, is unknown.

VII. CONSIDERATIONS FOR FORMULATING REGULATIONS AND OPERATIONAL PROCEDURES

In terms of the earthquake hazard associated with deep well injection, the three critical parameters that need to be evaluated are: the magnitude of the preexisting tectonic stress,

the injection pressure, and the proximity and characteristics of any faults or fractures that may be affected by pore pressure increases caused by fluid injection operations. The preexisting tectonic stress can be measured at the time of well completion, or extrapolated from measurements made in adjacent wells within the same geologic province. The injection pressure will be controlled by the desired injection rate and the hydrologic properties of the receiving reservoir. Although the presence of large faults may be obvious at the the surface, the presence of smaller faults in the projected reservoir may be extremely difficult to detect. Thus, the two earthquake-related factors that are most amenable to regulation or control are the site selection (and by inference, the characteristics of the reservoir chosen for injection), and the maximum injection pressure.

The following recommendations are made from the point of view of addressing the potential seismic hazard associated with injection-induced earthquakes. These recommendations are not intended to replace or reduce existing procedures or restrictions established on the basis of environmental concerns or other considerations, and therefore, do not comprise by any means a complete list of all the factors needed to be considered in discussing potential hazards associated with the disposal of hazardous waste by deep well injection.

Site selection

Reservoir with high transmissivity and storativity

The potential operator of a waste injection well desires a reservoir with high transmissivity and storativity, because for a given volume of fluid to be injected, the higher the transmissivity and storativity, the lower the required injection pressure. High transmissivity and storativity are also very desirable from the point of view of reducing earthquake hazard, because the lower the injection pressure, the less likely the prospect of inducing or triggering earthquakes.

Stress estimate

An estimate of the state of stress in the area of the projected reservoir is important at an early stage in the selection of a potential site of deep well injection because the state of

stress controls, to a large extent, both the formation fracturing pressure and the pressure threshold for triggering faulting, the Mohr-Coulomb failure pressure. An estimate of high deviatoric stress (the difference between the maximum and minimum principal stresses) in the reservoir region should serve as a warning that both the formation fracturing pressure and the Mohr-Coulomb failure pressures will be low.

The most reliable estimates of the state of stress in the reservoir will be those based upon measurements made in the reservoir rock itself. However, it is likely that a reasonable estimate prior to drilling can be made from the interpolation of regional stress measurements, particularly from hydrofracturing measurements made in the same reservoir rock at nearby wells. Surface or shallow well measurements may also be of value, although the extrapolation of such measurements to significant depth may be unreliable.

Absence of faults

The possibility for induced earthquakes appears to be significantly enhanced if any part of the reservoir affected by the planned injection, is cut by a fault or fracture. Obviously the presence of a fault that might present a flow path through the confining zone is also of concern in evaluating the integrity of the reservoir. Moreover, since the effect of the pressure increase typically extends to a significantly greater distance from the wellbore than the distance to which any of the injected fluid actually migrates, faults or fractures beyond the anticipated migration distance should also be considered carefully.

Clearly it is easier to prove the existence of a fault, than to prove the absence of a fault. Prior to drilling, the existence of a fault may be inferred from surface geologic mapping, from subsurface geologic studies in nearby wells, or from geophysical studies, such as gravity, magnetic, or seismic reflection surveys. It should be remembered, however, that should drilling or operation of the well reveal a previously unknown fault or fracture, then a re-evaluation and analysis of the fluid injection operations may be required.

Regional seismicity

In as much as the occurrence of earthquakes, even relatively small ones, indicates both the existence of faults or fractures and the presence of stresses sufficiently high to cause seismic fault slip, a proposal to locate a deep injection well in an area of significant

seismicity should be regarded with caution, particularly if there is any indication that some of the earthquakes occur near the depth of the reservoir.

Well drilling and completion

Transmissivity and storativity

Estimates of the transmissivity and storativity of the reservoir are critical to the estimate of the maximum injection pressures required over time to accommodate the desired volume and rate of injection. Estimates of these quantities should be made through *in situ* measurements at the time of well completion, in so far as possible, supplemented by laboratory measurements as required. Necessary measurements include the effective permeability and thickness of the potential injection zones, and related measurements, such as the porosity and elastic constants of the reservoir formation.

It would be highly desirable for the potential operator, prior to the beginning of injection operations, to present a calculation of the predicted injection pressure, and its expected increase through time, required to accommodate the desired rate of injection and based on the inferred values of transmissivity and storativity measured in the borehole. This calculation would then provide a standard against which any unusual or unanticipated changes in pressure history observed at the well could then be evaluated.

Stress measurement in reservoir rock

From the point of view of assessing the potential for inducing earthquakes through deep well injection, the most useful single measurement is a high quality stress measurement made in the reservoir rock within the injection well itself. Currently the most reliable and accurate method of making such a measurement is using the hydraulic fracturing technique described in Chapter V. In general, the measurements made in association with standard commercial hydraulic fracturing operations for well stimulation are not precise enough for this purpose. To make an adequate measurement, it is necessary to first select an unfractured length of hole, using an impression packer or borehole televiewer; to use a carefully controlled, low volume of fluid, generally requiring the use of a specially designed hydrofracture tool (called a double straddle-packer unit); and to monitor the operation

with sensitive fluid pressure equipment, as described in Chapter V. It is also highly desirable to repeat the measurement at several places along the unfractured drill hole, to obtain an estimate of the measurement uncertainty.

Given the importance of maintaining the integrity of the confining zone, there may be concern that even the small fractures created by the hydraulic fracture stress measurement technique, or the subsequent propagation of those fractures, could threaten the integrity of the confining zone. Certainly if the well is to be stimulated by hydraulic fracturing, then there is no incremental risk associated with the fractures created by the stress measurements. If the well is not to be stimulated by hydraulic fracturing, then if the stress measurements are done carefully, and at low injection volume, it should be possible to keep the fractures very close to the borehole, and nearly limited to the section of the borehole that has been packed off. The benefit of making these measurements is that the operator, and the regulator, will have a direct measurement of the formation fracture (or breakdown) pressure and a reliable estimate of the zero-cohesion, Mohr-Coulomb failure pressure. With these measurements in hand, the operator and the regulator will be in a position to establish maximum pressure levels for injection operations, using the relations described in Chapters IV and V, which will minimize both the possibility of creating uncontrolled fractures, as well as extending or causing seismic failure on preexisting faults.

If it is judged undesirable to carry out hydraulic fracturing measurements in the reservoir itself out of concern for the integrity of the confining zone, then it may be possible to obtain meaningful and relevant measurements at depths in the borehole above or below the confining zone. Ideally, such measurements should be carried out at sufficient depth to avoid near surface effects, and to avoid possible zones of stress decoupling caused by low-strength sedimentary layers or structures, such as salt beds (Figure 7*b*), between the measurement depth and the reservoir. Strictly from the point of view of the relevance of the stress measurements, the deeper the better.

Pore pressure measurement

An important measurement required to understand the state of stress in the reservoir prior to the beginning of injection, and to understand the influence of the subsequent

injection on the state of stress, is the initial pore pressure in the reservoir formation.

Faulting parameters

If there is any indication that the injection pressures will approach the zero-cohesion Mohr-Coulomb failure pressure, then it would be prudent to make measurements of the coefficient of friction (μ) of the reservoir rock, and adjacent basement rocks, as well as to estimate, if possible, the cohesion and shear strength of any adjacent faults or fractures present (or potentially present) in the reservoir or surrounding country rock.

Well operation and monitoring

Determination of maximum allowable injection pressure

From the point of view of earthquake hazard, assuming possession of the information requested above, the key decision facing the operator and the regulator is the establishment of the maximum allowable injection pressure.

An absolute upper limit of permissible injection pressure, without considering the potential for slip on preexisting faults, would presumably be the formation fracture (or breakdown) pressure. It should be emphasized, however, that estimates of the "safe" injection pressure, based on some percentage of the so-called "normal" gradient of formation fracture pressure of about 0.75–1.0 psi/foot may not be conservative at all. This is because, as described in Chapter V, the formation fracture pressure critically depends on the state of stress, and in particular on the difference between the maximum and minimum principal stresses. The higher the deviatoric stress, the lower the formation fracture pressure. Strict "rules-of-thumb" that do not account for the spatial variation in the state of stress will not adequately specify the "safe" upper limit of the formation fracture pressure.

The lowest critical injection pressure, in terms of possible earthquake triggering, is the zero-cohesion Mohr-Coulomb failure pressure. This is the pressure at which frictional sliding would occur on favorably-oriented preexisting faults or fractures, assuming no cohesion. If the projected injection pressures are below this threshold, no earthquake problems should be anticipated. In contrast, if the desired injection pressures are above

this threshold, then it is necessary to consider with care whether any faults or fractures exist in close proximity to the point of injection, what their orientation may be, and the magnitude of the cohesion on these faults or fractures. If the injection pressure is allowed to reach the Mohr-Coulomb failure pressure, taking into account the appropriate cohesion, then earthquake activity should be anticipated.

Comparison of actual and predicted pressure-time records

The pattern of the injection pressure over time, and indeed the fall of pressure with time during any interruption in injection, give important information about the average hydrologic characteristics of the reservoir. Comparison of the actual pressure *versus* time records with those predicted from the measured or estimated reservoir characteristics (transmissivity, storativity, shape and extent) would provide an assessment of whether the initial assumptions, such as radial flow in a confined homogeneous aquifer, were correct or require modification. Obviously any increase in the apparent transmissivity of the reservoir should be scrutinized as a possible indication that fluid has reached a fracture system.

Seismic monitoring

If there is any question about the possibility of inducing earthquakes, particularly if the projected injection pressure is above the zero-cohesion Mohr-Coulomb failure pressure, then it would be prudent to carry out a seismic monitoring program to detect the occurrence of any adjacent earthquake activity. This would also be advisable if the well is situated in an area with a previous well-defined history of seismic activity, or if the well site is in close (< 20 km) proximity to a known major fault structure. Preferably, this monitoring program should begin as far in advance of the anticipated injection operations as possible, to establish a background level of seismicity against which any potentially injection-induced earthquakes might be compared. To be meaningful, instrumentation should be sensitive enough to detect earthquakes in the magnitude 0 to 1 range located at the bottom of the well. Figure 18 is a seismogram of such a microearthquake detected within 3 km of the Calhio injection well discussed in Appendix A. To obtain this degree of sensitivity in the presence of high levels of seismic noise often associated with industrial activity in the vicinity of the well itself, it may be necessary to locate the instrumentation somewhat

off-site, or to locate it in an adjacent borehole. Significant reductions in noise level can be obtained by placing seismic instrumentation in boreholes at depths as small as a few tens of meters.

Monitoring should continue for as long as it takes to verify that elevated injection pressures are unlikely to trigger significant earthquake activity. This may require several years of observation, since the time involved to attain maximum (*i.e.*, critical) injection pressure at a constant injection rate may take a long time and the diffusion of significant pore fluid effects away from the well is often slow. The time interval between initiation of injection and the largest earthquakes at the Rocky Mountain Arsenal site near Denver was 5 years. For the Snipe Lake, Alberta, case (Appendix A), the time lag was 7 years. Similar time intervals between injection and the largest earthquakes in the triggered sequence have been observed in other cases, however, the time between initiation of injection and the onset of microearthquake activity is often short (*e.g.*, RMA, Dale, *etc.*).

While one seismic station may be adequate for detecting earthquakes (and in favorable cases for estimating the distance of the earthquake from the station), should earthquakes be detected in the vicinity of the well, a minimum of three stations would be necessary to accurately determine their location and focal depth. Thus, if there were any indication of induced seismic activity, it would then be appropriate to supplement an initial, single monitoring station, with additional stations to provide reliable and accurate earthquake locations and focal depths.

Consideration of small earthquakes near the bottom of the well

The occurrence of any earthquakes, even as small a magnitude zero, near the bottom of the well should be viewed with concern. Confirmation that earthquakes are indeed triggered by injection operations could be obtained by comparing the frequency of earthquakes with the cycling of the injection pressure. It should be noted, however, that the pressure changes immediately at the wellbore are damped out with distance from the well. Therefore, induced or triggered earthquakes at some distance from the wellbore should not be expected to correlate as well with the cycling of injection pressure as earthquakes in the immediate vicinity of the bottom of the well. If earthquakes thought to be related

to injection operations are detected, then the appropriate questions are: 1) Is there a possibility that induced earthquakes might cause damage or injury in the surrounding area? and 2) Is there a possibility that the earthquakes indicate fault displacement that might threaten the integrity of the confining zone? If the answer to either of these questions is yes, than consideration should be given to reducing the injection pressure. It should be remembered, however, that once the pore pressure in the reservoir or in adjacent rocks is raised above the critical pressure capable of triggering seismic faulting, lowering the pressure at the wellbore may not immediately lead to the cessation of earthquake activity. Seismicity would not be expected to stop until the pressure in the affected region has decayed below the critical value.

APPENDIX A—EARTHQUAKES ASSOCIATED WITH DEEP WELL INJECTION

Denver, Colorado

In this, the first well-documented case of injection induced seismicity, at the Rocky Mountain Arsenal near Denver, the injection of 17 to 21 million liters/month of hazardous waste into a 3671 m-deep disposal well was quickly followed by many felt earthquakes in a region were the last felt earthquake occurred in 1882 [*top,* Figure A1; Healy *et al.*, 1968]. A comparison between the onset of seismicity and well operations, as well as between earthquake frequency and average injection rate showed a convincing correlation [See Figure 3; Evans, 1966]. Injection ceased in February, 1966, however earthquakes resulting from the increased fluid pressure established around the wells continued for several years (*bottom,* Figure A1). In 1967, three large earthquakes—each with a magnitude greater than 5—occurred, causing minor structural damage in and near Denver.

A study of event locations indicated that earthquakes began initially near the bottom of the injection well, then migrated out along a northwesterly trend for a distance of about 6-7 km (*top,* Figure A1). After the sequence had been in progress for 5 years ($1\frac{1}{2}$ years after injection had stopped), earthquakes continued to occur, not near the base of the well, but primarily within the previously defined linear zone at a distance of 4–6 km and at depths of 4 to 7 km. The largest earthquakes in the sequence (between 5 and 5.5) occurred in April, August and November of 1967 (*middle,* Figure A1), after which activity began to decline.

A total of 620 million liters of fluid were injected at average rates of 478 liters/minute before well operations ceased. Maximum top hole pressure reached 72 bars, corresponding to an estimated bottom hole pressure of 415 bars [Evans, 1966]. Hsieh and Bredehoeft [1981] demonstrated that the records of pressure falloff at the disposal well were consistent with injection into a long, narrow reservoir, a conclusion supported by the elongate shape of the seismogenic zone. No hydraulic stress measurements were ever made near the Rocky Mountain Arsenal. Healy *et al.*[1968] inferred a least compressive stress of 362 bars at the bottom of the disposal well from the pressure at which the volume rate of injection increased rapidly and estimated a maximum compressive stress to be at least the

overburden pressure of 830 bars. This assumption proved valid when it was demonstrated that the three largest earthquakes exhibited predominantly normal faulting along nodal planes that paralleled the trend of earthquake epicenters [*middle,* Figure A1; Herrmann *et al.*, 1981]. Formation pressure prior to injection was estimated to be 269 bars. From these calculations and using the Mohr–Coulomb failure criterion, a fluid pressure increase of 32 bars was determined to be sufficient to trigger seismic activity along favorably oriented, preexisting fractures [Hsieh and Bredehoeft, 1981; Zoback and Healy, 1984]. The observation that the earthquake locations were confined to those parts of the reservoir where the pressure buildup from injection exceeded the critical threshold, as predicted by the Mohr-Coulomb failure criterion, strongly supports the conclusion that the earthquake activity was related to injection well operations and was consistent with fluid pressures within the reservoir initiating failure along favorably oriented fractures with cohesive strengths of as much as 82 to 100 bars. The continuation of seismicity with time and the outward migration of earthquakes from the well are then explained by the outward propagation of the critical levels of fluid pressure, even after the injection had stopped.

Rangely, Colorado

Waterflooding for the secondary recovery of oil near Rangely, Colorado, began in 1958. Wells were drilled to the producing horizon at a depth of about 2 km. As of June, 1970, 9,700 million liters of water were injected at a top hole pressure of about 83 bars, representing a net increase of 2,300 million liters after accounting for petroleum withdrawal [Gibbs *et al.*, 1973]. In 1962, with the installation of seismographic equipment, earthquakes were found to be occurring within the oilfield. A dense network of stations was then installed in 1969 to accurately determine the earthquake hypocenters and fault plane orientations. Seismic activity was found to be concentrated in a narrow zone about 4 km long and 1.5 km wide, crossing the boundary of the field to the south and east [*top,* Figure A2; Raleigh *et al.*, 1972]. Hypocenters tended to cluster in two groups, one located at depths of 2 to 2.5 km near the wells and within the injection zone, and the other group at depths of 3 to 5 km about 1 to 2 km from the wells. Maximum size of the earthquakes generated was 3.1.

Hydraulic fracture data obtained at the bottom of one of the wells (*top,* Figure A2) indicated values for the maximum compressive stress of 552 bars, vertical stress of 427 bars and least compressive stress of 314 bars. Raleigh *et al.*[1972] combined these hydraulic stress measurements with the locations and fault orientations of the earthquakes, as well as laboratory determined properties of the rock at depth, to calculate that a pore pressure of about 260 bars (or 90 bars above the original formation pressure of 170 bars) would have been sufficient to induce slip using the Mohr–Coulomb failure criterion. This value was consistent with the pressure of 275 bars measured in the oilfield at the time that the induced seismicity began, and corresponded to the critical pore pressure below and above which earthquakes could be turned off and on in a later controlled experiment [*bottom,* Figure A2; Raleigh *et al.*, 1976]. This experiment in earthquake control established the validity of the Mohr–Coulomb failure model in predicting the critical threshold of stress and pore pressure necessary for earthquake occurrence. Each time the pressure in the part of the field where earthquakes had previously appeared exceeded the predicted threshold, more earthquakes began to occur (Figure A2). Earthquake activity declined whenever the fluid pressure fell below the threshold.

Attica–Dale, New York

Solution mining for salt near Dale, New York, triggered a marked increase in microearthquake activity in 1971 (See Figure A3). As many as 80 earthquakes per day were concentrated within 1 km of a 426 m-deep injection well [Figure A4; Fletcher and Sykes, 1977] in an area where the previous record of activity was less than one event per month. All of these earthquakes were small, with estimated magnitudes from -1.0 to 1.0. Top-hole pressure at the injection well typically operated between 52 to 55 bars, or only a few bars less than that calculated to induce sliding on preexisting fractures with no cohesion, based on the Mohr–Coulomb failure criterion and analysis of hydrofracture stress measurements conducted about 100 km from the activity. Seismicity continued in the Dale brine field for as long as elevated pore pressure was maintained (Figure A5). The low level of background activity prior to high pressure injection, the dramatic increase in activity following injection, and the rapid cessation of activity following a decrease in

injection pressure below about 50 bars (Figure A6) strongly suggest this seismicity was induced by injection activities.

Texas oil fields

Permian Basin, West Texas

Cases of induced seismicity associated with fluid injection operations for the secondary recovery of oil and gas have been suggested in several areas in Texas. One of the earliest reports alludes to an increase in seismicity associated with petroleum production and water flooding operations in the Permian basin of West Texas near Kermit [Shurbet, 1969]. A marked increase in earthquakes above magnitude 3 was observed that correlated with a dramatic increase in the number of injection wells operating at pressures greater than 70 bars. This increase in seismicity was of particular interest because of its proximity to a radioactive waste disposal site in southeastern New Mexico [*right,* Figure A7; Rogers and Malkiel, 1979]. About 20 earthquakes (the largest of which was about magnitude 4.4) were recorded between November, 1964 and December, 1976. Eleven stations were then installed to monitor this seismicity and to determine whether in fact the earthquakes were directly related to oil field activities. Between December 12, 1975 to June 26, 1977, 406 earthquakes were detected, most at depths less than 5.0 km and nearly all in areas with active water-flooding operations (*left,* Figure A7). Eight of the local water flooding projects that typically operated at pressures greater than 100 bars are listed in Table A1 [Texas Railroad Commission, 1970; 1984]. The producing horizon for hydrocarbons in the Central Basin Platform ranges from 800 to 3700 m. Measurements of *in situ* stress determined from hydrofracturing indicated a maximum compressive stress of 150 bars and a minimum compressive stress of 85 bars at a depth of 485 m.

Cogdell Oil field, West Texas

The largest earthquake to occur in known association with oil field injection operations was a magnitude 4.6 event near Snyder in June, 1978. This earthquake was part of a sequence of events that had apparently been active since 1974 [Davis, 1985] and was located in the Cogdell Canyon Reef oil field of West Texas. Because of the proximity of

the earthquakes to oil field operations, a small local network of stations was operated from February, 1979 through August, 1981 [Figure A8; Harding, 1981]. As of 1985, a total of about 30 earthquakes have been spatially associated with the Cogdell field (Figure A8), most of which occurred between April, 1977 and August, 1979. Injection operations began near Snyder in the mid-1950's, however, a dramatic increase in numbers of injection wells, volumes of fluid pumped and effective pressures took place in the early 1970's. Injection pressures range from 45 to 185 bars, but typically operate between 95 to 145 bars. These values are sufficient to induce slip on favorably oriented fractures with little or no cohesion as determined by the Mohr–Coulomb failure criterion [Davis, 1985]. Most of the wells that penetrate to the Canyon Reef formation operate at depths between 2070 to 2265 m. These well depths coincide with the shallow focal depths of the earthquakes located within the oil field (on the order of 3 km or less)[Harding, 1981] and are nearly the same as the focal depth determined for the June, 1978 event (3 km)[Voss and Herrmann, 1980].

Atascosa County, South Texas

Seismic activity has also been identified with the *withdrawal* of oil and gas from two fields in south Texas [Pennington *et al.*, 1986]. Production from the Imogene oil and gas field began in 1944. Depth of the producing horizon is 2.4 km. Initial fluid pressure in the field was approximately 246 bars and was reduced to 146 bars by 1973. In the Flashing gas field, production began in 1958 at a depth of 3.4 km. Initial pore pressure in the producing formation was 352 bars, but was reduced to only 71 bars (or 20% of the original value) by 1983. The rapid withdrawal of fluid and gas apparently resulted in subsidence and differential compaction of the producing horizon in both fields. Seismic activity began in 1973, with the largest earthquake (magnitude 3.9) occurring in the Imogene field in March, 1984. In both cases, the sizes and numbers of earthquakes increased with time, consistent with a model for the evolution of the hydrologic characteristics of the field whereby the strength of the rock increases as fluid pressure decreases. Earthquakes are then generated as the formation pore pressure is reduced sufficiently such that further subsidence results in strain accumulation in the newly strengthened rock. If the strains are large enough, the amount of energy accumulated in the rock is sufficient to cause earthquakes as large as

magnitude 3 to 4 [Pennington *et al.*, 1986].

The Geysers, California

In a case similar to Atascosa County, Texas, a large number of small earthquakes ($M_L \leq 4.0$) have been triggered by the reduction in steam pressure caused by energy production in The Geysers geothermal area near Clear Lake in northwestern California [Figure A9; Oppenheimer, 1986]. The Geysers is the site of a vapor-dominated steam field where, by the early 1980's, 150 wells had been drilled to depths between 0.8 and 3.0 km. Earthquake activity has increased in The Geysers area by nearly a factor of two over seismicity levels prior to production, with about 10 microearthquakes greater than magnitude 0.5 typically occurring each day. Evidence that the increased seismicity was induced relied upon the spatial and temporal distribution of the microearthquakes in the vicinity of the producing steam wells. During the period 1975–1981, earthquakes were found to occur in previously aseismic areas within months following the initiation of steam extraction from newly developed regions of the reservoir. Seismic activity also correlated with energy production or rate of steam extraction (Figure A10). Earthquake hypocenters were found to extend from 0 to 6.5 km depth, but earthquakes shallower than 3.5 km typically located within a few hundred meters laterally from the sites of active steam wells [Eberhart-Phillips and Oppenheimer, 1984]. Although some of the extracted steam is condensed and re-injected, the reduction in effective normal stress caused by increased pore pressure is not considered the likely mechanism to explain the induced seismicity. Steam pressure in the field actually declined by about 1 bar/year since 1966 as a result of cooling, and numbers of earthquakes did not correlate with volumes of steam condensate injected into the wells. The two possible mechanisms thought to be responsible for the increased seismicity are: increased shear stresses as a result of volumetric thermal contraction caused by reservoir cooling [Denlinger *et al.*, 1981] and by reservoir subsidence arising from large fluid mass withdrawal [Majer and McEvilly, 1979]; or alternatively, the conversion of continuous aseismic slip into seismic slip (*i.e.*, earthquakes) by an increase in the coefficient of friction following the deposition of exsolved solids (probably silica) onto slipping fracture surfaces [Allis, 1982].

New Mexico

Several hundred microearthquakes were generated during a massive hydraulic fracturing experiment conducted at Fenton Hill, New Mexico in March, 1979. The purpose of the experiment was to stimulate a fracture in a deep (2930 m) injection well so as to intersect an adjacent production well for use in a hot-dry rock geothermal energy project. Hydraulic stimulation involved nearly 460,000 liters of water injected over a $5\frac{1}{2}$ hour period. Maximum top-hole pressure was held constant at 200 bars. During the experiment, microearthquake activity averaged 3 to 4 earthquakes per minute. Formation pore pressure prior to injection was measured to be about 265 bars. Maximum and minimum effective horizontal stresses were found to be 370 and 140 bars, respectively. Using the Mohr–Coulomb failure criterion, Pearson [1981] determined that only 30 bars of increased pore pressure was sufficient to initiate slip on favorably-oriented preexisting joints. Most of the small earthquakes appeared to be localized to within 30 m of the expanding hydraulic fracture. Unfortunately, the stimulated fracture failed to intersect the desired production well. In a subsequent attempt, 7.6 million liters of water was injected at a depth of 3400 m at a rate of 1,600 liters/minute, triggering an additional 850 microearthquakes in the vicinity of the well [House and McFarland, 1985].

Nebraska

With the installation of sensitive monitoring equipment in Nebraska in 1977, a concentration of seismic activity was identified near the Kansas–Nebraska border. Subsequent investigations using portable instruments (from March, 1979, to March, 1980) detected 31 earthquakes in close proximity to the most productive oil field in the state: the Sleepy Hollow oil field [Figure A11; Evans and Steeples, 1987]. Water flooding to enhance recovery had been in operation since 1966. Water injection typically operated at top-hole pressures of 52 bars within the Lansing Group (depths of 1050 to 1170 m) and 22 bars within the Sleepy Hollow sandstone (Reagan) formation (1150 to 1170 m depth)[*top*, Figure A12], corresponding to bottom-hole pressures of 172 and 142 bars, respectively. Most of the well-located earthquakes occurred within the confines of the producing field and at depths less than 2 km [Rothe and Lui, 1983], in an area where well-defined subsurface

faults were present based on structure contour maps (*bottom,* Figure A12). Maximum magnitude of the induced seismicity was 2.9. In a later monitoring program, an additional 250 microearthquakes were detected within the active field between April, 1982 and June, 1984 [*bottom,* Figure A11; Evans and Steeples, 1987], at a time when the average top-hole pressure in the field reached as high as 56 bars.

Southwestern, Ontario

Oil and gas production from the Gobles oil field in southwestern Ontario, about 55 km east-northeast of London, began in 1960 [*top,* Figure A13; Mereu *et al.*, 1986]. Lower than expected formation pressure resulted in water flooding operations to enhance recovery starting in 1969. The producing horizon is 884 m deep. Historically, this area of southwestern Ontario has had a very low level of seismic activity. In December, 1979, a magnitude 2.8 earthquake was detected in the vicinity of the oil field. A portable network of stations has since recorded 478 earthquakes within and around the oil field from July, 1980, through August, 1984 (*bottom,* Figure A13). All the locatable events are shallow and exhibit travel-times consistent with hypocenters at a focal depth coincident with the producing horizon. No spatial correlation with specific wells is identifiable, however, and although earthquake activity varies considerably in time, fluctuations in activity rate do not correlate with injection pressure, which for the most part has remained nearly constant. This area is located just west of the Dale brine field in western New York and just north of possible triggered seismicity in northeastern Ohio (see below).

Matsushiro, Japan

One of the few attempts besides the Rangely Oil field experiment to specifically manipulate earthquake behavior by fluid injection occurred near Matsushiro, Japan. In 1970, 2.9 million liters of water were injected at a depth of 1800 meters using a top hole pressure of 14 to 50 bars and injection rates of 120 to 300 liters/minute [Ohtake, 1974]. During the two month duration of the experiment, several hundred small earthquakes were triggered within 4 km of the well and at depths of 1.5 to 7.5 km. A delay of 5 to 9 days was observed between the onset of increased seismicity and increased injection

pressure. Activity was significantly greater during injection than either before or after the experiment, with most of the induced seismicity localized to the northeast-dipping Matsushiro fault zone, whereas most of the background seismicity was scattered in the hanging wall [Ohtake, 1974]. No attempts were made to determine the *in situ* state of stress or the critical threshold for failure as indicated by the Mohr–Coulomb failure criterion, but the observed time delay for the onset of seismicity and the subsequent migration in depth of the earthquakes was consistent with inferred values of permeability and the time required for pore pressure effects to migrate to the area where the earthquakes were observed.

Other less-well documented or possible cases

Western Alberta, Canada

On March 8, 1970, a magnitude 5.1 earthquake occurred near Snipe lake in western Alberta [Milne, 1970]. No significant earthquakes had previously occurred in the area, and based on the limited felt area and preliminary determinations of focal depth (<9 km), the event appeared to have occurred at relatively shallow depths [Milne, 1976]. At the time of the earthquake, 646 oil and gas wells were in operation within 80 km (50 miles) of Snipe Lake. Production began in 1954, and water injection to maintain field pressure had been in effect in 56 wells since 1963. Although little else is known about this event, since it occurred within the Snipe Lake oil field, where fluid injection was actively taking place, this earthquake is considered the first and largest known Canadian example of an earthquake induced by fluid injection into a producing oil field [Milne, 1976].

Historical seismicity and solution mining in Western New York

Solution salt mining operations have been in operation in the northwest region of New York since the late 19th century [Dunrud and Nevins, 1981]. In 1929, a large (magnitude 5.2) earthquake occurred near Attica, New York, causing significant damage (intensity VIII) in the epicentral region (Figure A3). Subsequent earthquakes in 1966 (magnitude 4.6) and 1967 (magnitude 3.8) also generated relatively high intensities for their size [Herrmann, 1978]. These observations were attributed to the shallow focal depths of the earthquakes (about 2 km) or roughly on the same order as the depth of solution salt mining.

Past investigators have attributed these earthquakes near Attica to tectonic slip along the Clarenden–Linden fault system [Figure A3; *e.g.,* Fletcher and Sykes, 1977], however, their shallow focal depths and proximity to protracted mining operations is suggestive that these earthquakes may also have been triggered by adjacent solution mining operations. Unfortunately, the lack of detailed records of injection activities, or direct measurements of the state of stress in the epicentral region make any definitive correlation between these older historical earthquakes and mining operations difficult. The identification of more recent seismic activity with the Dale brine field [Fletcher and Sykes, 1977], however, suggests that a relationship may have existed between the older historical earthquakes and adjacent solution mining operations.

Historical seismicity and solution mining in Northeastern Ohio

The association of solution mining with the occurrence of small earthquakes in western New York State [Fletcher and Sykes, 1977], and the extensive salt mining operations in northeastern Ohio [Clifford, 1973], suggested the possibility that some of the earthquake activity in Ohio may be related to solution salt mining (Figure A14). Solution mining for salt began in northeastern Ohio in 1889 [Clifford, 1973; Dunrud and Nevins, 1981] and continues to the present, although several previously active operations have been closed down. The target horizon for the mining operations is the Silurian Salina formation at a depth of 600 to 900 m depending on distance from Lake Erie. Based on their spatial proximity and temporal association, it could be argued that several earthquakes in the northeast region of the state could be associated with active solution salt mining operations. In particular, earthquakes in 1898, 1906 and 1907 [Stover *et al.*, 1979] located within the Cleveland metropolitan area, as well as earthquakes in 1932, and 1940, 35 km southeast of Cleveland are possible examples (Figure A14). However, in view of the large number of earthquakes reported prior to the initiation of solution mining, and the apparent occurrence of at least some earthquakes in northeastern Ohio beyond the range of expected influence from mining operations, it seems reasonably clear that at least some of the earthquakes are natural and that solution mining is not a necessary condition for the occurrence of earthquake activity.

Recent seismicity and injection operations in Northeastern Ohio

On January 31, 1986, at 11:46 EST an earthquake of magnitude 5.0 occurred about 40 km east of Cleveland, Ohio, and about 17 km south of the Perry Nuclear Power Plant (Figure A15). Only thirteen aftershocks were detected as of April 15th, with six occurring within the first 8 days. Three deep injection wells are currently operating within 15 km of the epicentral region and have been responsible for the injection of nearly 1.2 billion liters of fluid at a nominal depth of 1.8 km since 1975. Injection pressures at a typical injection rate of 320 liters/min (85 gal/min) have reached a maximum of 112 bars top-hole pressure. Although the distance from the major injection wells to the January 31st earthquake (12 km) is greater than the corresponding distances in either the Denver or Dale earthquakes, the total volume of fluid injected and the pressures involved are proportionately greater. Estimates of stress inferred from commercial hydrofracturing measurements suggest that the state of stress in northeastern Ohio is close to the theoretical threshold for failure along favorably oriented, preexisting fractures, as determined by the Mohr–Coulomb failure criterion. Maximum horizontal compressive stress is greater than the vertical stress of 460 bars, the minimum horizontal stress is about 300 bars, and the initial formation pore pressure is measured to be about 200 bars [Wesson and Nicholson, 1986]. This implies that at a nominal injection pressure of 110 bars, the zone immediately surrounding the well bottom would be in a critical stress state for favorably oriented fractures with cohesive strengths of as much as 40 bars and a friction coefficient of 0.6 (Figure 6). Calculations of the pressure effect in the epicentral region based on modelling the fluid flow away from the wells, and comparison with the history of pressure increase at the wells with time and continued pumping, suggest that a radial flow model (instead of a narrow confined aquifer implicated in the Denver case) is more appropriate, implying a pressure increase near the earthquakes of only a few bars. Several small earthquakes, however, have occurred at shallow depths and within less than 5 km from the wells since 1983 [Figure A15; Nicholson *et al.*, 1987]. The increased depth and distance from the wells to the mainshock epicenter and its aftershocks, the lack of large numbers of small earthquakes typical of many induced sequences, the history of small to moderate earthquakes in the region prior to the initiation of injection, and the attenuation of the

pressure field with distance from the injection wells, all argue for a "natural" origin for the January 31st earthquake. In contrast, the proximity to failure conditions at the bottom of the well and the spatial association of at least a few small events, suggest that triggering by well activities can not be precluded.

Los Angeles Basin, California

Teng *et al.*[1973] report on seismic activity associated with fourteen oil fields operating within the Los Angeles Basin, where water flooding for secondary recovery of hydrocarbons began in 1954. Total fluid injection as of 1970 was 250,000 million liters at depths ranging from 910 to 1520 meters. Earthquakes with depths as deep as 16 km predominantly occur along the Newport–Inglewood fault, which acts as a major structural trap for hydrocarbon deposits. Seismic activity during 1971 appears to correlate, at least in part, with injection volume from nearby wells (Figure A16) [Teng *et al.*, 1973]. However, many of these earthquakes are small (less than magnitude 3.2), and occur at depths of 5 km or greater, making them difficult to distinguish from the natural background seismicity that normally occurs along major right-lateral strike-slip faults in the area. Subsequently, injection operations have stabilized to the point where fluid injection nearly equals fluid withdrawal, and little, if any, seismic activity can be directly attributable to injection well operations [E. Hauksson, personal communication, 1986].

Gulf Coast Region: Louisiana and Mississippi

In 1978, a magnitude 3.5 earthquake was strongly felt in Melvin, Alabama. Portable monitoring equipment was installed shortly after the earthquake, but only one small aftershock was detected. Based on this one event, both earthquakes appeared to be at a depth of about 1 km and with 1–2 km of the Hunt Oil field, located just across the state border in Mississippi [J. Zollweg, personal communication]. Four earthquakes of similar magnitude (3.0-3.6) had previously been detected in the area since 1976. Although no injection procedures were in operation at the time of the earthquake, waterflooding to enhance extraction had previously occurred.

A similar situation was noted in 1983, when a magnitude 3.8 earthquake was detected in southwestern Louisiana near Lake Charles. Oil and gas operations had been active in

the region for several decades, as well as injection activities from a nearby waste disposal well, but lack of station coverage precluded accurate determination of the earthquake's location and focal depth, and so made any direct correlation with particular well operations unresolvable.

APPENDIX B—SUMMARY OF RESERVOIR-INDUCED SEISMICITY

The phenomenon of seismicity induced by the impoundment of reservoirs is more widespread and better documented than that of injection induced seismicity; however, the mechanism of reservoir-induced seismicity is more complicated and less well understood [*c.f.*, Simpson, 1986; Gupta and Rastogi, 1976]. Reservoir-induced earthquakes were first described in association with the filling of Lake Mead, Nevada [Carder, 1945], but it was not until the late 1960's, when earthquakes larger than magnitude 5.5 occurred at four major reservoirs (Hsinfengkiang, China; Kremasta, Greece; Lake Kariba, Rhodesia; and Koyna Reservoir, India), that sufficient concern was raised to warrant investigation of the mechanism controlling reservoir-induced seismicity. The largest of the earthquakes believed to have been induced by the impoundment of a reservoir was a magnitude 6.5 earthquake at Koyna Reservoir in 1967. It caused some 200 deaths, 1500 injuries, and considerable damage to both the nearby town, and the dam itself. Thus, the hazard associated with reservoir-induced seismicity is significant.

Unlike injection operations, which only affect pore pressure, the presence of a large reservoir modifies the environment in several ways. First, the large mass of the reservoir represents a large increase in the imposed load, increasing the *in situ* elastic stresses. The load of water also affects the pore pressure both directly (by the infiltration of the reservoir water and subsequent raising of the water table), and indirectly (through the closure of water-saturated pores and fractures in the rock beneath the reservoir load). This coupling between the elastic and fluid effects in the rock, as well as the poorly understood response of inhomogeneities in material and hydrologic properties of the rock to changes in stress induced by the reservoir load, make modeling of the impact of reservoirs much more difficult than for cases of fluid injection [Simpson, 1986]. Nevertheless, there are a number of similarities between injection-induced and reservoir-induced earthquakes to provide added constraints on the mechanism of triggered seismicity.

Although the magnitude of the net pore pressure change produced by reservoirs may be considerably less than at many fluid injection sites, the larger physical dimensions of reservoirs allows their influence to extend over much broader areas. There are, however, a number of cases of reservoir-induced seismicity in which the load effect from

the reservoir is believed to be minimal. These cases may arguably include some of the largest earthquakes associated with reservoir-impoundment, and are usually characterized by a large distance between the earthquake and the reservoir, as well as a long time interval between impoundment and the earthquake occurrence (*e.g.*, Oroville, Califonia, 1975, $M_S = 5.7$; Aswan, Egypt, 1981, $m_b = 5.3$). If these cases do indeed represent seismicity induced by the reservoir, the triggering mechanism is believed to be similar in many respects to injection-induced seismicity. In many of these cases, the mainshocks occurred along major mapped surface faults that intersected the reservoir. Increases in fluid pressure as a result of impoundment may have been able to migrate out along the fault zones, reducing effective stress levels, and thereby enhancing the probability for failure in an earthquake. Since the changes in pore pressure as a result of impoundment are believed to be relatively small at the increased distances involved in these cases, this suggests that the states of stress in those areas was already near critical levels for failure prior to impoundment [Simpson, 1986].

A particularly good example of reservoir-induced seismicity occurred at the Nurek Reservoir in southcentral Soviet Asia [Figure B1; Simpson and Negmatullaev, 1981]. Here, both the water height and the rate-of-change in water height proved to be critical parameters (Figure B2). The observation that at some sites of reservoir-induced seismicity, like Nurek, changes in water height of only a few meters, corresponding to pressure changes of less than a bar, have triggered swarms of small earthquakes (see Figure B2) suggests that seismicity can be triggered on faults that otherwise remain stable even at stress levels extremely close to failure [Leith and Simpson, 1985]. Accurate assessment of the magnitude of the critical stress change necessary for failure is difficult in many cases of reservoir-induced seismicity because major heterogeneities in elastic and hydrologic properties of the rock may tend to concentrate or amplify changes in pore pressure caused by compaction and the redistribution of pore fluids in response to changes in water level [Simpson, 1986b]. In the case of fluid injection, however, the total mass of the fluid involved is relatively small, and so the need to consider the coupled interaction between applied load, elastic stresses, and pore pressure is absent.

ACKNOWLEDGEMENTS

Preparation of this report was funded by the Office of Drinking Water, U.S. Environmental Protection Agency. Discussions with John Bredehoeft, Evelyn Roeloffs, Keith Evans, David Simpson, and Scott Davis are much appreciated. We thank Pradeep Talwani and Mary Lou Zoback for copies of their papers and figures in advance of publication, and Carl Stover for a timely copy of his latest map on United States seismicity. We appreciate reviews and comments on the manuscript from John Bredehoeft, Bob Hamilton, Bill Leith and Evelyn Roeloffs.

REFERENCES

The following reference materials were assembled and were evaluated for use in the report:

Allis, R.G., Mechanisms of induced seismicity at The Geysers geothermal reservoir, California, *Geophys. Res. Lett., 9,* 629–632, 1982.

Anderson, E.M., *The Dynamics of Faulting and Dyke Formation with Applications to Britain,* 206 pp., Oliver and Boyd, Edinburgh and London, 1951.

Angelier, J., Determination of the mean principal directions of stresses for a given fault population, *Tectonophysics, 56,* T17–T26, 1979.

Bardwell, G.E., Some statistical features of the relationship between Rocky Mountain Arsenal waste disposal and frequency of earthquakes, *Mountain Geologist, 3,* 37–42, 1966.

Bell, J.S., and D.I. Gough, Northeast-southwest compressive stress in Alberta: Evidence from oil wells, *Earth Planet. Sci. Lett., 45,* 475–482, 1979.

Bell, J.S., and D.I. Gough, The use of borehole breakouts in the study of crustal stresses, in *Hydraulic Fracturing Stress Measurements,* 201–209, National Academy Press, Washington, D.C., 1983.

Borcherdt, R.D., ed., Preliminary Report on aftershock sequence for earthquake of January 31, 1986 near Painesville, Ohio (Time Period: 2/1/86-2/10/86), *U.S. Geol. Surv. Open-file Report 86-181,* 109 pp., 1986.

Bredehoeft, J.D., R.G. Wolff, W.S. Keys, and E. Shuter, Hydraulic fracturing to determine the regional in-situ stress field, Piceance Basin, Colorado, *Geol. Soc. Am. Bull., 87,* 250–258, 1976.

Byerlee, J.D., Friction of Rock, *Pure Appl. Geophysics, 116,* 615–626, 1978.

Byerlee, J.D., and W.F. Brace, Fault stability and pore pressure, *Bull. Seismol. Soc. Am., 62,* 657–660, 1972.

Carder, D.S., Seismic investigations in the Boulder Dam area, 1940–1944, and the influence of reservoir loading on earthquake activity, *Bull. Seismol. Soc. Am., 35,* 175–192, 1945.

Carlson, S., Investigations of recent and historical seismicity in East Texas, M.S. Thesis, 197 pp., University of Texas at Austin, Austin, Texas, 1984.

Cleveland Electric Illuminating Company, The Perry Nuclear Power Plant Units I and II, *Final Safety Analysis Report*, North Perry, Ohio, 1982.

Clifford, M.J., Silurian rock salt of Ohio, *Report of Investigations No. 90,* 42 pp., Ohio Department of Natural Resources, Division of Geological Survey, Columbus, Ohio, 1973.

Clifford, M.J., Subsurface liquid-waste injection in Ohio, *Information Circular No. 43,* 27 pp., Ohio Department of Natural Resources, Division of Geological Survey, Columbus, Ohio, 1975.

Coffman, J.L., and C.A. von Hake, (eds.), *Earthquake History of the United States: Revised Edition (Through 1970),* 207 pp., U.S. Department of Commerce Publication 41-1, Washington, D.C., 1973.

Costain, J.K., and G.A. Bollinger, A hydrological model for intraplate seismicity in the southeastern United States (abstract), *Earthquake Notes,56,* 67, 1985.

Costain, J.K., G.A. Bollinger and J.A. Speer, Hydroseismicity: A hypothesis for intraplate seismicity near passive rifted margins (abstract), *Earthquake Notes, 57,* 13, 1986.

Davis, S.D., Investigations of natural and induced seismicity in the Texas panhandle, M.S. Thesis, 230 pp., University of Texas at Austin, Austin, Texas, 1985.

Davis, S.D., and W.D. Pennington, Induced seismic deformation in the Cogdell oilfield of west Texas, *Bull. Seismol. Soc. Am., 77,* preprint, 1987.

Davis, S.N., and R.J.M. DeWiest, *Hydrogeology,* 463 pp., John Wiley and Sons, New York, 1966.

Denlinger, R.P., and C.G. Bufe, Reservoir conditions related to induced seismicity at the Geysers steam reservoir, northern California, *Bull. Seismol. Soc. Am., 72,* 1317–1327, 1982.

Denlinger, R.P., W.F. Isherwood, and R.L. Kovach, Geodetic analysis of reservoir depletion at The Geysers steam field in northern California, *J. Geophys. Res., 86,* 6091–6096, 1981.

Dewey, J.W., and D.W. Gordon, Map showing recomputed hypocenters of earthquakes in the eastern and central United States and adjacent Canada, 1925–1980, 1:2,500,000, *U.S. Geol. Surv. Misc. Field Studies Map MF-1699* 1984.

Dieterich, J.H., C.B. Raleigh, and J.D. Bredehoeft, Earthquake triggering by fluid injection at Rangely, Colorado, in *Percolation Through Fissured Rock,* 12 pp., *Proc. Int. Soc. Rock Mech. and Int. Assoc. Eng. Symp. Paper T2-B,* 1972.

Dumas, D.B., H.J. Dorman, and G.V. Latham, A reevaluation of the August 16, 1931 Texas earthquake, *Bull. Seismol. Soc. Am., 70,* 1171–1180, 1980.

Dunrud, C.R., and B.B. Nevins, Solution mining and subsidence in evaporite rocks in the United States, *U.S. Geol. Surv. Misc. Inf. Map I-1298,* 1981.

Eberhart-Phillips, D., and D.H. Oppenheimer, Induced seismicity in the Geysers Geothermal Area, California, *J. Geophys. Res., 89,* 1191–1207, 1984.

EPA, Compilation of industrial and municipal injection wells in the United States, *U.S. Environ. Protec. Agency EPA-520/9-74-020,* 700 pp., Washington, D.C., 1974.

EPA, Report to Congress on Injection of Hazardous Waste, *U.S. Environ. Protec. Agency EPA-570/9-85-003,* 266 pp., Washington, D.C., 1985.

EPRI, Earthquake Catalog of the United States, 1985.

Evans, D.G., and D.W. Steeples, Microearthquakes near the Sleepy Hollow oilfield, southwestern Nebraska, *Bull. Seismol. Soc. Am., 77,* 132–140, 1987.

Evans, D.M., The Denver area earthquakes and the Rocky Mountain Arsenal disposal well, *Mountain Geologist, 3,* 23–36, 1966.

Evans, D.M., Man-made earthquakes in Denver, *Geotimes, 10,* 11–17, 1966.

Evans, M.A., Fractures in oriented Devonian shale cores from the Appalachian Basin, M.S. Thesis, 278 pp., W. Virginia University, 1979.

Fetter, C.W., Jr., *Applied Hydrogeology,* 488 pp., Charles E. Merrill Publishing Co., Columbus, Ohio, 1980.

Fletcher, J.B., and L.R. Sykes, Earthquakes related to hydraulic mining and natural seismic activity in western New York State, *J. Geophys. Res., 82,* 3767–3780, 1977.

Freeze, R.A., and J.A. Cherry, *Groundwater,* 604 pp., Prentice-Hall, Inc., Englewood Cliffs, N.J., 1979.

Frohlich, C., and D.B. Dumas, The seismicity of the Gulf of Mexico (abstract), *EOS Trans. AGU, 61,* 288, 1980.

Frohlich, C., Seismicity of the central Gulf of Mexico, *Geology, 10,* 103–106, 1982.

GangaRao, H.V.S., S.H. Advani, P. Cheng, S.C. Lee, and C.S. Dean, In-situ stress determination based on fracture responses associated with coring operations, in *Proceedings of the 20th U.S. Symposium on Rock Mechanics,* 683–690, Austin, Texas, 1979.

Gibbs, J.F., J.H. Healy, C.B. Raleigh, and J. Coakley, Seismicity in the Rangely, Colorado, area: 1962–1970, *Bull. Seismol. Soc. Am., 63,* 1557–1570, 1973.

Glassmoyer, G., and R. Borcherdt, Effects of local geology on high-frequency ground motions observed near Painesville, Ohio (abstract), *EOS Trans. AGU,67,* 1092, 1986.

Glassmoyer, G., R. Borcherdt, J. King, C. Dietal, E. Sembera, E. Roeloffs, C. Valdes, and C. Nicholson, Source and propagation characteristics for aftershock sequence near Painesville, Ohio (abstract), *EOS Trans. AGU, 67,* 314, 1986.

Gough, D.I., Induced Seismicity, in *The Assessment and Mitigation of Earthquake Risk,* 91–117, UNESCO, Paris, 1978.

Gough, D.I., and J.S. Bell, Stress orientations from oil-well fractures in Alberta and Texas, *Can. J. Earth Sci., 18,* 638–645, 1981.

Gupta, H.K., and B.K. Rastogi, *Dams and Earthquakes,* 229 pp., Elsevier Scientific Publishing Co., Amsterdam, 1976.

Haimson, B.C., Earthquake stresses at Rangely, Colorado, in *New Horizons in Rock Mechanics: Earthquakes and Other Dynamic Phenomena,* H.R. Hardy and R. Stefanko, eds., *Proc. U.S. Symp. Rock Mechanics, 14,* 680–708, 1972.

Haimson, B.C., Crustal stress in the continental United States as derived from hydrofracturing tests, in *The Earth's Crust,* J.C. Heacock, ed., 575–592, *AGU Geophys. Monograph Ser. 20,* 1977.

Haimson, B.C., Crustal stress in the Michigan Basin, *J. Geophys. Res., 83,* 5857–5863, 1978.

Haimson, B.C., The hydrofracturing stress measuring method and recent field results, *Int. J. Rock Mech. Min. Sci. and Geomech. Abstr., 15,* 167–178, 1978.

Haimson, B.C., and T.W. Doe, State of stress, permeability, and fractures in the Precambrian granite of northern Illinois, *J. Geophys. Res., 88,* 7355–7372, 1983.

Haimson, B.C., and C. Fairhurst, Initiation and extension of hydraulic fractures in rock, *Soc. Petrol. Eng. J., 7,* 310–318, 1967.

Haimson, B.C., and C. Fairhurst, In-situ stress determinations at great depth by means of hydraulic fracturing, in *Proc. 11th U.S. Symp. Rock Mechanics,* 539–584, A.I.M.E., New York, 1970.

Harding, S.T., Induced seismicity in the Cogdell Canyon Reef Oil Field, *U.S. Geol. Surv. Open-file Rep. 81-833,* 547, 1981.

Harding, S.T., D. Carver, R.F. Henrissy, R.L. Dart, and C.J. Langer, The Scurry County, Texas, earthquake series of 1977-1978: Induced seismicity? (abstract), *Earthquake Notes, 49,* 14–15, 1978.

Healy, J.H., W.W. Rubey, D.T. Griggs, and C.B. Raleigh, The Denver earthquakes, *Science, 161,* 1301–1310, 1968.

Herrmann, R.B., A seismological study of two Attica, New York earthquakes, *Bull. Seismol. Soc. Am., 68,* 641–651, 1978.

Herrmann, R.B., Earthquake hazard in the central United States, *U.S. Geol. Surv. Open-file Rep. 86-383,* 641–651, 1986.

Herrmann, R.D., S.-K. Park, and C.Y. Wang, The Denver earthquakes of 1967–1968, *Bull. Seismol. Soc. Am., 71,* 731–745, 1981.

Hickman, S.H., J.H. Healy, and M.D. Zoback, In situ stress, natural fracture distribution, and borehole elongation in the Auburn Geothermal Well, Auburn, New York, *J. Geophys. Res., 90,* 5497–5512, 1985.

Hickman, S.H., and M.D. Zoback, The interpretation of hydraulic fracture pressure-time data for in-situ stress determination, in *Hydraulic Fracturing Stress Measurements,* 44–54, National Academy Press, Washington, D.C., 1983.

House, L.S., and N. McFarland, Locations of microearthquakes induced by hydraulic fracturing at Fenton Hill, New Mexico, in May 1984 (abstract), *Earthquake Notes, 56,* 12, 1985.

Hsieh, P.A., and J.S. Bredehoeft, A reservoir analysis of the Denver earthquakes: A case of induced seismicity, *J. Geophys. Res., 86,* 903–920, 1981.

Hubbert, M.K., and D.G. Willis, Mechanics of hydraulic fracturing, *Trans. AIME Soc. Petrol. Eng., 210,* 153–166, 1957.

Hubbert, M.K., and W.W. Rubey, Role of fluid pressure in overthrust faulting, *Geol. Soc. Am. Bull., 70,* 115–206, 1959.

Jaeger, C.J., and N.G.W. Cook, *Fundamentals of Rock Mechanics,* 593 pp., Methuen, London, 1979.

Keller, G.R., A.M. Rogers, R.J. Lund, and C.D. Orr, A seismicity and seismotectonic study of the Kermit seismic zone, Texas, *U.S. Geol. Surv. Open-file Rep. 81-37,* 1981.

Kisslinger, C., A review of theories of mechanisms of induced seismicity, *Eng. Geol., 10,* 1970.

Knape, B.K., (compiler), Underground Injection Operations in Texas: A classification and assessment of underground injection activities, *Texas Department of Water Resources Report 291,* 1984.

Kulander, B.R., S.L. Dean, and C.C. Barton, Fractographic logging for determination of pre-core and core-induced fractures: Nicholas Combs well No. 7239, Hazard, Kentucky, *U.S. Energy Research and Development Agency MERC /CR/3,* 44 pp., 1977.

Lavin, P.M., D.L. Chaffin, and W.F. Davis, Major lineaments and the Lake Erie-Maryland crustal block, *Tectonics, 1,* 431–440, 1982.

Leith, W., and D.W. Simpson, Seismic domains within the Gissar-Kokshal seismic zone, Soviet Central Asia, *J. Geophys. Res., 91,* 689–700, 1986.

Linder, E.N., and J.A. Halpern, In-Situ stress in North America: A compilation, *Int. J. Rock Mech. Min. Sci. and Geomech. Abstr., 15,* 183–203, 1978.

Lockner, D.A., P.G. Okubo, and J.H. Dieterich, Containment of stick- slip failures on a simulated fault by pore fluid injection, *J. Geophys. Res. Lett., 9,* 801–804, 1982.

Majer, E.L., and T.V. McEvilly, Seismological investigations at The Geysers geothermal field, *Geophysics, 44,* 246–269, 1979.

Martin, J.C., The effect of fluid pressure on effective stresses and induced faulting, *J. Geophys. Res., 80,* 3783–3785, 1975.

McClain, W.C., On earthquakes induced by underground fluid injection, *Oak Ridge National Laboratory Rep. ORNL-TM-3154,* 16 pp., 1970.

McGarr, A., Some constraints on levels of shear stress in the crust from observations and theory, *J. Geophys. Res., 85,* 6231–6238, 1980.

McKenzie, D.P., The relationship between fault plane solutions for earthquakes and the directions of the principal stresses, *Bull. Seismol. Soc. Am., 59,* 591–601, 1969.

Mereu, R.F., J. Brunet, K. Morrissey, B. Price, and A. Yapp, A study of the microearthquakes of the Gobles oilfield area of southwestern Ontario, *Bull. Seismol. Soc. Am., 76,* 1215–1223, 1986.

Michael, A.J., Determination of stress from slip data: Faults and folds, *J. Geophys. Res., 89,* 11517–11576, 1984.

Michael, A.J., Use of focal mechanisms to determine stress: A control study, *J. Geophys. Res., 92,* 357–368, 1987.

Milne, W.G., The Snipe Lake, Alberta earthquake of March 6, 1970, *Can. J. Earth Sci., 7,* 1564–1567, 1970.

Milne, W.G., and M.J. Berry, Induced seismicity in Canada, *Eng. Geol.,10,* 219–226, 1976.

Munson, R.C., Relationship of effect of water flooding of the Rangely Oil Field on seismicity, in *Engineering Seismology: The Works of Man,* W.M. Adams, ed., *Geol. Soc. Am. Eng. Case Hist. 8,* 39–49, 1970.

Musman, S.A., and T. Schmidt, The relationship of intraplate seismicity to continental scale strains (abstract), *EOS Trans. AGU, 67,* 307, 1986.

Nealon, D.J., A hydrological simulation of hazardous waste injection in the Mt. Simon, Ohio, M.S. Thesis, Ohio University, 1982.

Neuzil, C.E., Groundwater flow in low-permeability environments, *Water Resource Res., 22,* 1163–1195, 1986.

Nicholson, C., E. Roeloffs, and R.L. Wesson, The northeastern Ohio earthquake of January 31, 1986: Was it induced?, *EOS Trans. AGU, 68,* 354–355, 1987.

Nottis, G.N., A chronology of events and review of the association of seismicity with well #11 and #12 at the Dale Brine Field, Dale, New York, 19 pp., Geoscience Services, Summit, New Jersey, 1986.

Ohio Environmental Protection Agency, Ohio UIC Permit Application for Class I Injection Well: Perry, Ohio Injection Well #1, Calhio Chemicals, Inc., 1985.

Ohio River Valley Water Sanitation Commission, Evaluation of the Ohio Valley region basal sandstone as a wastewater injection interval, 98 pp., Cincinnati, Ohio, 1976.

Ohio River Valley Water Sanitation Commission, Registry of wells for use in underground injection of wastewater: 1972–1975, 57 pp., Cincinnati, Ohio, 1976.

Ohtake, M., Seismic activity induced by water injection at Matsushiro, Japan, *J. Phys. Earth, 22,* 163–174, 1974.

Oppenheimer, D.H., Extensional tectonics at The Geysers geothermal area, California, *J. Geophys. Res., 91,* 11463–11476, 1986.

Orr, C.D., and G.R. Keller, Keyston Field, Winkler County, Texas: An examination of seismic activity, in-situ stresses, effective stresses, and secondary recovery (abstract), *Earthquake Notes, 52,* 29–30, 1981.

Pearson, C., The relationship between microseismicity and high pore pressures during hydraulic stimulation experiments in low permeability granitic rocks, *J. Geophys. Res., 86,* 7855–7864, 1981.

Pennington, W.D., and S.D. Davis, Changing pore-fluid pressures and the evolution of seismic barriers and asperities in Texas oil and gas fields (abstract), *Earthquake Notes, 56,* 17–18, 1985.

Pennington, W.D., S.D. Davis, S.M. Carlson, J. DuPree, and T.E. Ewing, The evolution of seismic barriers and asperities caused by the depressuring of fault planes in oil and gas fields of south Texas, *Bull. Seismol. Soc. Am., 76,* 939–948, 1986.

Plumb, R.A., and J.W. Cox, Deep crustal stress directions in eastern North America determined from borehole elongation, *J. Geophys. Res.,* in press, 1987.

Plumb, R.A., and S.H. Hickman, Stress-induced borehole elongation: A comparison between the four-arm dipmeter and borehole televiewer in the Auburn geothermal well, *J. Geophys. Res., 90,* 5513–5521, 1985.

Raleigh, C.B., J.H. Healy, and J.D. Bredehoeft, Faulting and crustal stresses at Rangely, Colorado, in *Flow and Fracture of Rocks,* 275–284, *AGU Geophys. Monograph Ser. 16,* 1972.

Raleigh, C.B., J.H. Healy, and J.D. Bredehoeft, An experiment in earthquake control at Rangely, Colorado, *Science, 191,* 1230–1237, 1976.

Rogers, A.M., and A. Malkiel, A study of earthquakes in the Permian Basin of Texas-New Mexico, *Bull. Seismol. Soc. Am., 69,* 843–865, 1979.

Rondout Assoc. Inc., Tectonic framework and seismic source zones of the Eastern United States, A Report Prepared for the Electric Power Research Institute/Seismicity Owners Group, 1985.

Rothe, G.H., and C.-Y. Lui, Possibility of induced seismicity in the vicinity of the Sleepy Hollow Oil Field, southwestern Nebraska, *Bull. Seismol. Soc. Am., 73,* 1357–1367, 1983.

Sanford, A.D., and T.R. Toppozada, Seismicity of proposed radioactive waste disposal site in southeastern New Mexico, *New Mexico Bur. Mines and Min. Res. Circ. 143,* 15 pp., 1974.

Sanford, A.D., S. Sanford, T.A. Wallace, L. Barrows, J. Sheldon, R.M. Ward, S. Johansen, and L. Merritt, Seismicity in the area of the Waste Isolation Pilot Plant (WIPP), *Sandia Laboratories Rep. SAND 80-7096,* 1980.

Sbar, M.L., and L.R. Sykes, Contemporary compressive stress and seismicity in eastern North America: An example of intra-plate tectonics, *Geol. Soc. Am. Bull., 84,* 1861–1882, 1973.

Segall, P., Stress and subsidence resulting from subsurface fluid withdrawal in the epicentral region of the 1983 Coalinga earthquake, *J. Geophys. Res., 90,* 6801–6816, 1985.

Stover, C.W., B.G. Reagor, and S.T. Algermissen, Seismicity map of the state of Ohio, *U.S. Geol. Surv. Misc. Field Studies Map MF-1142,* 1979.

Stover, C., Seismicity map of the conterminous United States and adjacent areas: 1974–1984, *U.S. Geol. Surv. Geophys. Investigation Map GP-984,* 1986.

Shurbet, D.H., Induced seismicity in Texas, *Texas J. Sci., 21,* 37–41, 1969.

Simpson, D.W., Seismicity changes associated with reservoir impounding, *Eng. Geol., 10,* 371–385, 1976.

Simpson, D.W., Triggered Earthquakes, *Ann. Rev. Earth Sci., 14,* 21–42, 1986.

Simpson, D.W., Reservoir-induced earthquakes and the hydraulic properties of the shallow crust (abstract), *EOS Trans. AGU, 67,* 242, 1986.

Simpson, D.W., and S.Kh. Negmatullaev, Induced seismicity at the Nurek reservoir, Tadjikistan, U.S.S.R., *Bull. Seismol. Soc. Amer., 71,* 1561–1586, 1981.

Snow, D.T., Hydrogeology of induced seismicity and tectonism: case histories of Kariba and Koyna, *Geol. Soc. Am. Spec. Paper, 189,* 3117–3360, 1982.

Steeples, D.W., Induced seismicity in the Sleepy Hollow Oil Field, Red Willow County, Nebraska, *U.S. Geol. Surv. Open-File Rep. 85-464,* 429–432, 1985.

Talwani, P. and S. Acree, Deep well injection at the Calhio Wells and the Leroy, Ohio earthquake of January 31, 1986, *A Report to the Cleveland Electric Illuminating Co.,* 92 pp., North Perry, Ohio, 1986.

Teng, T.L., C.R. Real, and T.L. Henyey, Microearthquakes and water flooding in Los Angeles, *Bull. Seismol. Soc. Am., 63,* 859–875, 1973.

Terashima, T., Survey on induced seismicity at Mishraq area in Iraq, *J. Phys. Earth, 29,* 371–375, 1981.

Texas Railroad Commission, A Survey of Secondary Recovery and Pressure Maintenance Operations in Texas to 1970, 650 pp., *Bulletin 70,* Austin, Texas, 1971.

Texas Railroad Commission, A Survey of Secondary Recovery and Pressure Maintenance Operations in Texas to 1984, 650 pp., *Bulletin 84,* Austin, Texas, 1985.

Thatcher, W., and T.C. Hanks, Source parameters of southern California earthquakes, *J. Geophys. Res., 78,* 3821–3845, 1973.

van Poollen, H.K., and D.B. Hoover, Waste disposal and earthquakes at the Rocky Mountain Arsenal, Derby, Colorado, *J. Petrol. Tech., 22,* 983–993, 1970.

Voss, J.A., and R.B. Herrmann, A surface wave study of the June 16, 1978 Texas earthquake, *Earthquake Notes, 51,* 3–14, 1980.

Walker, W.R., and W.E. Cox, Deep Well Injection of Industrial Wastes: Government controls and legal constraints, 163 pp., Virginia Water Resources Research Center, 1976.

Warner, D.L., Survey of Industrial Waste Injection Wells, 3 vols., *U.S. Geol. Surv. Final Technical Report,* 1972.

Wesson, R.L., and C. Nicholson, (eds.), Studies of the January 31, 1986 northeastern Ohio earthquake: A Report to the U.S. Nuclear Regulatory Commission, 109 pp., *U.S. Geol. Surv. Open-file Rep. 86-331,* 1986.

Weston Geophysical Corporation, Investigations of confirmatory seismological and geological issues: Northeastern Ohio earthquake of January 31,1986, *A Report to the Cleveland Electric Illuminating Co.,* 233 pp., North Perry, Ohio, 1986.

Wong, I.G., J.R. Humphrey, W. Silva, D.A. Gahr, and J. Huizingh, A case of microseismicity induced by solution mining, southeastern Utah (abstract), *Earthquake Notes, 56,* 18, 1985.

Zoback, M.D., and J.H. Healy, Friction, faulting and "in situ" stress, *Annales Geophysicae, 2,* 689–698, 1984.

Zoback, M.D., and S. Hickman, In situ study of the physical mechanisms controlling induced seismicity at Monticello Reservoir, South Carolina, *J. Geophys. Res., 87,* 6959–6974, 1982.

Zoback, M.D., and M.L. Zoback, State of stress and intraplate earthquakes in the United States, *Science, 213,* 96–104, 1981.

Zoback, M.L., and M.D. Zoback, State of stress in the conterminous United States, *J. Geophys. Res., 85,* 6113–6156, 1980.

Zoback, M.L., and M.D. Zoback, Tectonic stress field of the continental United States, *Geol. Soc. Am. Memoir,* in press, 1987.

Table 1. Well-documented cases of injection-induced seismicity.

Well or Oil Field	Type	Depth m	Injection Pressure bars	Maximum Earthquake Magnitude	Year Injection Began-Ended	Year of Earthquakes
Cogdell, TX	secondary recovery	2071	199	4.6	1956-	1974-1979
Dale, NY	solution mining	426	55	1.0	1971	1971
Denver, CO (RMA)	waste disposal	3671	76	5.5	1962-1966	1962-1967
Fenton Hill, NM	geothermal/stimulation	2700	200	<1.0	1979	1979
The Geysers, CA	geothermal	3000		4.0	1966-	1975-
Matsushiro, Japan	research	1800	50	2.8	1970	1970
Perry, OH (Calhio)	waste disposal	1810	114	2.7?	1975-	1983-1987
Rangely, CO	secondary recovery/research	1900	83	3.1	1958-	1962-1975
Gobles Field, Ontario	secondary recovery	884		2.8	1969-	1979-1984
Sleepy Hollow, NE	secondary recovery	1150	56	2.9	1966-	1977-1984
Snipe Lake, Alberta	secondary recovery			5.1	1963-	1970
Permian Basin Fields				4.4		1964-1977
Dollarhide, TX	secondary recovery	2590	138	~3.5	1959-	"
Dora Roberts, TX	secondary recovery	3661	431	~3.0	1961-	"
Kermit Field, TX	secondary recovery	884	106	~4.0	1964-	"
Keystone I Field, TX	secondary recovery	975	103	~3.5	1957-	"
Keystone II Field, TX	secondary recovery	2987	176	~3.5	1962-	"
Monahans, TX	secondary recovery	2530	207	~3.0	1965-	"
Ward-Estes Field, TX	secondary recovery	914	117	~3.5	1961-	"
Ward-South Field, TX	secondary recovery	741	138	~3.0	1960-	"

Table A1. Injection wells with adjacent seismicity

Well or Oil Field	Depth m	Thickness m	K md	Porosity %	THP bars	BHP bars	Fm Pres bars	Sh bars	SH bars	Sv bars	Max Mag	Year of Earthquakes
Cogdell, TX	2071	43	18-30	7	199	406				476	4.6	1974-1979
Dale, NY	426	16			55	98		76	>109	109	1.0	1929?,1966?,1971
Denver, CO (RMA)	3671		0.03	2	76	415	269	362	<830	830	5.5	1962-1967
East Texas, TX	1113	3	200	25	103	214	70			256	~3.5	1957
Fenton Hill, NM	2700		0.01		200	493	265	405	<635	635	<1.0	1979
Flashing Field, TX	3400	50	13	15	* * *	71	352			768	3.4	1973-1983
The Geysers, CA	3000		<0.05	3			<35	245	785	785	4.0	1975-
Hunt Field, MS											3.6	1976-1978
Imogene Field, TX	2400	33	14	17	* * *	146	246			542	3.9	1973-1984
Lake Charles, LA	1411	49			93	234			<325	325	3.8	1983
Matsushiro, Japan	1800				50	230				460	2.8	1970
Perry, OH (Calhio)	1810	88	6	8	114	294	200	320	>460	460	2.7?	1983-1987
Rangely, CO	1900	350	1	12	83	275	170	314	552	427	3.1	1962-1975
Gobles Field, Ontario	884	9					45			225	2.8	1979-1984
Sleepy Hollow, NE	1150	100	26		56	171	115		<265	265	2.9	1977-1984
Snipe Lake, Alberta											5.1	1970
Permian Basin Fields											4.4	1964-1977
Dollarhide, TX	2590	59	9	6	138	397	179			596	~3.5	"
Dora Roberts, TX	3661		1	7	431	797	324			842	~3.0	"
Kermit Field, TX	884	8	10	18	106	194	35			203	~4.0	"
Keystone I Field, TX	975	11	21	20	103	200	90			224	~3.5	"
Keystone II Field, TX	2987	101	7	3	176	475	204			687	~3.5	"
Monahans, TX	2530	12	6	4	207	460	131			582	~3.0	"
Ward-Estes Field, TX	914		35	16	117	208	103			210	~3.5	"
Ward-South Field, TX	741	5	30	21	138	212	76			170	~3.0	"

FIGURE CAPTIONS

Figure 1. Earthquakes in the continental United States (1975-84) [from Stover, 1986] and sites of earthquakes associated with deep well injection. Double-bordered open symbols represent sites of well-documented cases of injection-induced seismicity; single-bordered sites are less-well established.

Figure 2. Epicentral distribution of earthquakes near the Rocky Mountain Arsenal well during January–February, 1966 [from Healy *et al.*, 1968].

Figure 3. Correlation between seismic activity and volume of injected fluid at the Rocky Mountain Arsenal well [from Evans, 1966].

Figure 4. Maximum shear stress (τ) as a function of effective normal stress (σ_n) for a variety of rock types [after Byerlee, 1978]. The data suggest that the coefficient of friction (μ) ranges between 0.6 and 1.0.

Figure 5. (*a*) Coulomb's law for failure in dry rock, showing the relationship between the shear stress (τ) required for failure and the normal stress (σ_n) across the plane. Here τ_0 is the cohesion and μ is the coefficient of friction. (*b*) The Mohr circle diagram, which provides a graphical method by which the principal (compressive) stresses can be resolved into shear (τ) and normal (σ_n) components on a plane at angle α to the σ_3 direction. (*c*) The Mohr–Coulomb failure criterion. Given a maximum (σ_1) and minimum (σ_3) principal stresses, failure will occur on a plane containing the intermediate stress (σ_2) and at an angle α to σ_3 if the circle containing points σ_1 and σ_3 intersects the failure curve defined in (*a*).

Figure 6. Mohr circle diagram showing state of stress at a nominal depth of about 1.8 km near the bottom of an injection well near Perry, Ohio (see Table 1).

Figure 7. (*a*) Map of maximum horizontal stress directions based on borehole measurements: borehole elongation data (dots); hydraulic fracture data (squares); and overcoring measurements (circled dots). (*b*) Map showing the strike of centerline fractures observed in Eastern Gas Shales Project cores. ENE trending centerline fractures found throughout the Appalachian Basin correlate with contemporary stress directions shown in

(*a*). (*c*) Diagram showing the relationship between various indicators of stress direction observed in wells from the Appalachian Basin [all three parts from Plumb and Cox, 1987].

Figure 8. Surface pressure and flow *versus* time records during an hydraulic fracture stress measurement made at a depth of 185 m in the Limekiln C well, drilled 4 km from the San Andreas fault in central California [from Hickman and Zoback, 1983]. The breakdown, fracture opening, and instantaneous shut-in surface pressures (ISIP) are indicated.

Figure 9. (*top*) Pressure *versus* time records showing differences between the initial cycle in which the fracture occurs (breakdown) and subsequent cycles that reopen (fracture opening pressure) and possibly extend the previously formed crack. (*bottom*) Multiple pumping cycles showing the decrease in fracture opening pressure with each cycle [from Hickman and Zoback, 1983].

Figure 10. Surface pressure and flow records illustrating the three different types of hydraulic fracture pressure-time histories. These examples are taken from wells drilled near the San Andreas fault in southern California. These 3 types are defined by the relative magnitudes of the breakdown and fracture opening pressures and the minimum horizontal principal stress, S_h. The calculated magnitude of the vertical stress, S_v, is shown for comparison [from Hickman and Zoback, 1983].

Figure 11. Map of maximum horizontal compressive stress orientations throughout the conterminous United States [Zoback and Zoback, 1987]. Solid lines define physiographic provinces typically exhibiting nearly uniform stress fields.

Figure 12. Generalized stress map for the conterminous United States [Zoback and Zoback, 1987]. Outward-pointing arrows are given for areas characterized by extensional deformation (*i.e.*, normal faulting); inward-pointing arrows are shown for regions dominated by compressional tectonism (thrust and strike-slip faulting). Horizontal stress provinces are delineated by the thick dashed lines: CC–Cascade convergent province; PNW–Pacific Northwest; SA–San Andreas province; and CP–Colorado Plateau interior.

Figure 13. Injection pressure *versus* time as calculated using the expressions in the text for: a) radial flow; b) an infinite strip 1 km wide; and c) an infinite strip 7.5 km wide

[from Wesson and Nicholson, 1986].

Figure 14. Pressure *versus* distance for injection into a confined reservoir of infinite extent [from Wesson and Nicholson, 1986]. Time intervals are 5, 10, 15, and 20 years.

Figure 15. Pressure *versus* distance at 5 year intervals along the axis of an infinite strip reservoir 7.5 km wide [from Wesson and Nicholson, 1986].

Figure 16. Pressure *versus* distance at 5 year intervals along the axis of an infinite strip reservoir 1 km wide [from Wesson and Nicholson, 1986].

Figure 17. Example of the relationship between magnitude and fault length [from Thatcher and Hanks, 1973].

Figure 18. Example of a seismogram recorded for a earthquake with magnitude about 0.5 located at a depth of about 2 km near the bottom of an injection well in northeastern Ohio [from Wesson and Nicholson, 1986].

Figure A1. (*top*) Locations of earthquakes near Denver, Colorado, associated with the fluid-injection well at the Rocky Mountain Arsenal [after Healy *et al.*, 1968]. (*middle*) Surface wave focal mechanism solutions of the three largest Denver earthquakes [after Herrmann *et al.*, 1981]. (*bottom*) Numbers of earthquakes per month and average monthly injection pressure at the bottom of the arsenal well [Healy *et al.*, 1968].

Figure A2. (*top*) Local map of the Rangely Oil field showing approximate boundary of the field (dashed lines), reservoir pressure contours (solid lines), seismicity (hatchured region) and the location of the well used for hydrofracture stress measurements (solid square). (*bottom*) Seismicity correlated with monthly reservoir pressure at Rangely Oil field. Shaded bars in bottom figure represent events located within 1 km of the active injection well [after Raleigh *et al.*, 1976].

Figure A3. Map showing the location of the Dale brine field (box) in western New York. Clarendon–Linden fault is the heavy dashed line; lesser secondary faults are lighter dashed lines. Stars represent epicenters of large historical earthquakes near Attica [from Nottis, 1986].

Figure A4. Epicenters of earthquakes (solid circles) near the Dale brine field in October and November, 1971. Monitoring stations are squares; injection wells are triangles. Epicenters with poor resolution are shown as open circles [from Fletcher and Sykes, 1977].

Figure A5. Numbers of earthquakes and pumping pressures in the Dale brine field with time. (*a*) Note the abrupt cessation of activity after pumping was shut down on November 9 and the fact that top-hole injection pressures were typically greater than 50 bars. (*b*) Similar plot to (*a*) but for a period when the maximum injection pressure did not exceed about 40 bars [from Fletcher and Sykes, 1977].

Figure A6. Enhanced section of Figure A5*a* showing the rapid decrease in seismicity with a decrease in pressure below about 50 bars.

Figure A7. Seismicity located in the Central Basin Platform of the Permian Basin, west Texas, since 1976. (*left*) Earthquake epicenters and outlines of oil fields with active water-flooding operations; (*right*) Epicenters and known pre-Permian basement faults [after Rogers and Malkiel, 1979].

Figure A8. Earthquake epicenters in the Cogdell oil field near Snyder, Texas [from Harding, 1981].

Figure A9. Seismicity and fault map of The Geysers geothermal area, California (box), and surrounding region [from Oppenheimer, 1986].

Figure A10. Yearly net mass of water withdrawn (*left*) and monthly power generated (*right*) as compared with numbers and moments of earthquakes [from Oppenheimer, 1986].

Figure A11. (*top*) Location of the Sleepy Hollow, Nebraska, oil field and seismic monitoring stations (triangles). (*bottom*) Earthquake epicenters in the vicinity of the field between April, 1982, and June, 1984 [Evans and Steeples, 1987].

Figure A12. (*top*) Average monthly pressures in the two reservoirs used for injection in the Sleepy Hollow oil field, and the number of earthquakes per month. Ten injection wells were added in May and June, 1983. (*bottom*) Mapped faults in the Precambrian basement in the vicinity of the Sleepy Hollow oil field [after Rothe and Lui, 1983].

Figure A13. (*top*) Location map of the Gobles oil field in Southwestern Ontario, Canada. (*bottom*) Epicenter map of earthquakes in the vicinity of the Gobles field [Mereu *et al.*, 1986].

Figure A14. Map of northeastern Ohio showing the location of the Perry Nuclear Power Plant (PNPP), the January 31 earthquake (large square), and significant historical seismicity (open symbols scaled according to intensity). Solid circles identify sites of solution salt mining, typically in operation from 1900–1940; solid triangles are deep waste injection wells drilled in 1968 to 1971. Most of the seismicity precedes initiation of injection activities. Diamonds are poorly located earthquakes, typically based on felt reports; squares are instrumentally located earthquakes. Modified from Stover *et al.*[1979]. Recent regional earthquakes ($M \geq 4.5$) are shown in inset.

Figure A15. (*top*) Location of deep injection wells and earthquake epicenters in Lake County, Ohio, through early 1987. Large uncertainties in location are associated with both the 1943 and 1983 earthquake epicenters. Local quarry blasts are shown as crosses. CH#1 and CH#2 are the deep waste disposal wells, SALT is the Painesville brine well. (*bottom*) Vertical cross section, no exaggeration, along the line A–A' shown in above [Nicholson *et al.*, 1987].

Figure A16. Seismicity and volumes of fluid injected along the Newport–Inglewood fault, Los Angeles County, California [Teng *et al.*, 1973].

Figure B1. (*left*) Location map of the Nurek Reservoir in southcentral Soviet Asia. (*right*) Historical seismicity in the vicinity of the dam [Simpson and Negmatullaev, 1981].

Figure B2. Seismicity and water height with time at the Nurek Reservoir, Tadjikistan, Soviet Central Asia [Simpson and Negmatullaev, 1981].

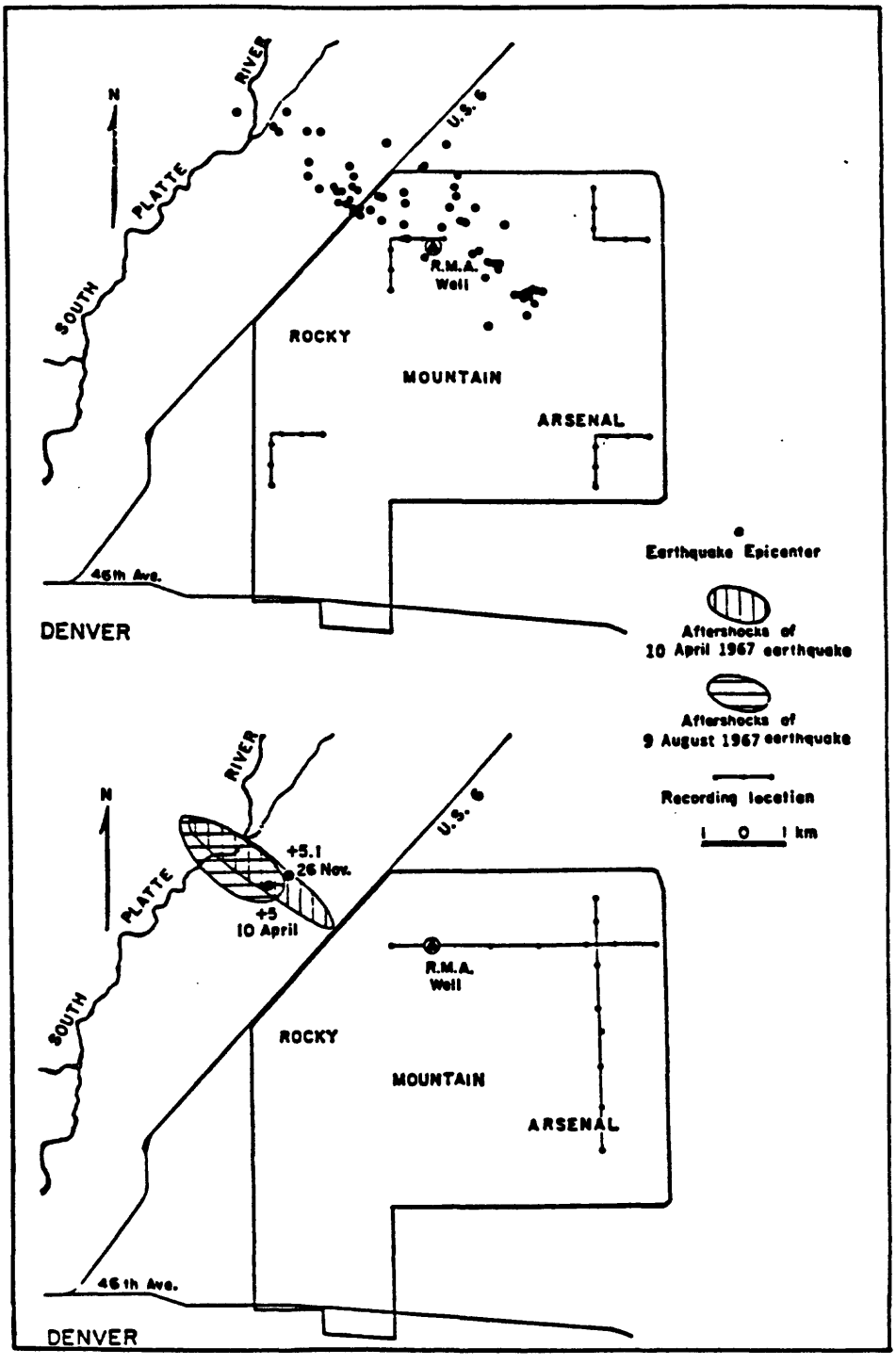

(From Healy et al., 1968)

FIGURE 2 Epicentral area surrounding the Rocky Mt. Arsenal during January-February 1966.

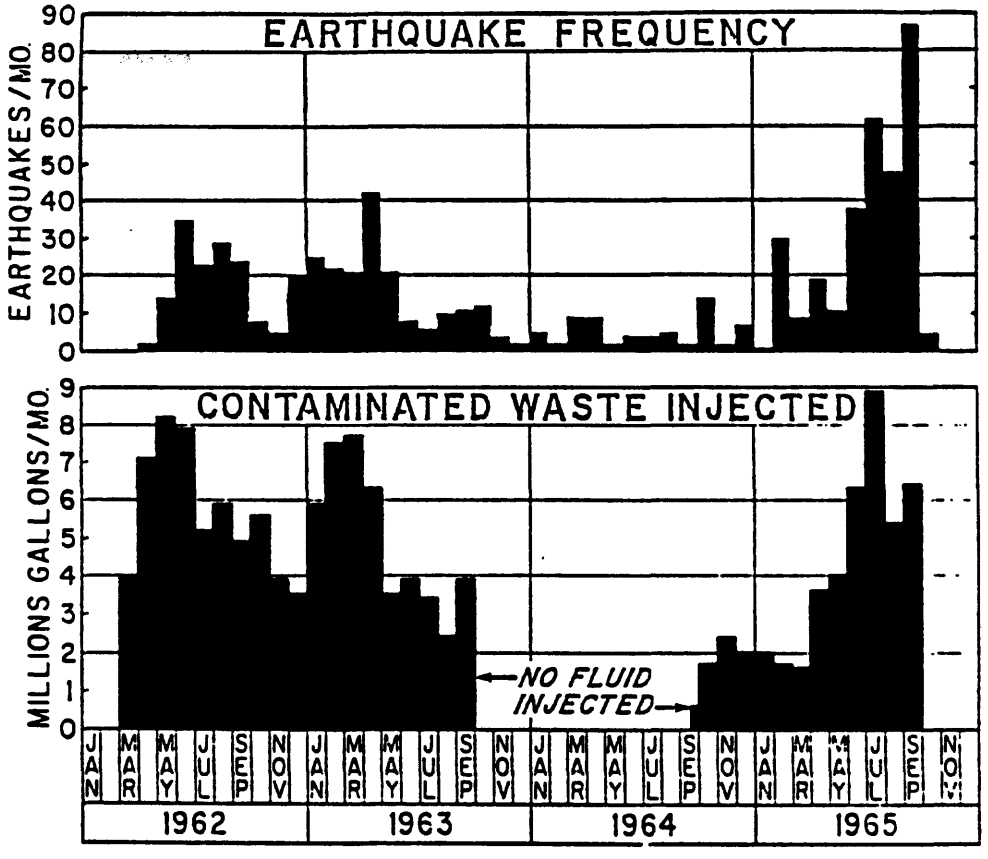

(From Evans, 1966)

FIGURE 3 Correlation between seismic activity and volume of injected fluid at the Rocky Mt. Arsenal well.

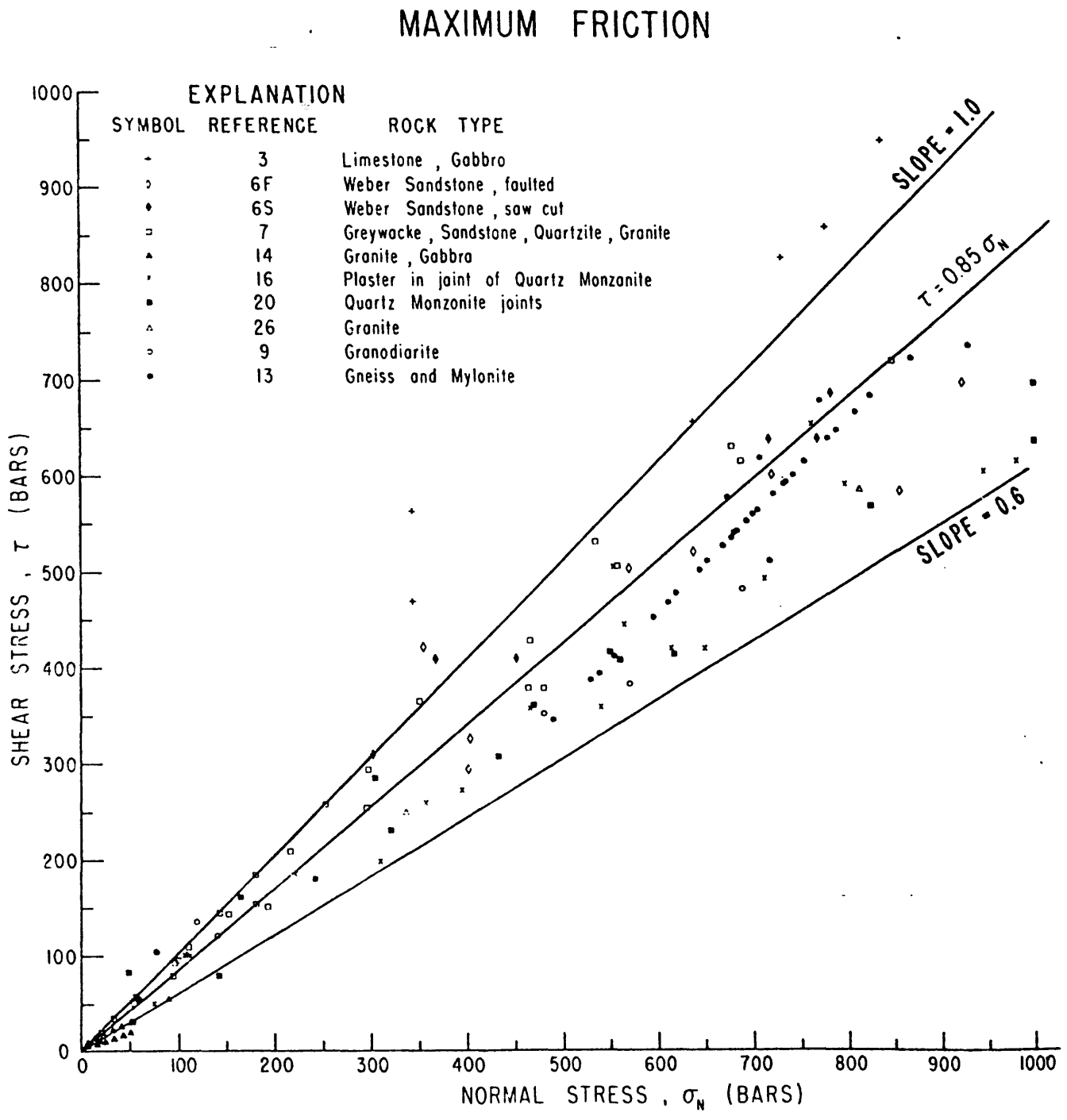
MAXIMUM FRICTION
EXPLANATION
SYMBOL REFERENCE ROCK TYPE
3 Limestone , Gabbro
6F Weber Sandstone , faulted
6S Weber Sandstone , saw cut
7 Greywacke , Sandstone , Quartzite , Granite
14 Granite , Gabbro
16 Plaster in joint of Quartz Monzonite
20 Quartz Monzonite joints
26 Granite
9 Granodiarite
13 Gneiss and Mylonite
SLOPE = 1.0
τ = 0.85 σN
SLOPE = 0.6
SHEAR STRESS , τ (BARS)
NORMAL STRESS , σN (BARS)
0
100
200
300
400
500
600
700
800
900
1000

FIGURE 4

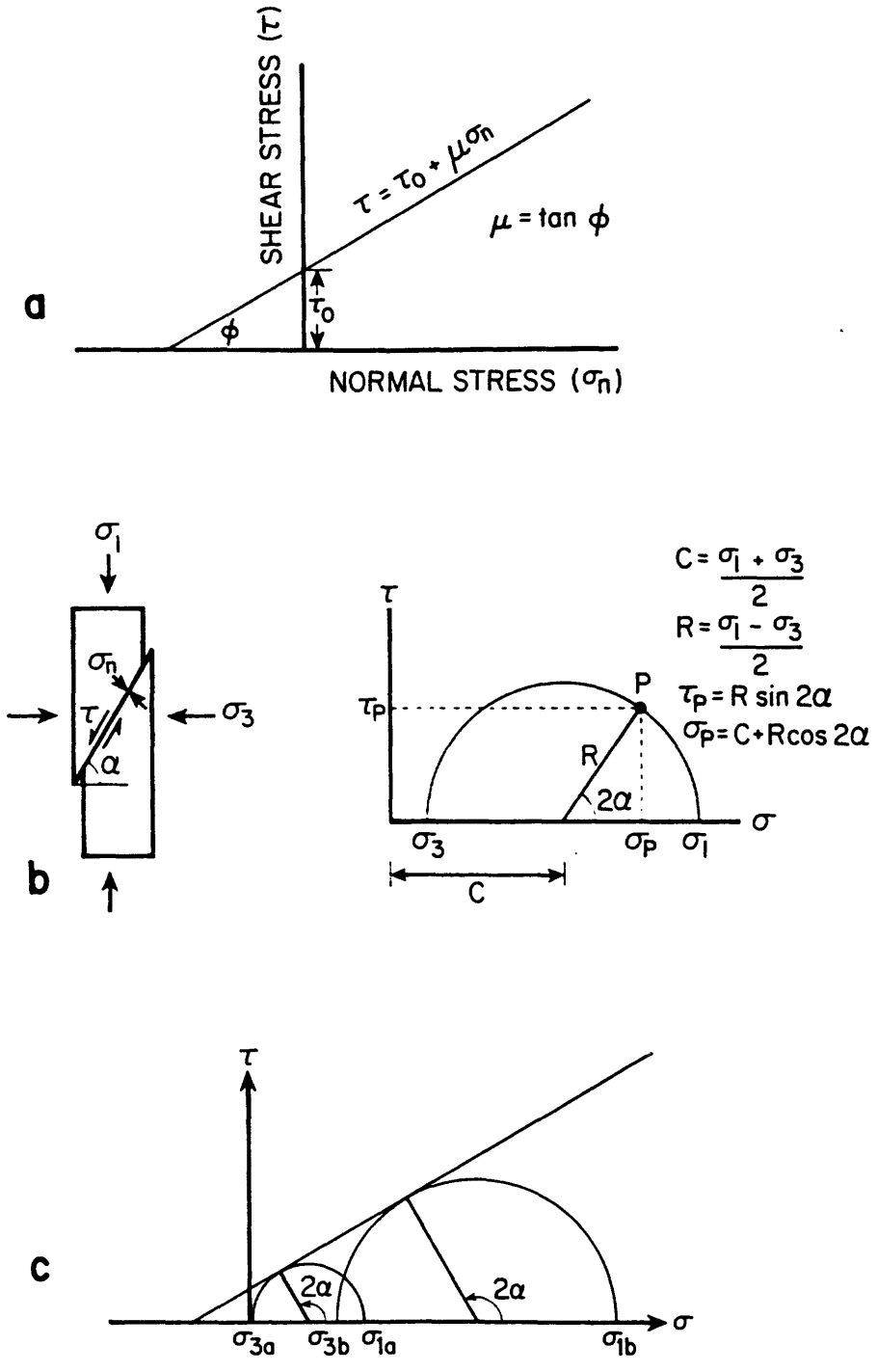

FIGURE 5 (*a*) Coulomb's law for failure in dry rock, showing the relationship between the shear stress (τ) required for failure and the normal stress σ_n across the plane. Here τ_0 is the cohesion and μ is the coefficient of friction. (*b*) The Mohr circle diagram, which provides a graphical method by which the principal (compressive) stresses (σ_i) can be resolved into shear (τ) and normal (σ_n) components on a plane at angle α to the σ_3 direction. (*c*) The Mohr-Coulomb failure criterion. Given maximum (σ_1) and minimum (σ_3) principal stresses, failure will occur on a plane containing the intermediate stress (σ_2) and at an angle α to σ_3 if the circle containing points σ_1 and σ_3 intersects the failure curve defined in (*a*).

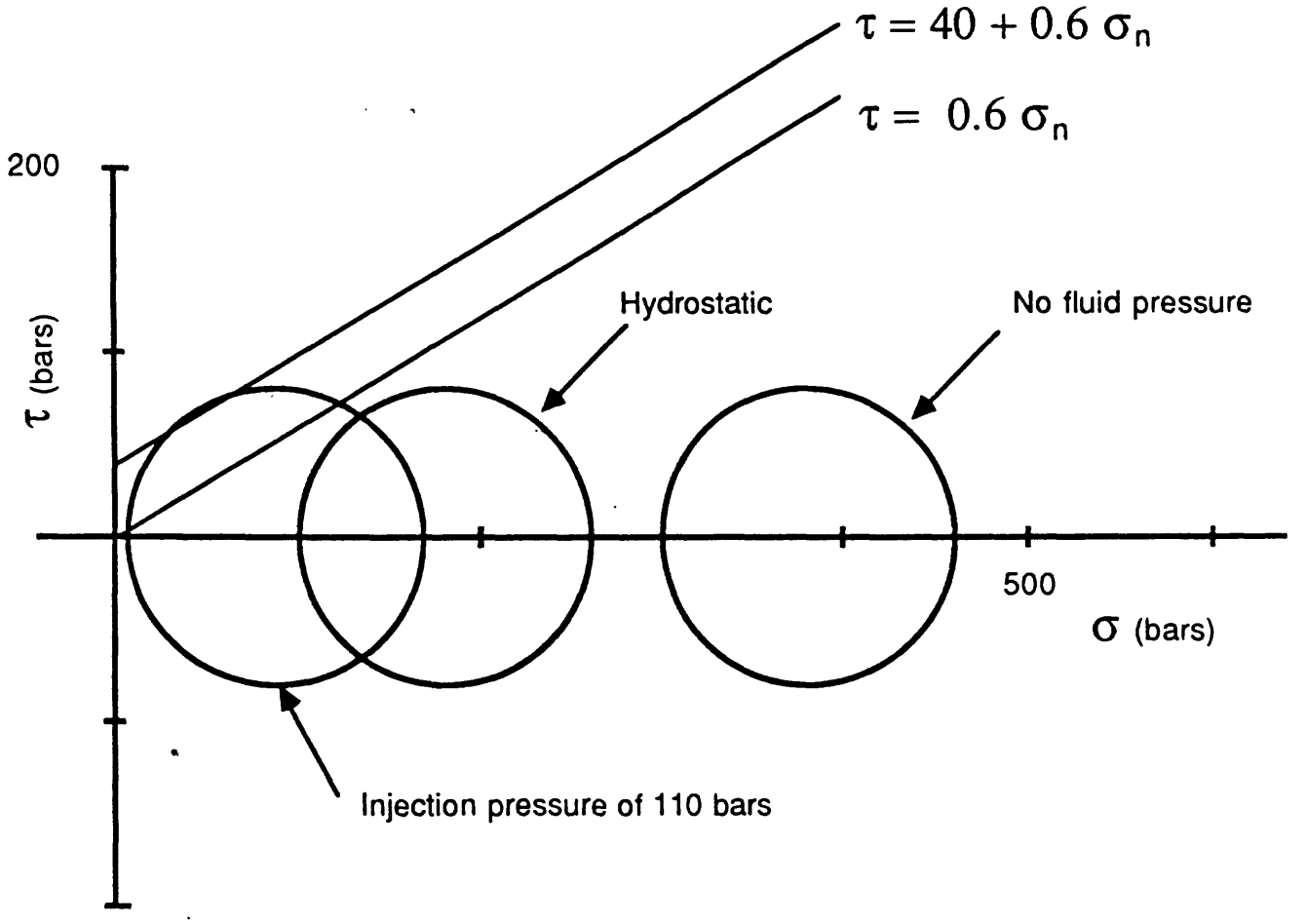
$\tau = 40 + 0.6\ \sigma_n$
$\tau = 0.6\ \sigma_n$
200
τ (bars)
Hydrostatic
No fluid pressure
500
σ (bars)
Injection pressure of 110 bars

FIGURE 6

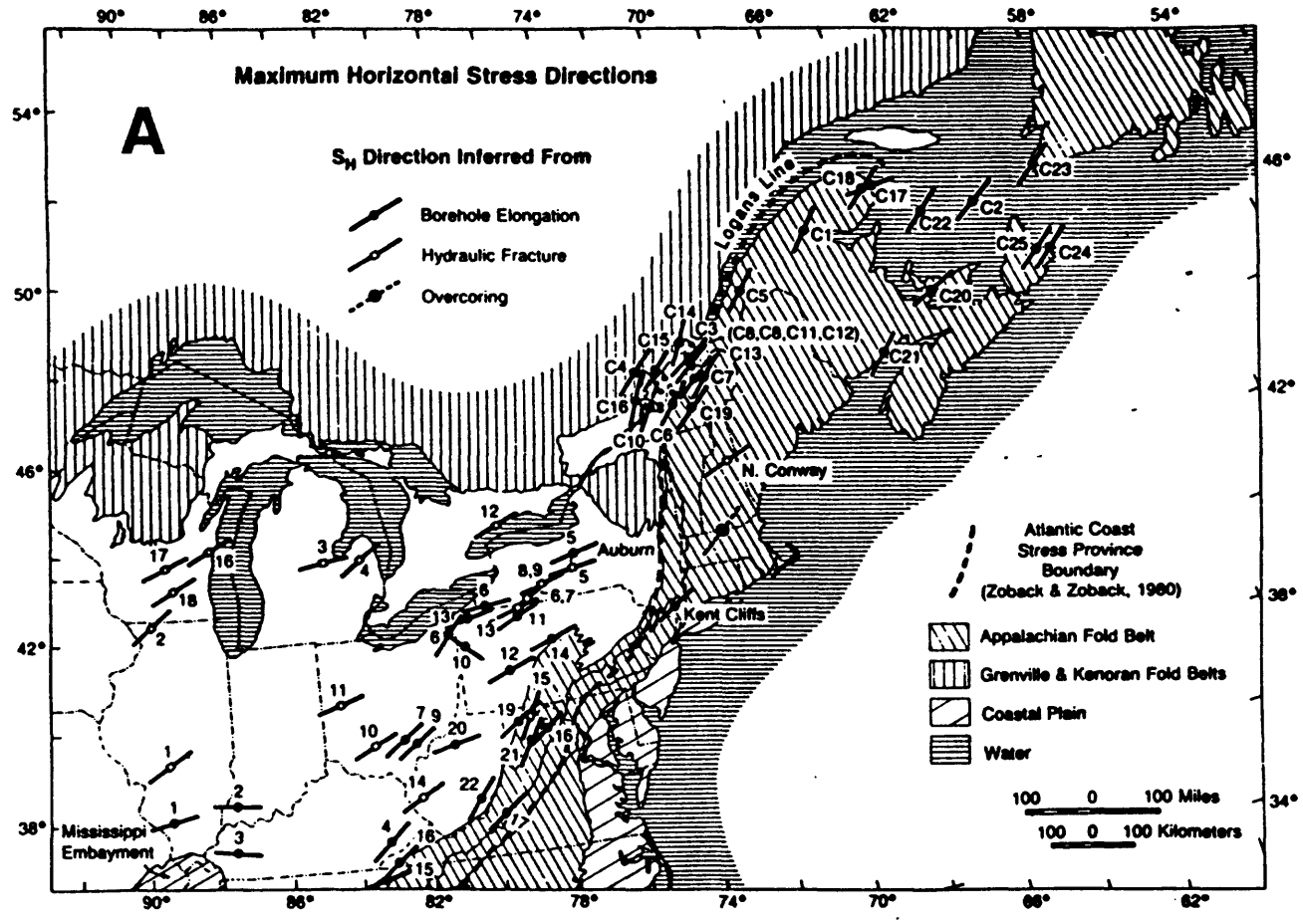
A
Maximum Horizontal Stress Directions
S_H Direction Inferred From
Borehole Elongation
Hydraulic Fracture
Overcoring
Logans Line
N. Conway
Auburn
Kent Cliffs
Mississippi Embayment
Atlantic Coast Stress Province Boundary (Zoback & Zoback, 1980)
Appalachian Fold Belt
Grenville & Kenoran Fold Belts
Coastal Plain
Water
100 0 100 Miles
100 0 100 Kilometers

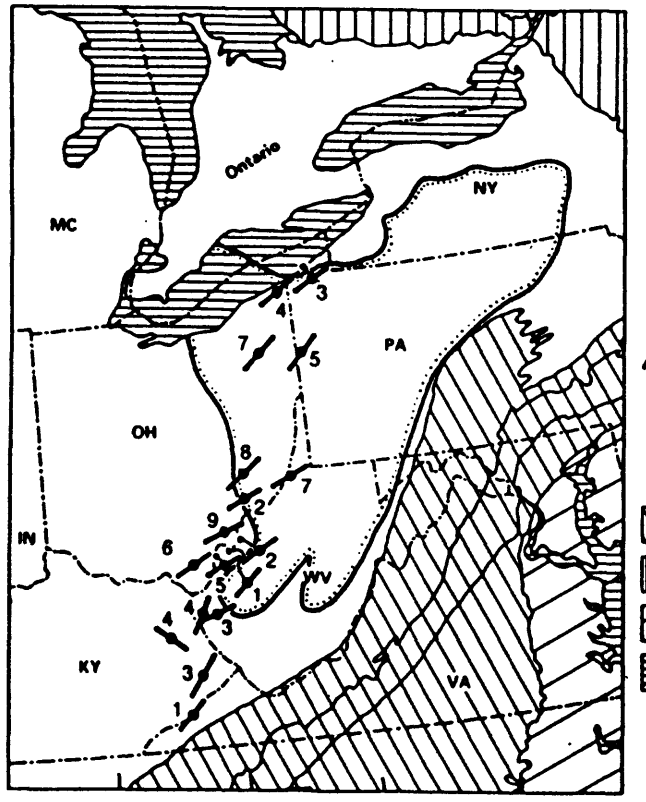
B
Coring-Induced Fractures
Ontario
NY
MC
PA
OH
IN
WV
KY
VA
Approximate Edge of Silurian Salt; 75 m Isopach
EGSP Well Number
Strike of Centerline Fractures
Appalachian Fold Belt
Grenville & Kenoran Fold Belts
Coastal Plain
Water
100 0 100 Miles
100 0 100 Kilometers

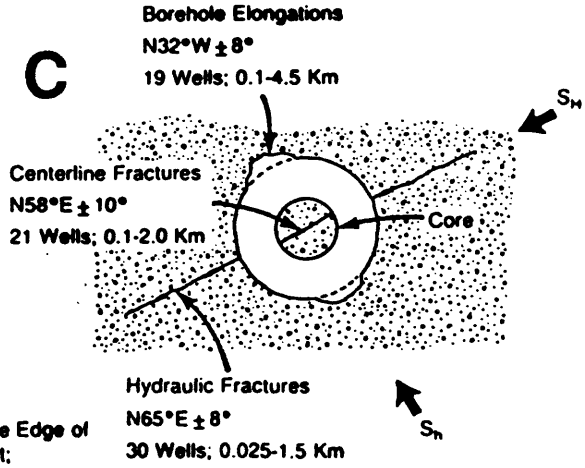
C
Borehole Elongations
N32°W ± 8°
19 Wells; 0.1-4.5 Km
S_H
Centerline Fractures
N58°E ± 10°
21 Wells; 0.1-2.0 Km
Core
Hydraulic Fractures
N65°E ± 8°
30 Wells; 0.025-1.5 Km
S_h

FIGURE 7

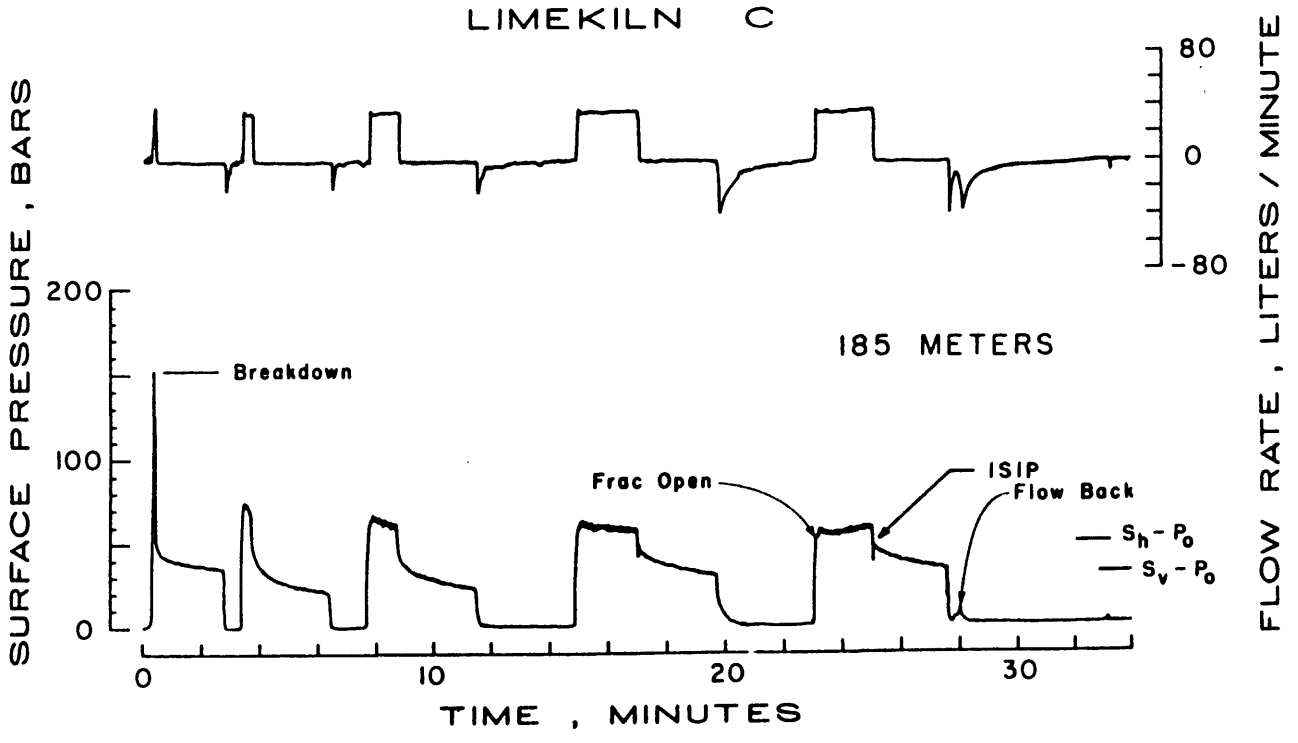
LIMEKILN C
SURFACE PRESSURE , BARS
200
100
0
80
0
-80
FLOW RATE , LITERS / MINUTE
185 METERS
Breakdown
Frac Open
ISIP
Flow Back
$S_h - P_o$
$S_v - P_o$
0
10
20
30
TIME , MINUTES

FIGURE 8

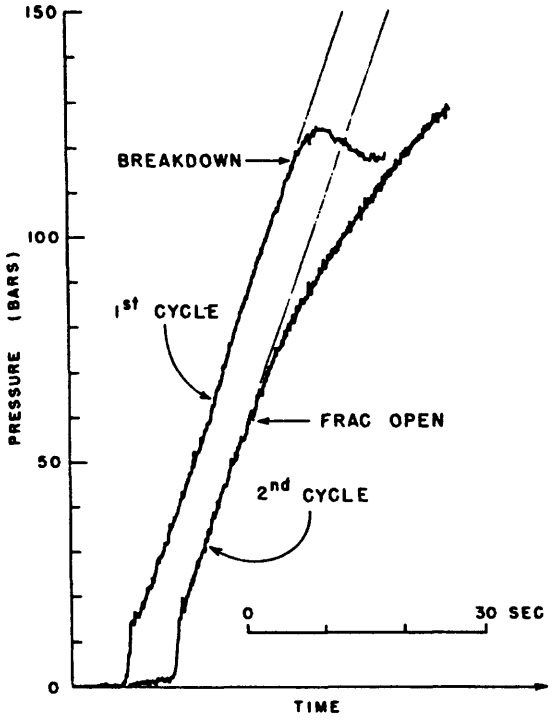
150
100
50
0
PRESSURE (BARS)
BREAKDOWN
1st CYCLE
FRAC OPEN
2nd CYCLE
0
30 SEC
TIME

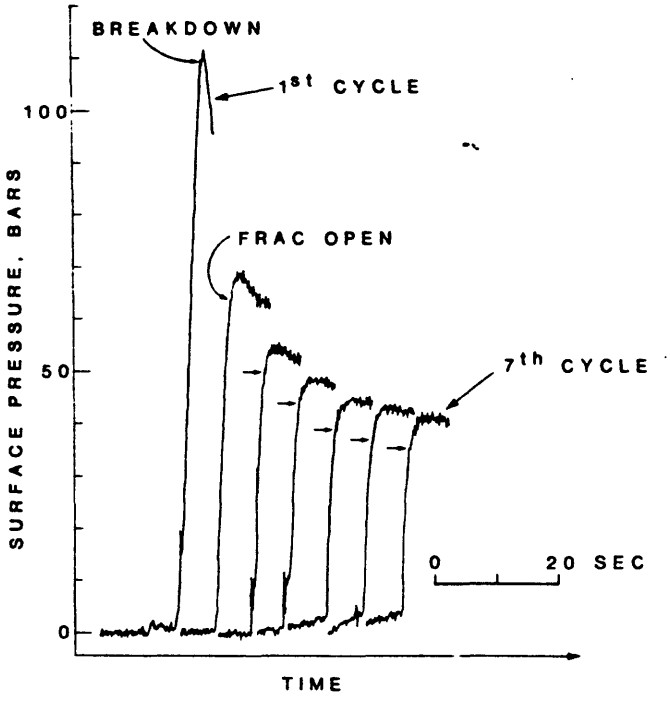
BREAKDOWN
1st CYCLE
100
FRAC OPEN
50
7th CYCLE
SURFACE PRESSURE, BARS
0
20 SEC
TIME

FIGURE 9

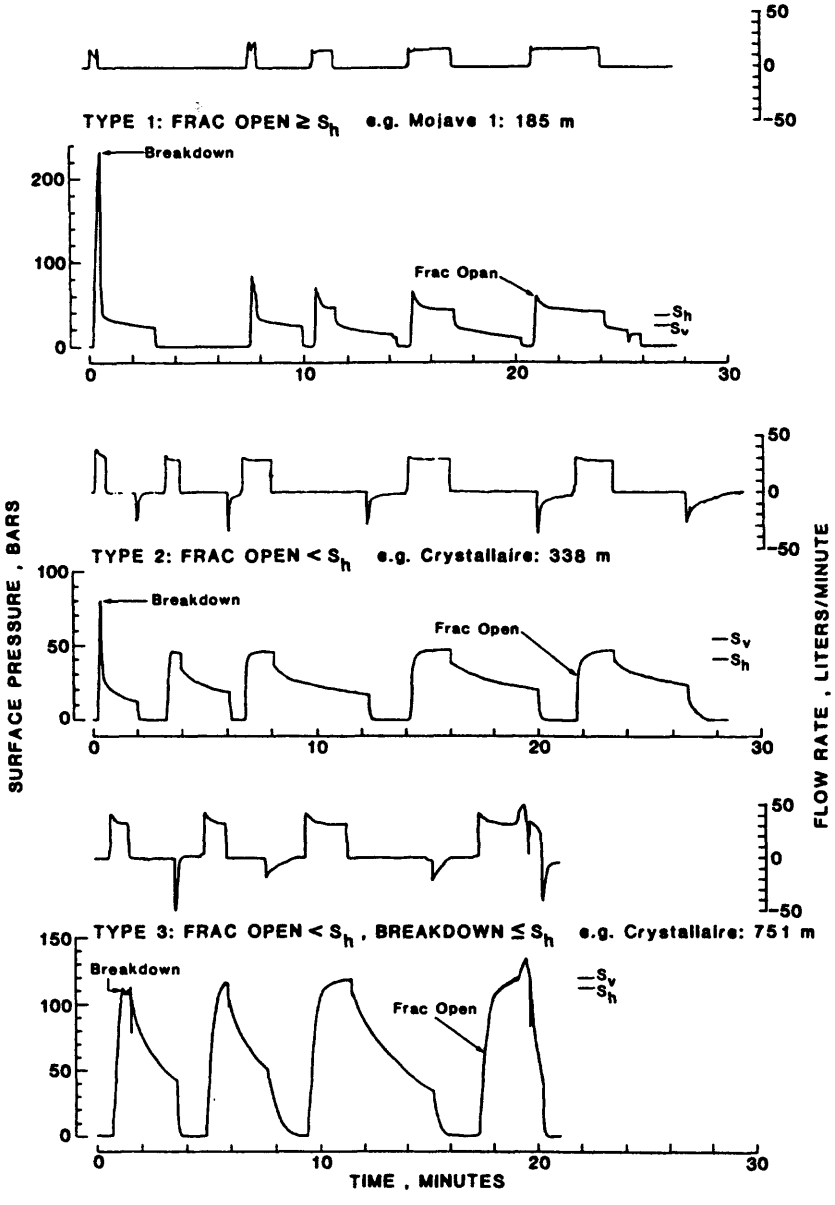
TYPE 1: FRAC OPEN ≥ S_h e.g. Mojave 1: 185 m
Breakdown
Frac Open
S_h
S_v
TYPE 2: FRAC OPEN < S_h e.g. Crystallaire: 338 m
Breakdown
Frac Open
S_v
S_h
TYPE 3: FRAC OPEN < S_h , BREAKDOWN ≤ S_h e.g. Crystallaire: 751 m
Breakdown
Frac Open
S_v
S_h
SURFACE PRESSURE , BARS
FLOW RATE , LITERS/MINUTE
TIME , MINUTES

FIGURE 10

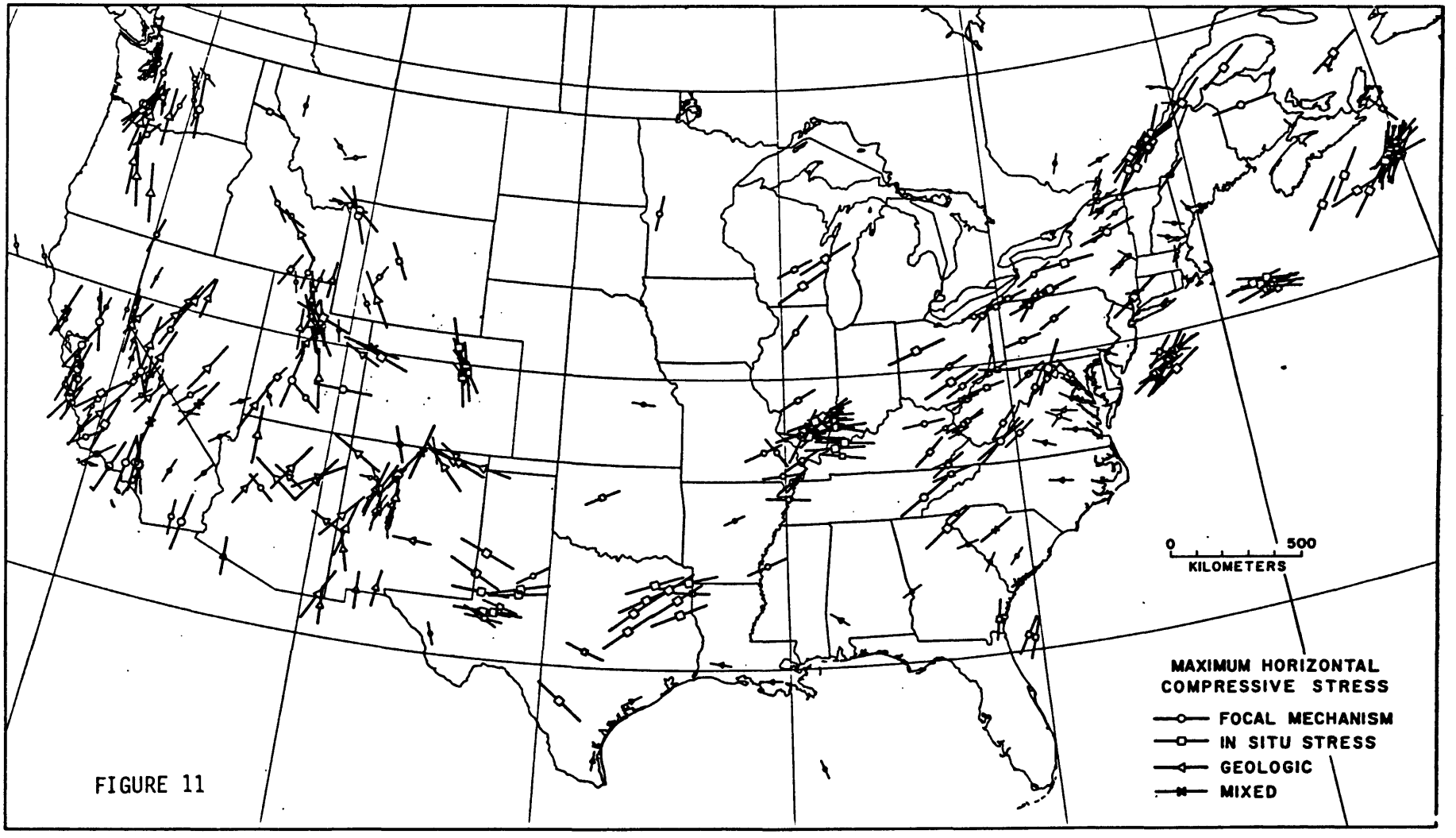
0
500
KILOMETERS
MAXIMUM HORIZONTAL
COMPRESSIVE STRESS
FOCAL MECHANISM
IN SITU STRESS
GEOLOGIC
MIXED

FIGURE 11

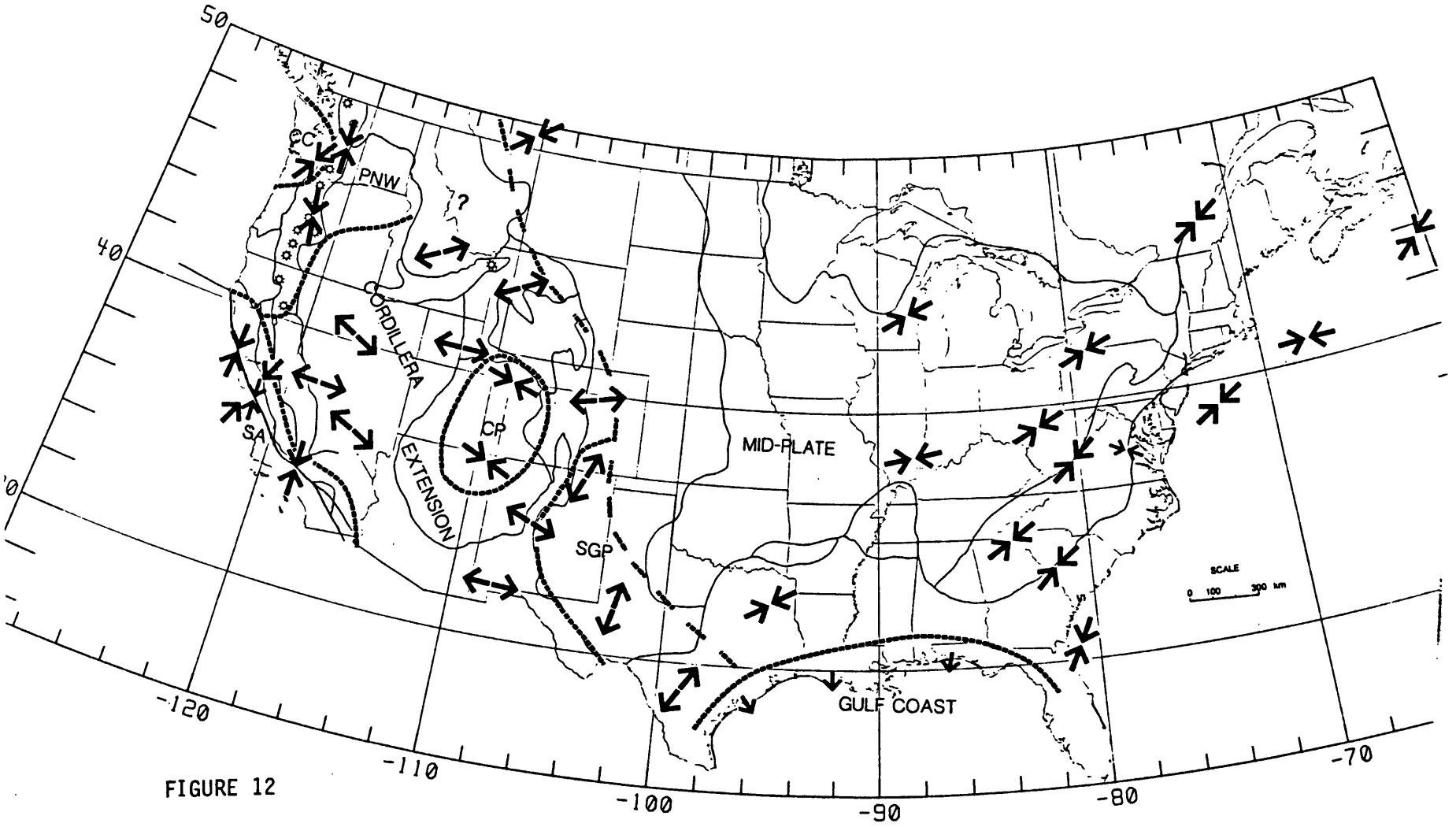
50
40
-120
-110
-100
-90
-80
-70
EC
PNW
?
CORDILLERA
CR
SA
EXTENSION
SGP
MID-PLATE
GULF COAST
SCALE
0 100 300 km

FIGURE 12

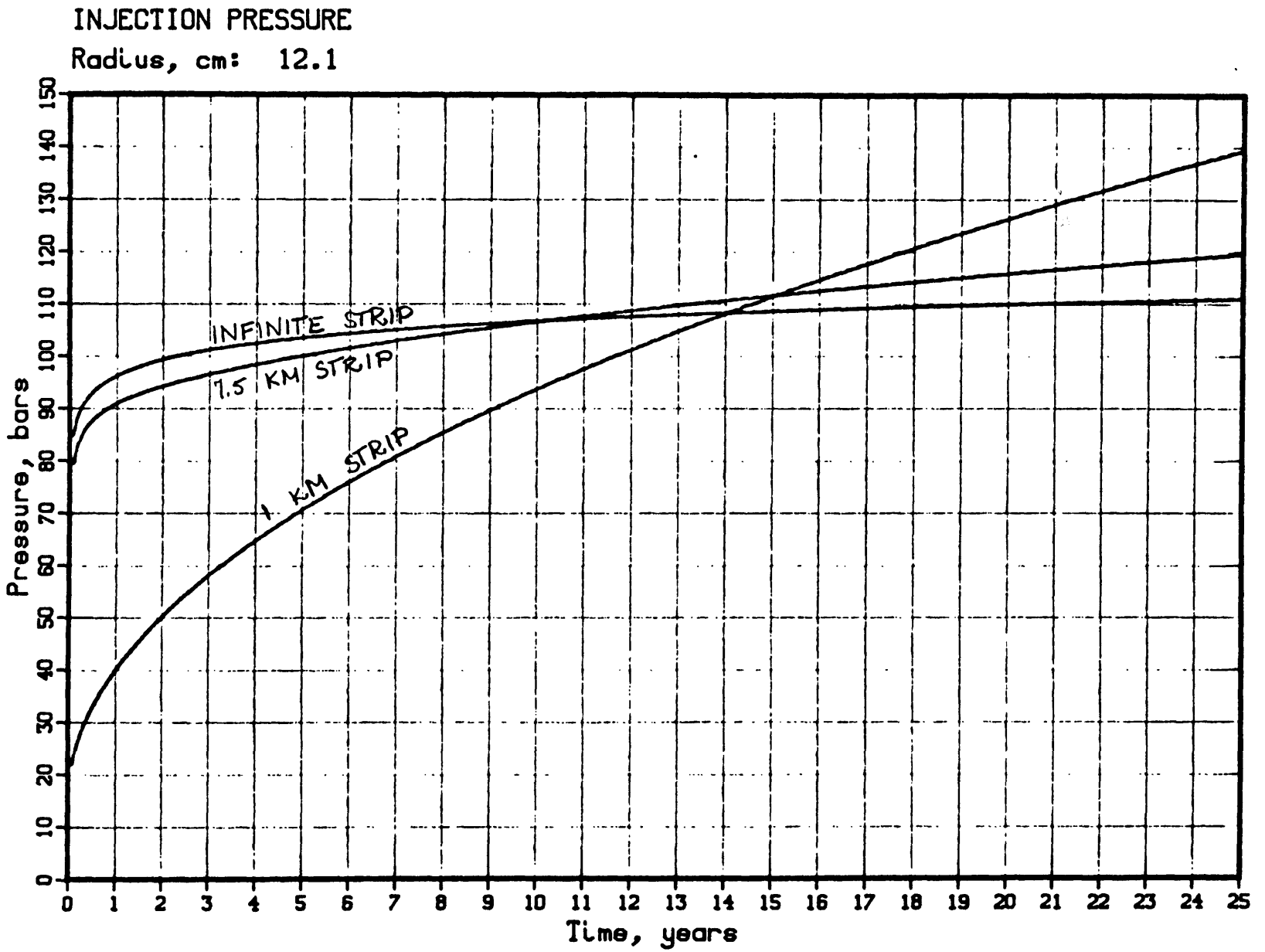
INJECTION PRESSURE
Radius, cm: 12.1
INFINITE STRIP
7.5 KM STRIP
1 KM STRIP
Pressure, bars
Time, years
0 10 20 30 40 50 60 70 80 90 100 110 120 130 140 150
0 1 2 3 4 5 6 7 8 9 10 11 12 13 14 15 16 17 18 19 20 21 22 23 24 25

FIGURE 13

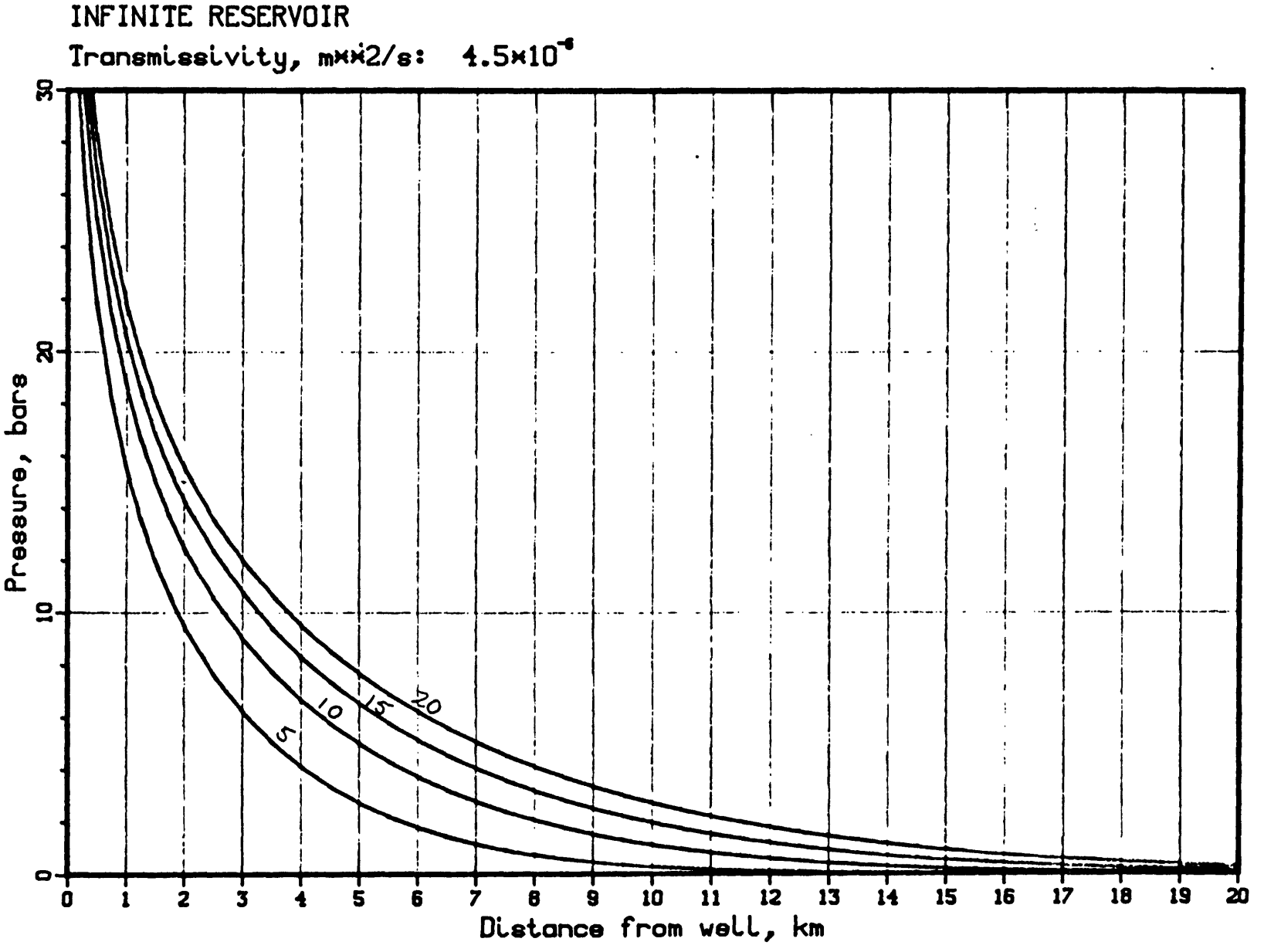
INFINITE RESERVOIR
Transmissivity, m**2/s: 4.5*10**-6
Pressure, bars
0
10
20
30
0 1 2 3 4 5 6 7 8 9 10 11 12 13 14 15 16 17 18 19 20
Distance from well, km
5
10
15
20

FIGURE 14

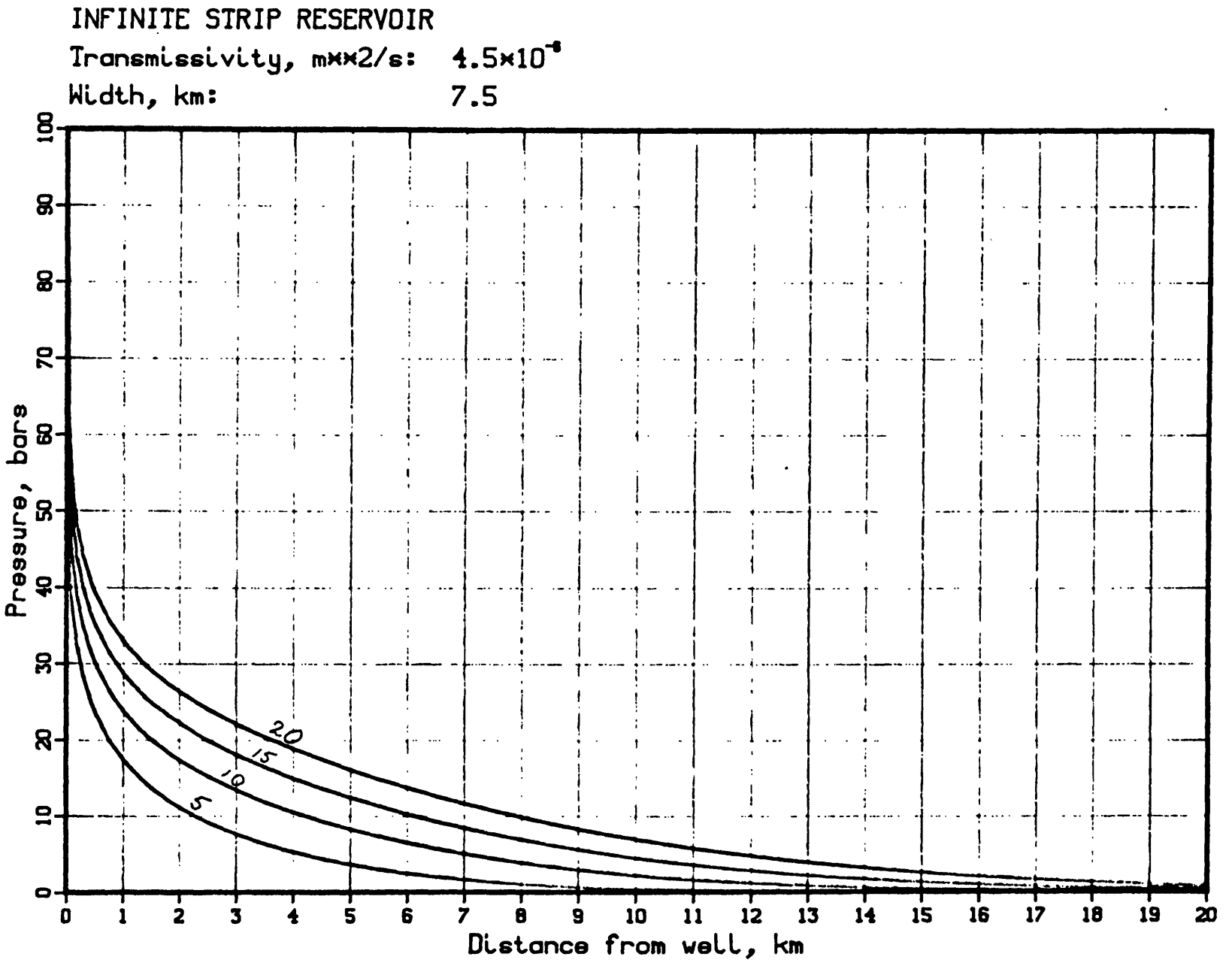
INFINITE STRIP RESERVOIR
Transmissivity, m**2/s: 4.5x10**-6
Width, km: 7.5
Pressure, bars
Distance from well, km
0
10
20
30
40
50
60
70
80
90
100
0
1
2
3
4
5
6
7
8
9
10
11
12
13
14
15
16
17
18
19
20
20
15
10
5

FIGURE 15

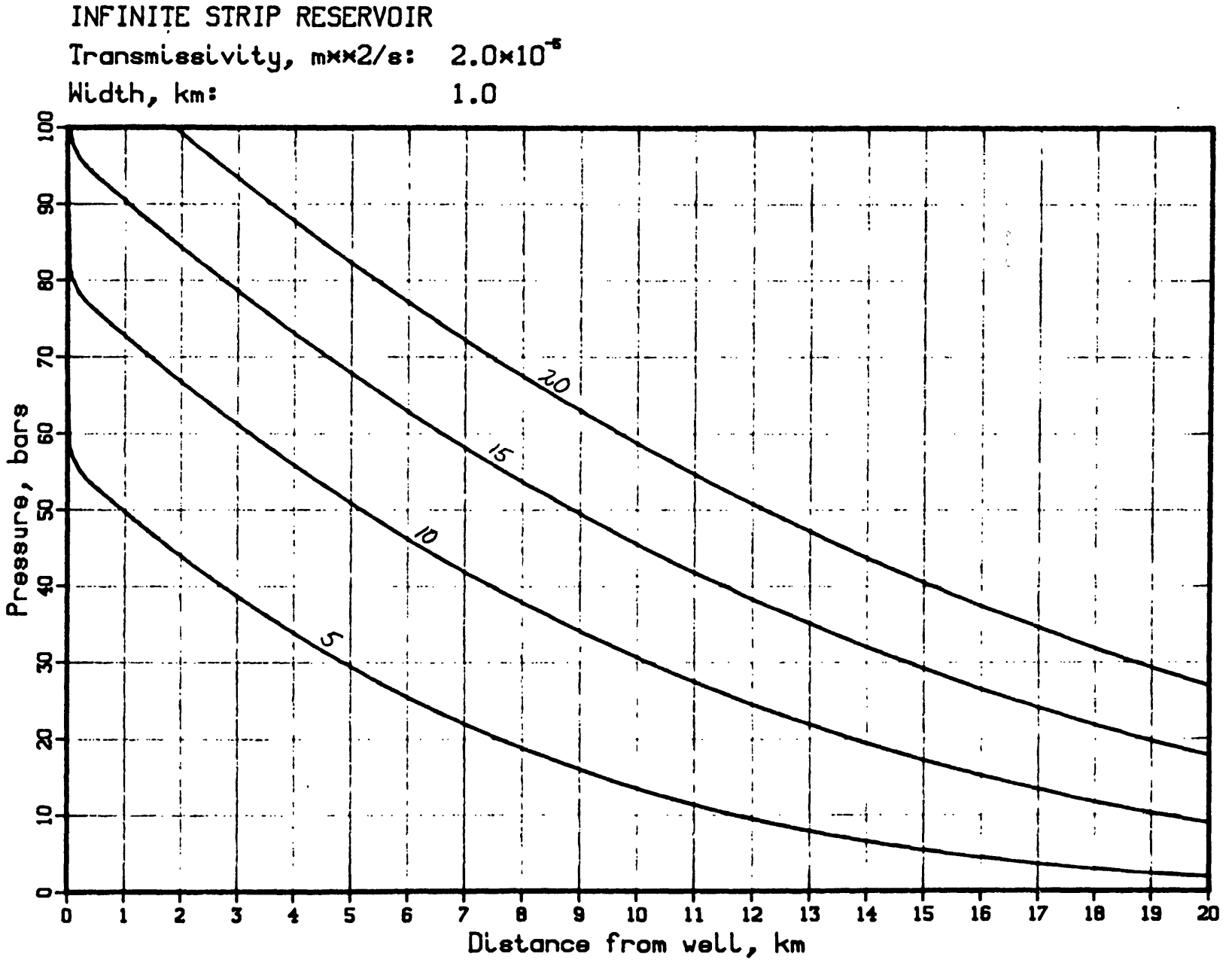
INFINITE STRIP RESERVOIR
Transmissivity, m**2/s: 2.0*10**-5
Width, km: 1.0
Pressure, bars
Distance from well, km
20
15
10
5
0
10
20
30
40
50
60
70
80
90
100
0
1
2
3
4
5
6
7
8
9
10
11
12
13
14
15
16
17
18
19
20

FIGURE 16

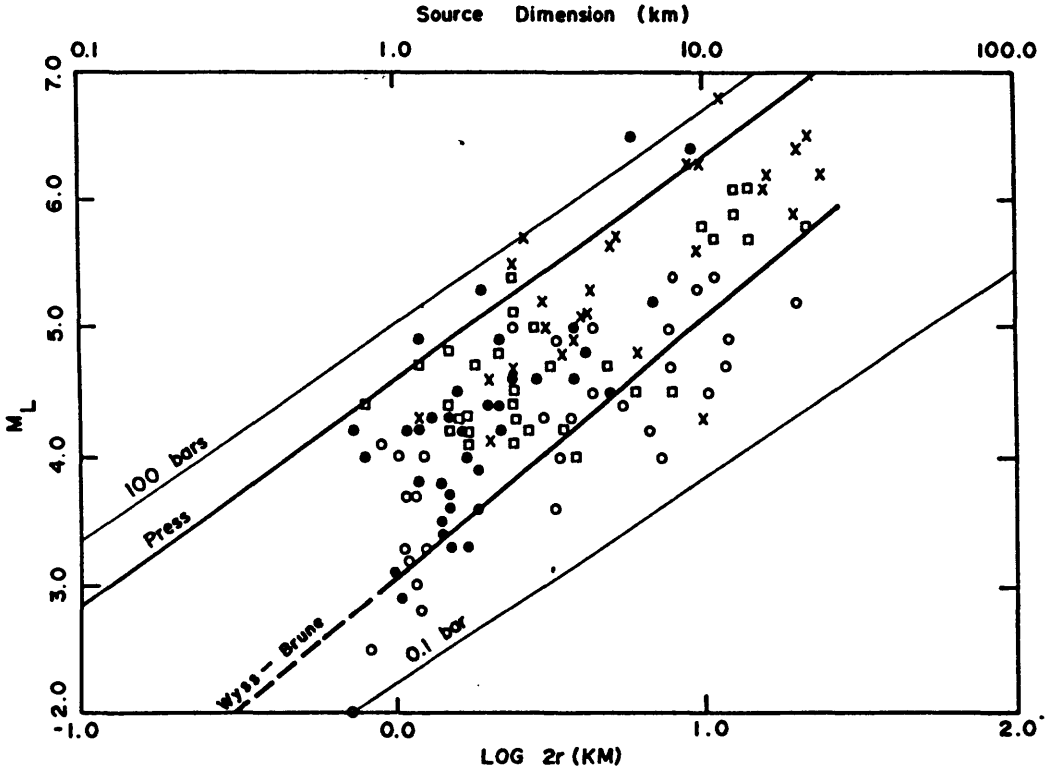

Local magnitude versus log source dimension. Source size is here taken as twice the radius of a circular dislocation. Shown for reference are the empirical relations proposed by *Press* [1967] and *Wyss and Brune* [1968]. Constant stress drop lines come from a theoretical relation discussed in the text. Open circles represent earthquakes in the offshore province and San Andreas fault; solid circles, in Transverse Ranges; squares, in Kern county; crosses, in other southern California locations.

FIGURE 17

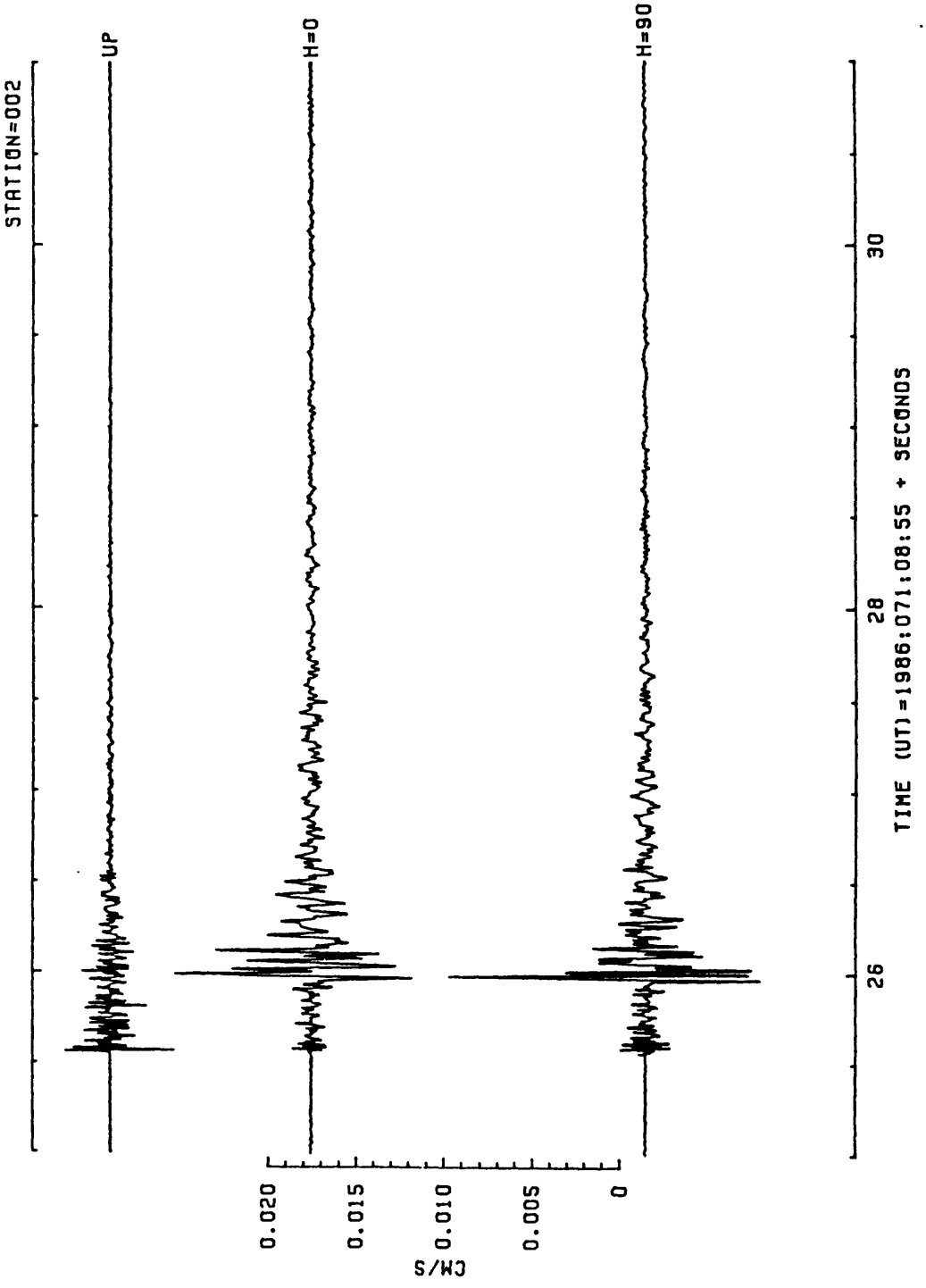
STATION=002
UP
H=0
H=90
0.020
0.015
0.010
0.005
0
CM/S
26
28
30
TIME (UT)=1986:071:08:55 + SECONDS

Figure 18

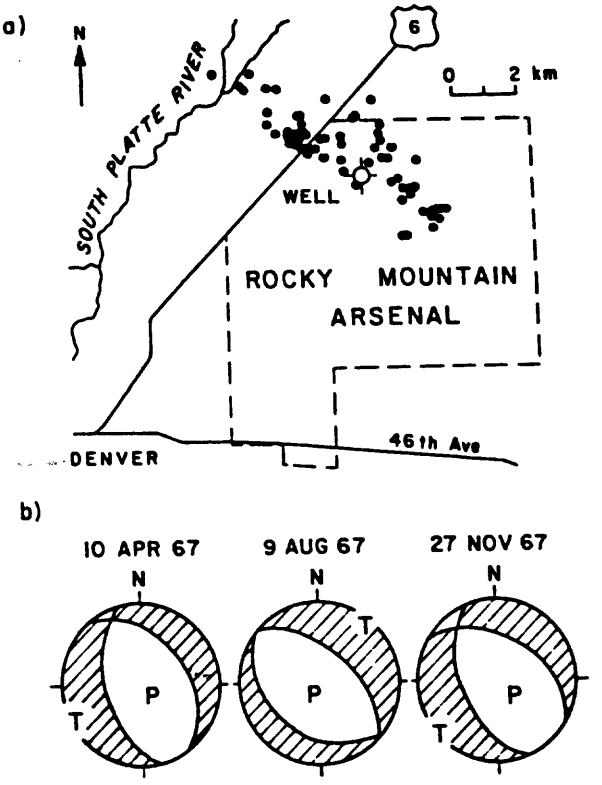

FIGURE A1

(a) *Location of earthquakes near Denver, Colorado associated with fluid-injection at the Rocky Mountain Arsenal (after Healy* et al., 1968*).*

(b) *Surface wave focal plane mechanisms of three of the larger Denver earthquakes (after Herrmann* et al., 1981*).*

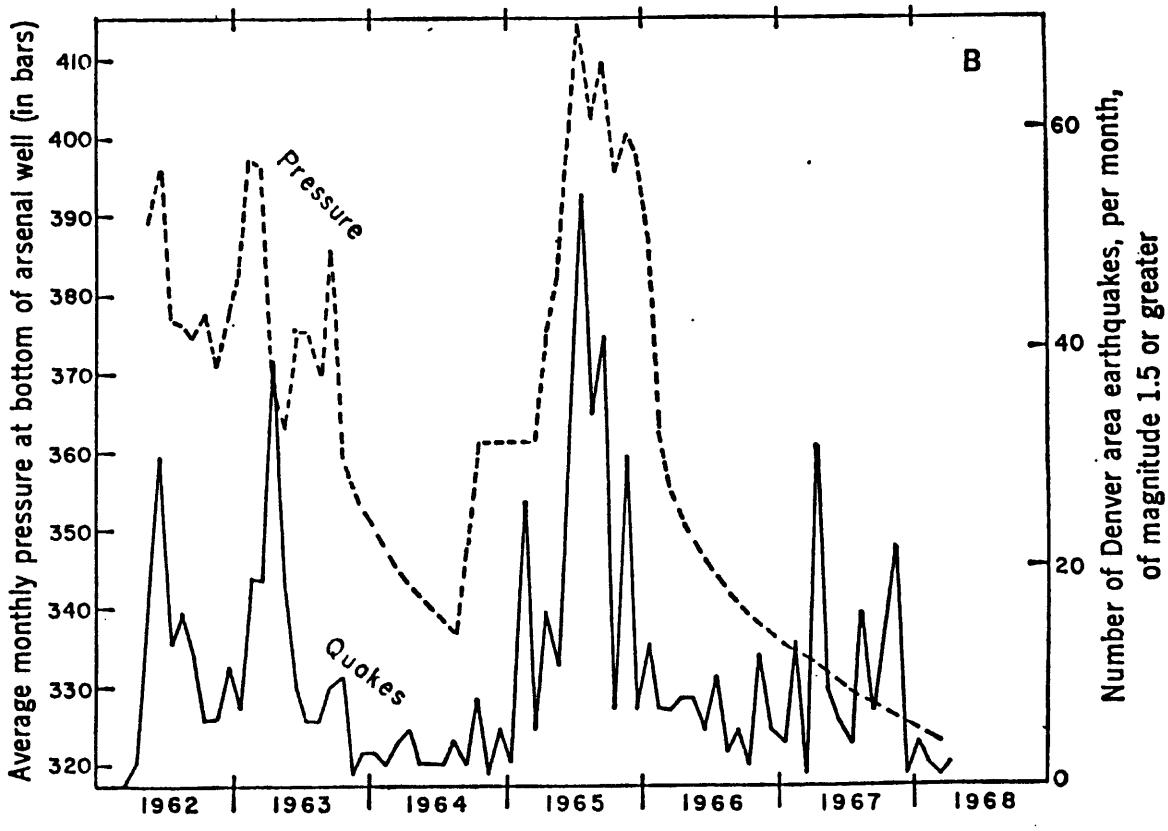

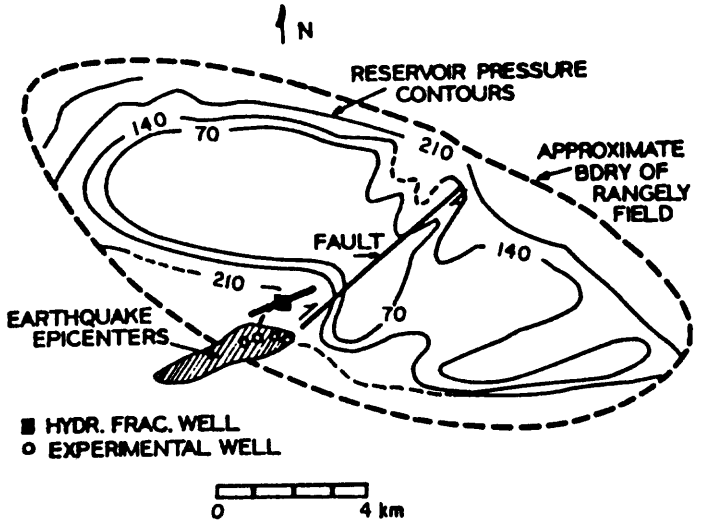

The Rangely Oil Field and the area where most earthquake epicenters concentrated. Shown also are the pressure contours (in bars) in the oil-bearing Weber sandstone formation, the major fault, the 4 experimental wells through which reservoir pressure in the earthquake zone was controlled and monitored, and the hydrofracturing well. The short line crossing the latter is in the direction of the largest horizontal compressive stress.

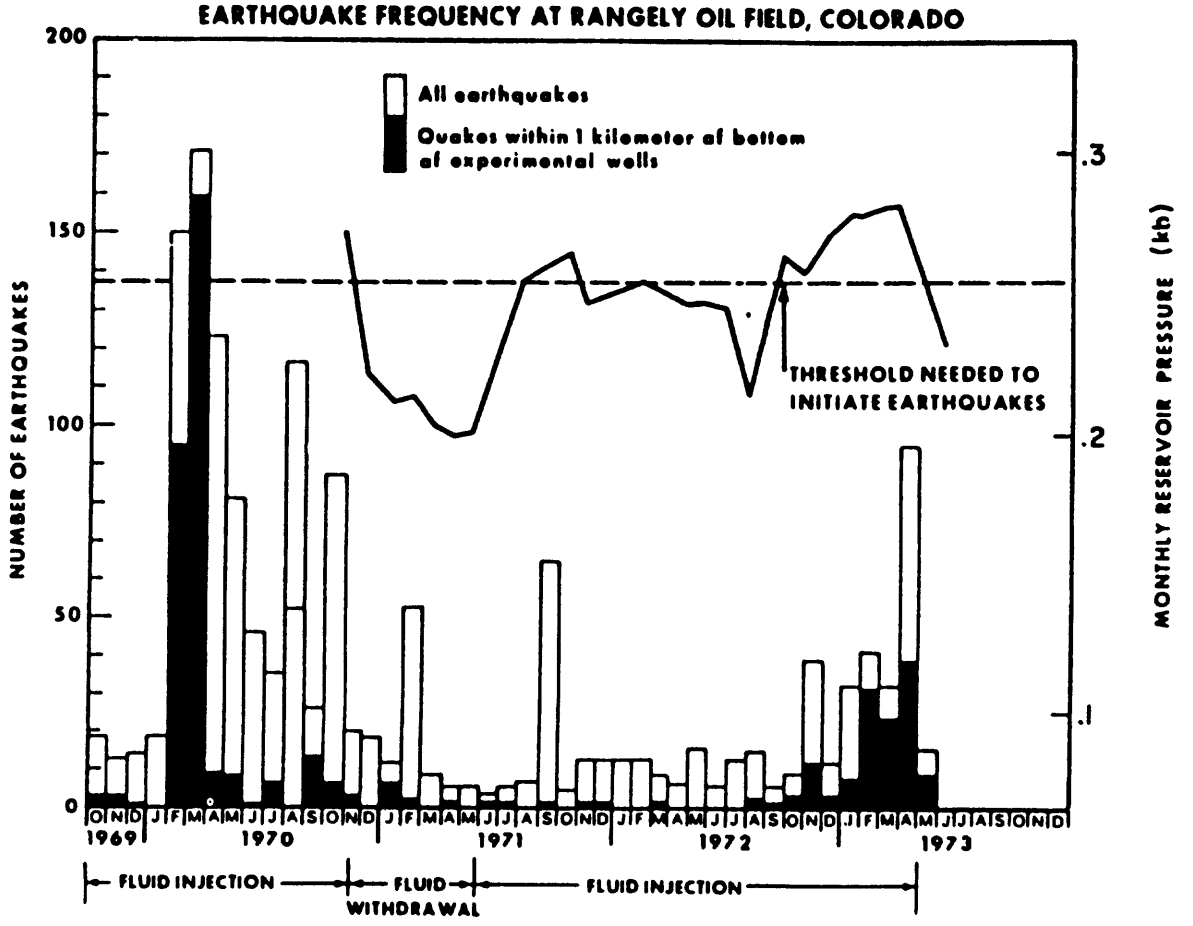

FIGURE A2

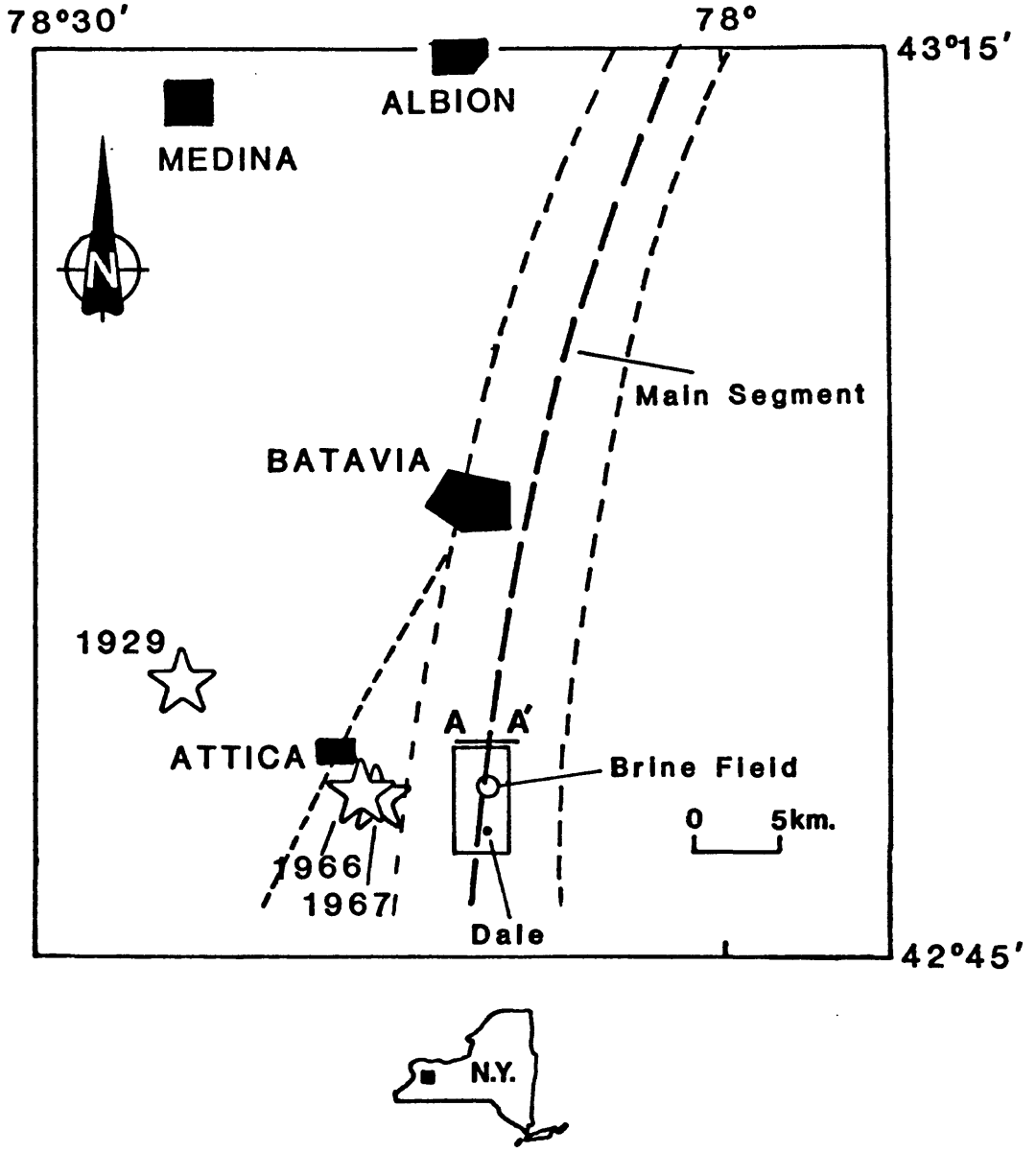
78°30'
78°
43°15'
ALBION
MEDINA
N
Main Segment
BATAVIA
1929
A
A'
ATTICA
Brine Field
0
5km.
1966
1967
Dale
42°45'
N.Y.

FIGURE A3

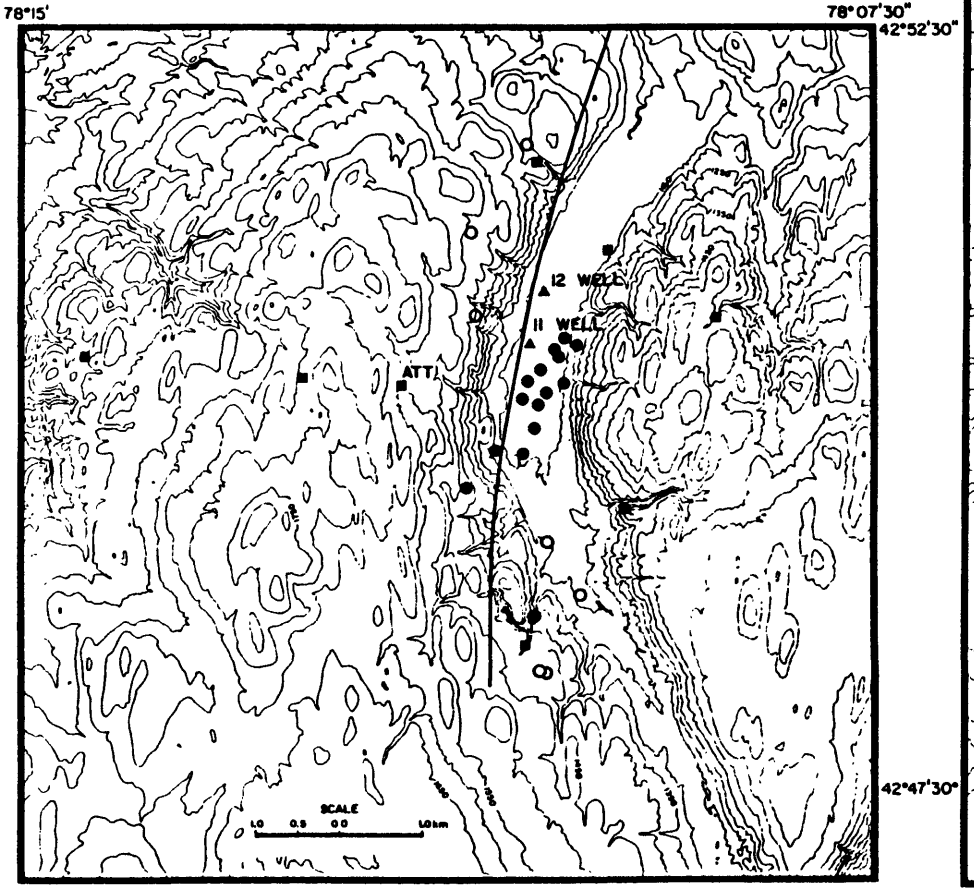
78°15'
78°07'30"
42°52'30"
42°47'30"
12 WELL
11 WELL
ATT
SCALE
1.0 0.5 0.0 1.0km

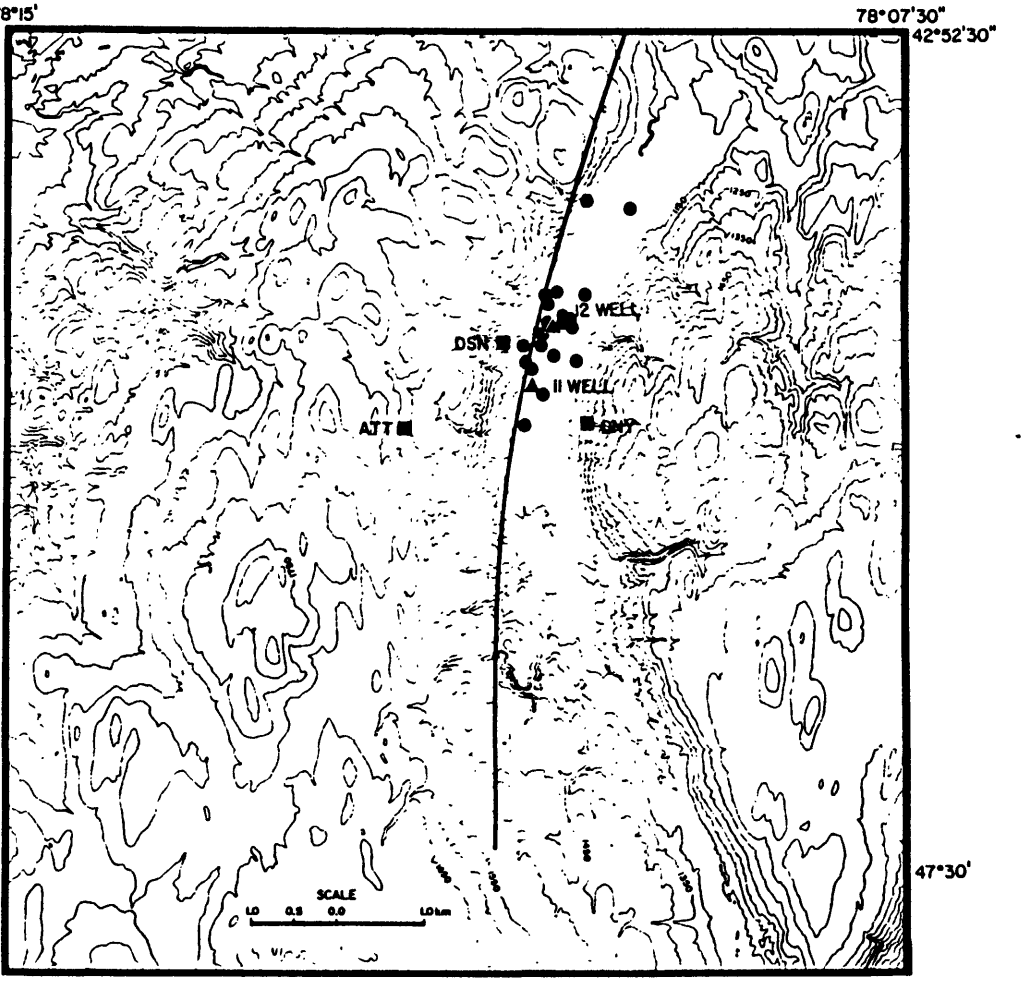
78°15'
78°07'30"
42°52'30"
47°30'
12 WELL
DSN
11 WELL
ATT
GMT
SCALE
1.0 0.5 0.0 1.0km

FIGURE A4

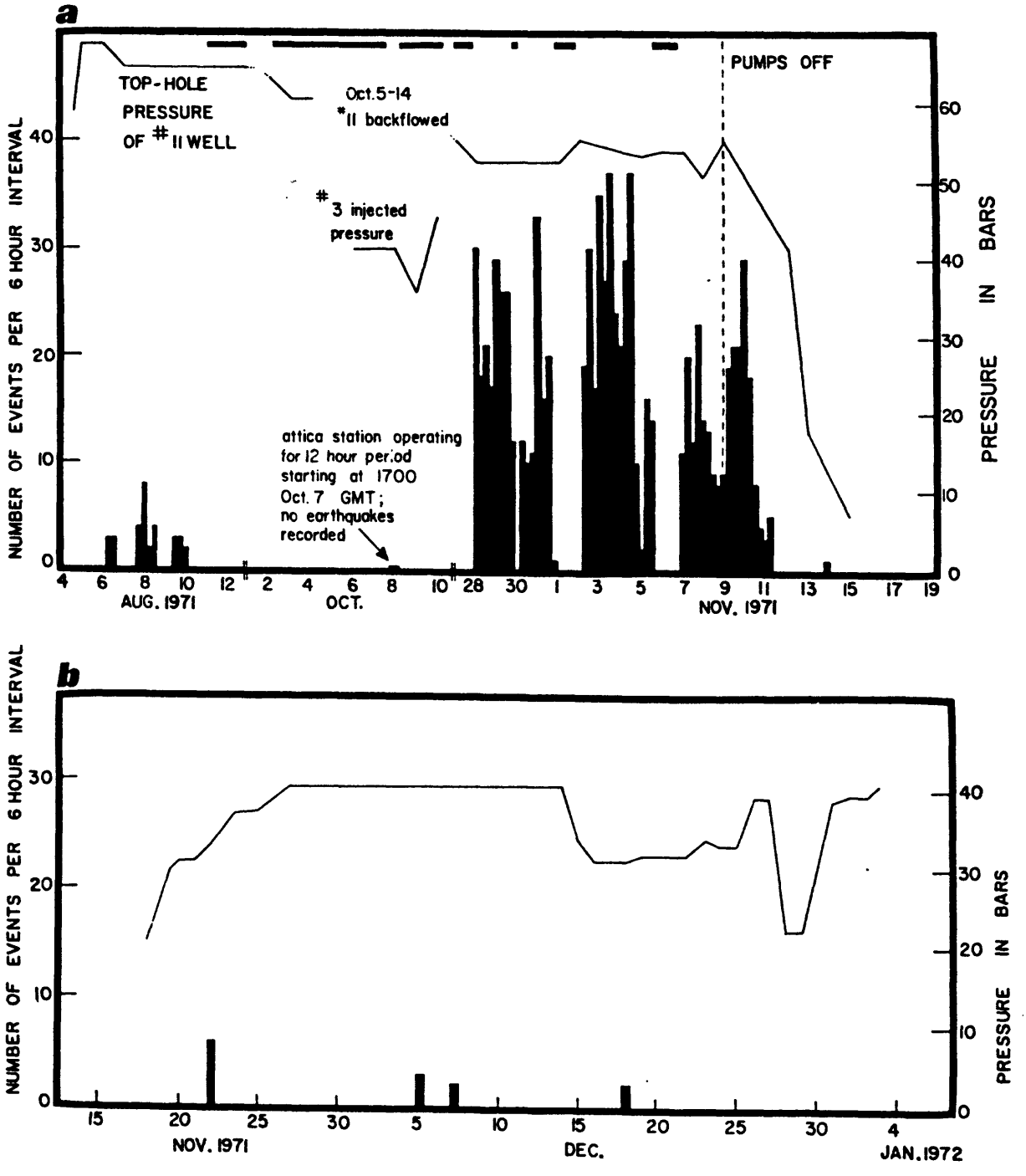
a
TOP-HOLE PRESSURE OF # 11 WELL
Oct. 5-14 *11 backflowed
3 injected pressure
PUMPS OFF
attica station operating for 12 hour period starting at 1700 Oct. 7 GMT; no earthquakes recorded
NUMBER OF EVENTS PER 6 HOUR INTERVAL
PRESSURE IN BARS
AUG. 1971
OCT.
NOV. 1971
b
NUMBER OF EVENTS PER 6 HOUR INTERVAL
PRESSURE IN BARS
NOV. 1971
DEC.
JAN. 1972

FIGURE A5

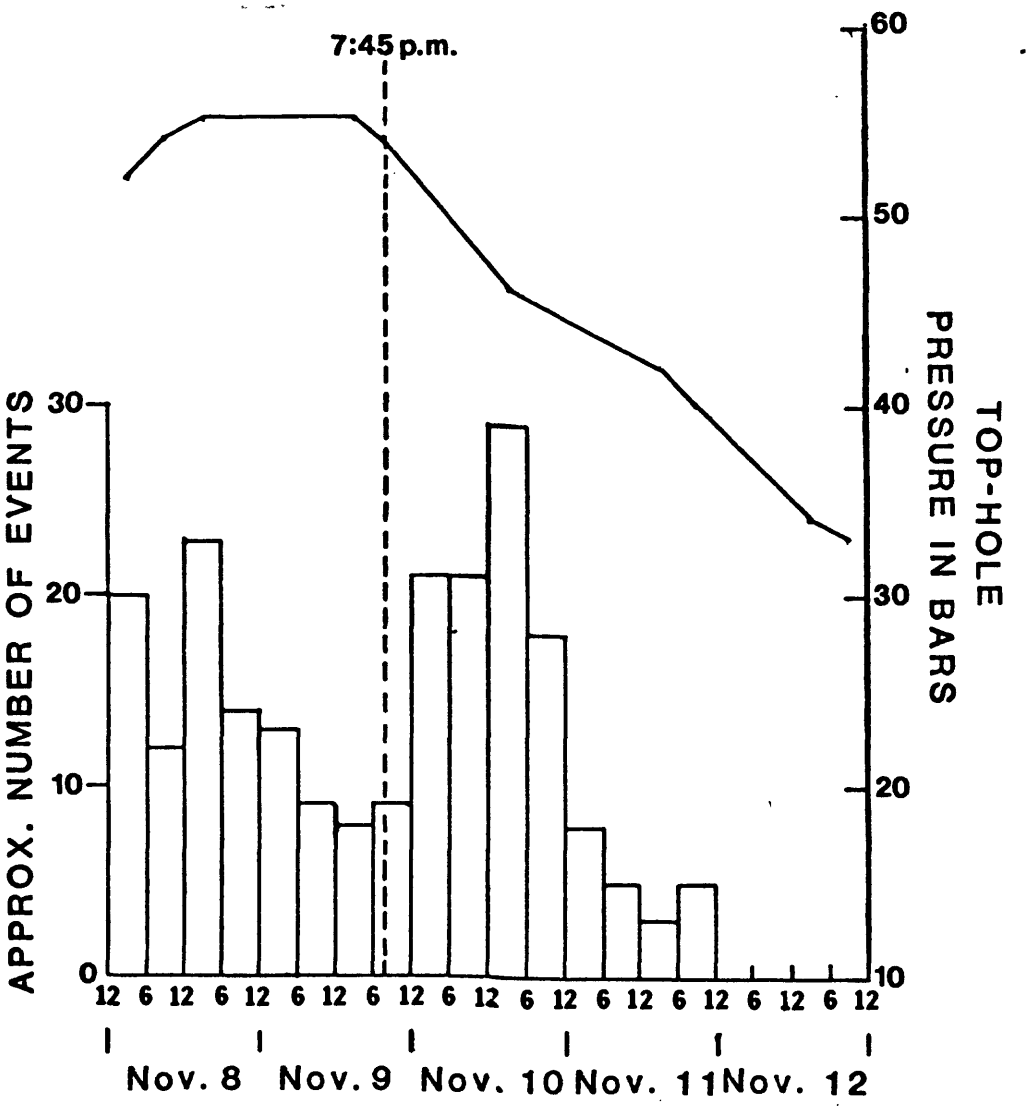
7:45 p.m.
APPROX. NUMBER OF EVENTS
TOP-HOLE PRESSURE IN BARS
0
10
20
30
10
20
30
40
50
60
12 6 12 6 12 6 12 6 12 6 12 6 12 6 12 6 12 6 12 6 12
Nov. 8
Nov. 9
Nov. 10
Nov. 11
Nov. 12

FIGURE A6

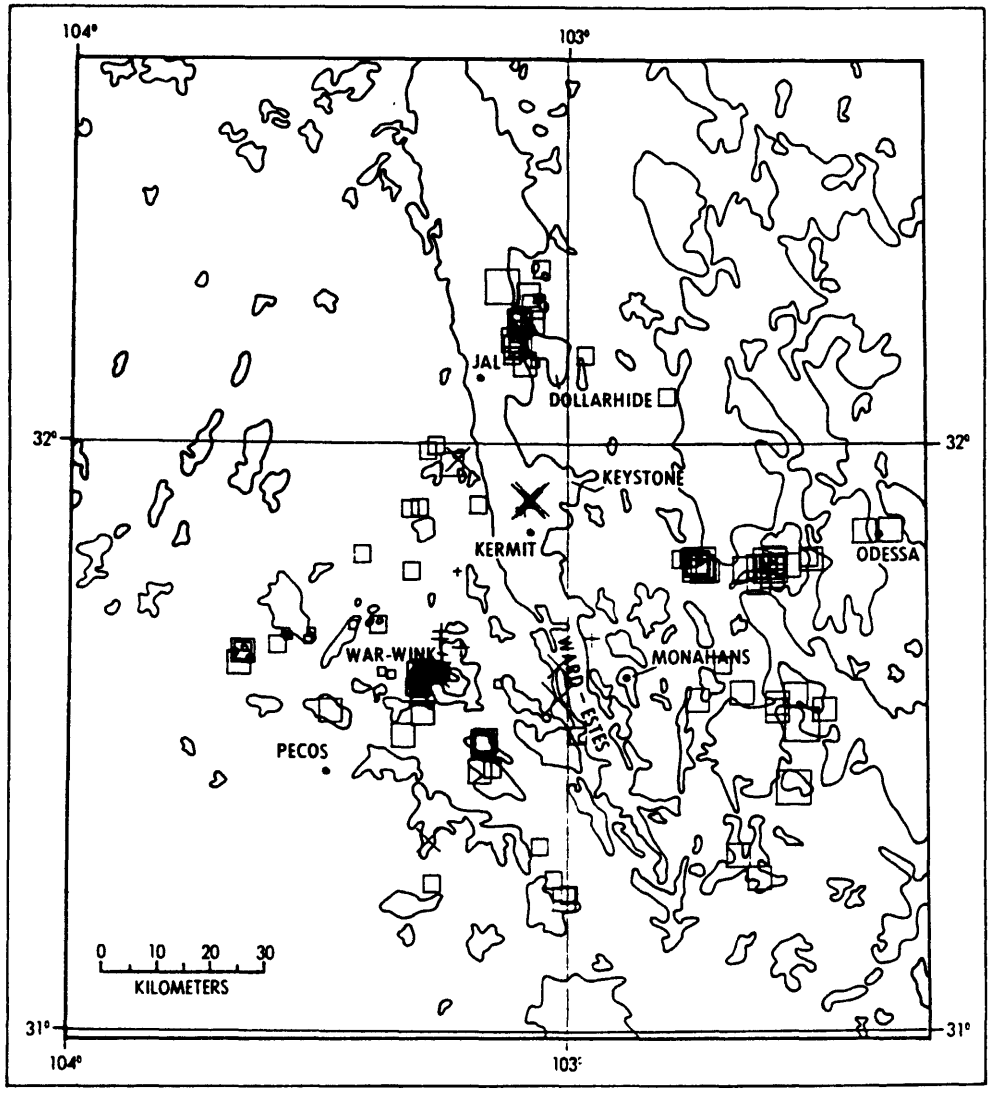

Earthquakes located after January 1976 using the current operating network. Large X's are earthquakes in the range: $3.0 < M_{LD} \leq 4.0$; small x's: $2.0 < M_{LD} \leq 3.0$; large +'s: $1.0 < M_{LD} \leq 2.0$; small +'s: $M_{LD} \leq 1.0$. The square figures in 4 sizes indicate earthquakes in the same magnitude ranges given above with the largest square indicating the largest range. Earthquakes indicated by a square are less reliable with a quality of C or D and gap >180°. All oil fields are indicated by solid lines, and the location of several major fields is shown.

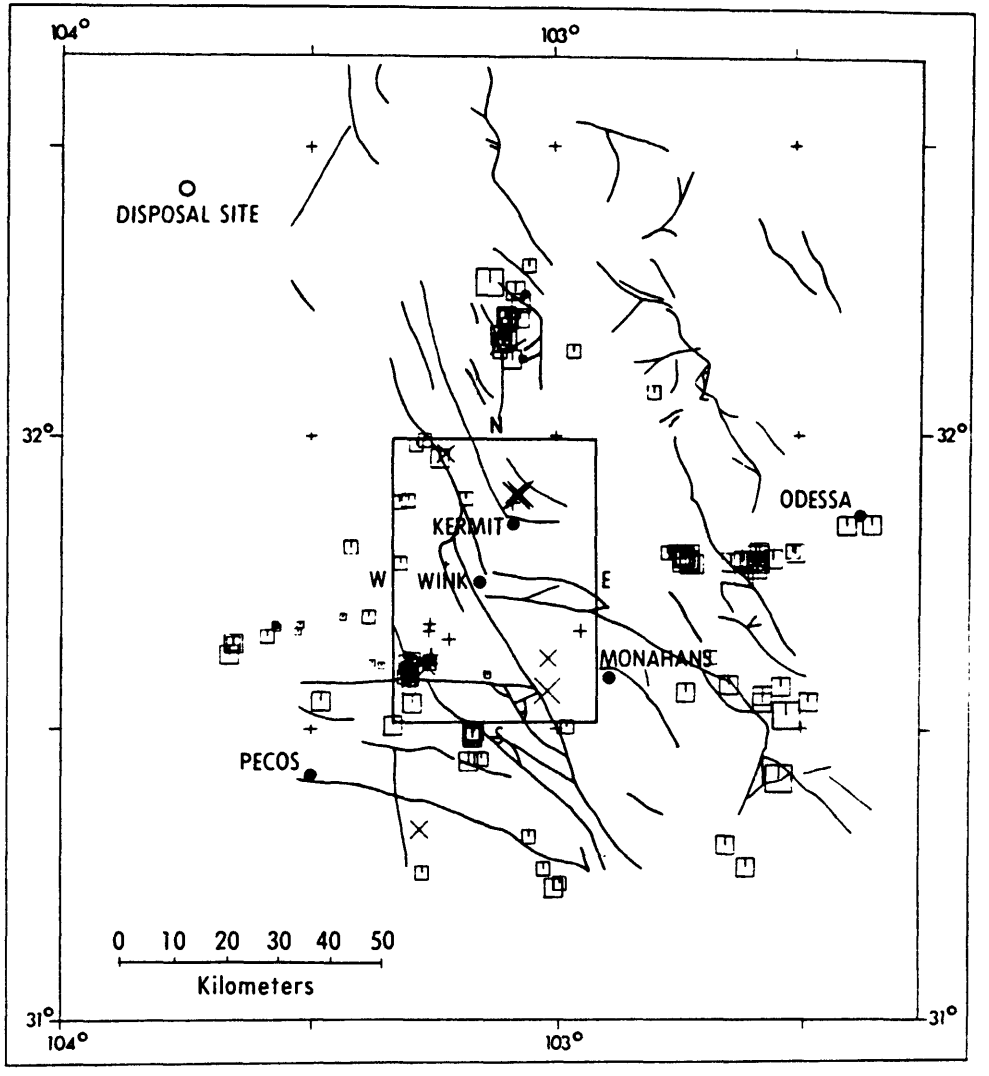

All located earthquakes and inferred pre-Permian faults taken from a 1:9600 scale map provided by Geomap Corp. (R. D. Wilde, written communication). The rectangular figure encloses the events that are shown in cross section in Figure 7. Large X's are earthquakes in the range: $3.0 < M_{LD} \leq 4.0$; small x's: $2.0 < M_{LD} \leq 3.0$; large +'s: $1.0 < M_{LD} \leq 2.0$; small +'s: $M_{LD} \leq 1.0$. The square figures in 4 sizes indicate earthquakes in the same magnitude ranges given above with the largest square indicating the largest range. Earthquakes indicated by a square are less reliable with a quality of C or D and gap >180°.

FIGURE A7

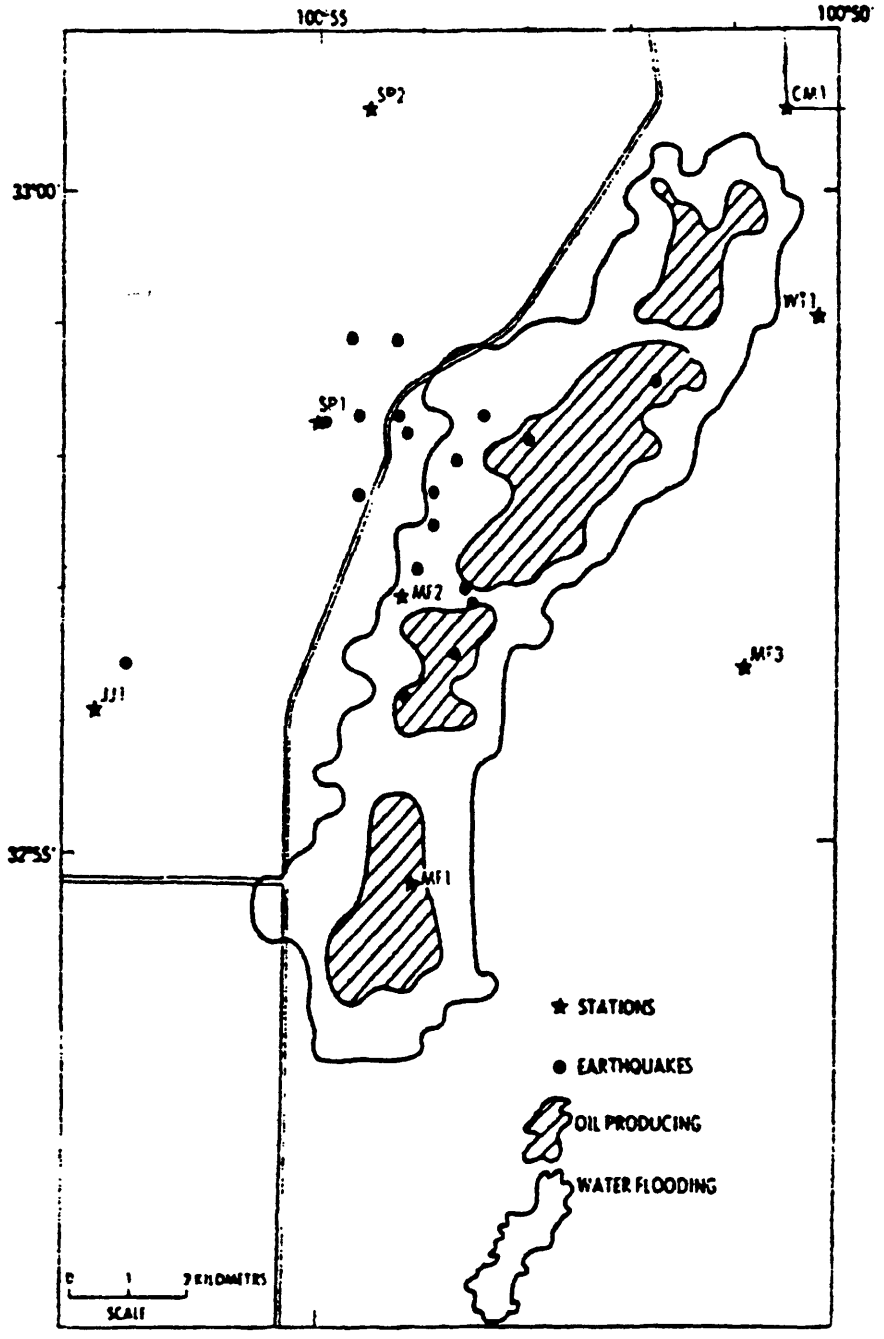

Earthquake epicenters in the Cogdell oil field. From Harding (1981).

FIGURE A8

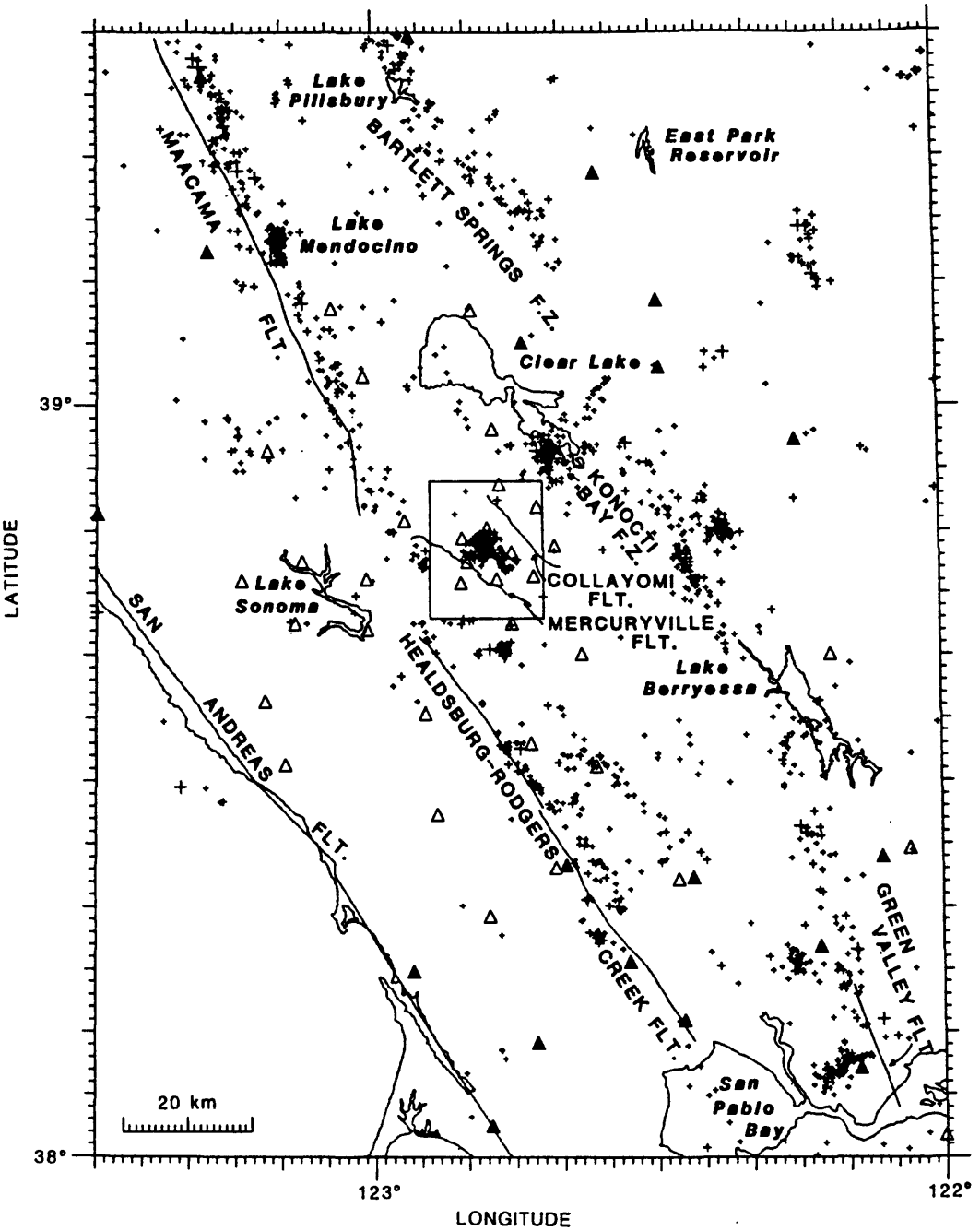

Seismicity and fault map of The Geysers and surrounding region. Pluses outside of box represent earthquakes for time period January 1976 through December 1984 with $M \geq 1.5$ and quality A–C [*Lee and Lahr*, 1975]. Seismicity inside box depicts earthquake locations for which fault plane solutions have been determined in this study for time period January 1984 through October 1985. Open triangles depict locations of CALNET stations used in computation of fault plane solutions. Solid triangles depict locations of stations used only for location of regional seismicity. Many of the latter stations were not in operation during period of this study.

FIGURE A9

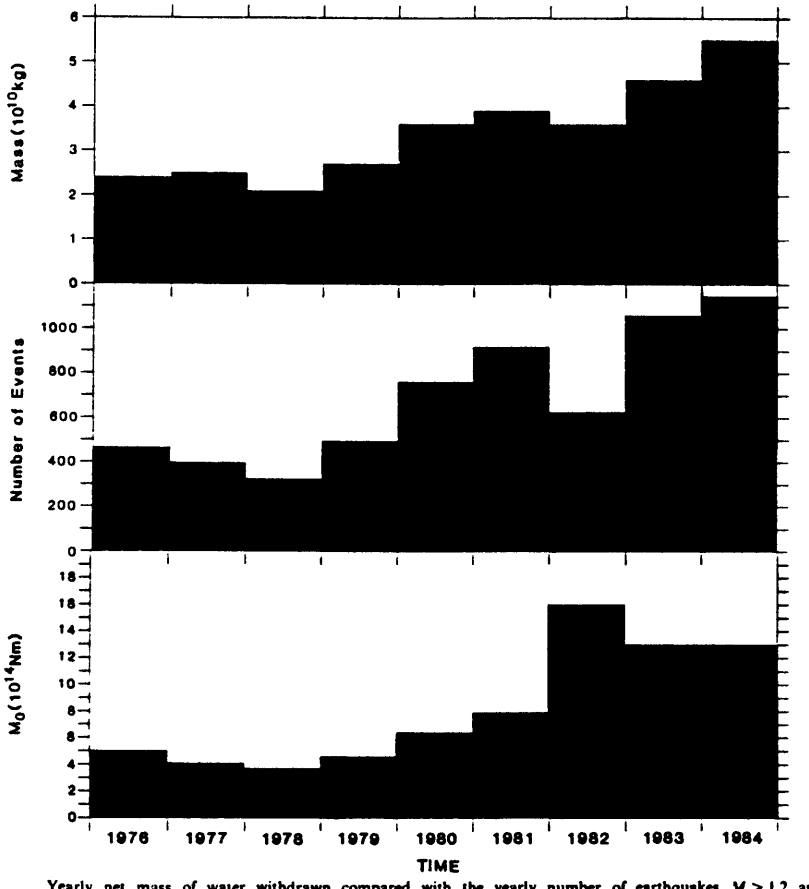

Yearly net mass of water withdrawn compared with the yearly number of earthquakes $M \geq 1.2$ and quality = A–C [*Lee and Lahr*, 1975] and the associated moment sum (Table 2) for entire The Geysers geothermal reservoir. The presence of a few $M3+$ earthquakes greatly influences the moment sum calculation and explains the better correlation between yearly mass withdrawn and number of earthquakes.

OPPENHEIMER: EXTENSIONAL TECTONICS AT THE GEYSERS, CALIFORNIA

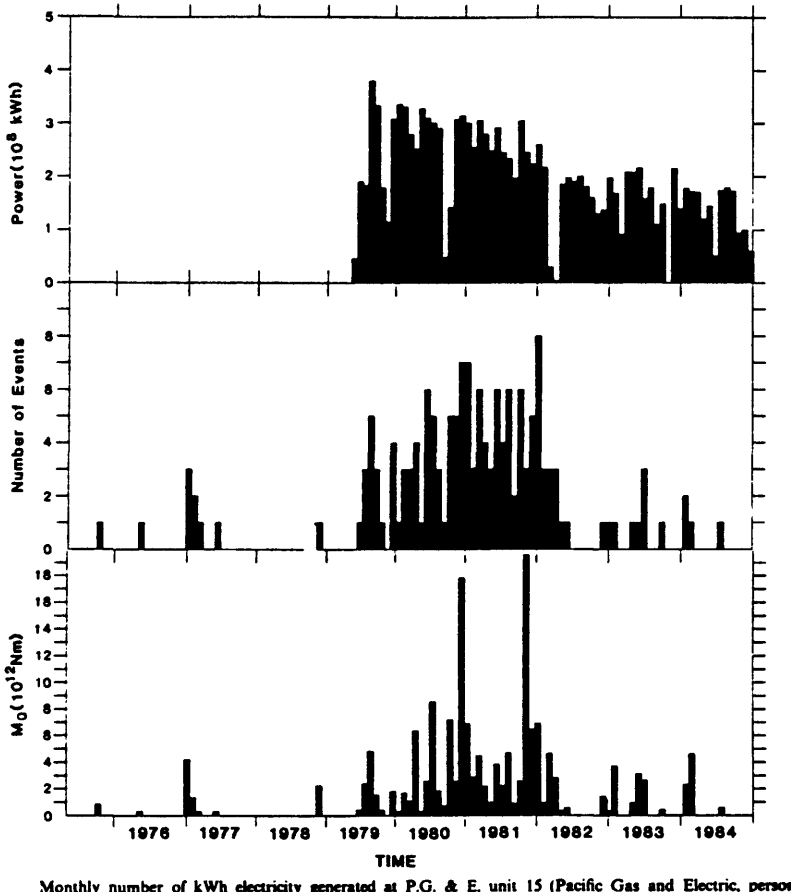

Monthly number of kWh electricity generated at P.G. & E. unit 15 (Pacific Gas and Electric, personal communication, 1985) compared with the number of earthquakes $M \geq 1.2$ and quality = A–C [*Lee and Lahr*, 1975] per month and the associated moment sum. Note increase of seismicity following commencement of power generation and subsequent abatement of seismicity following the decrease in the number of kWh generated.

FIGURE A10

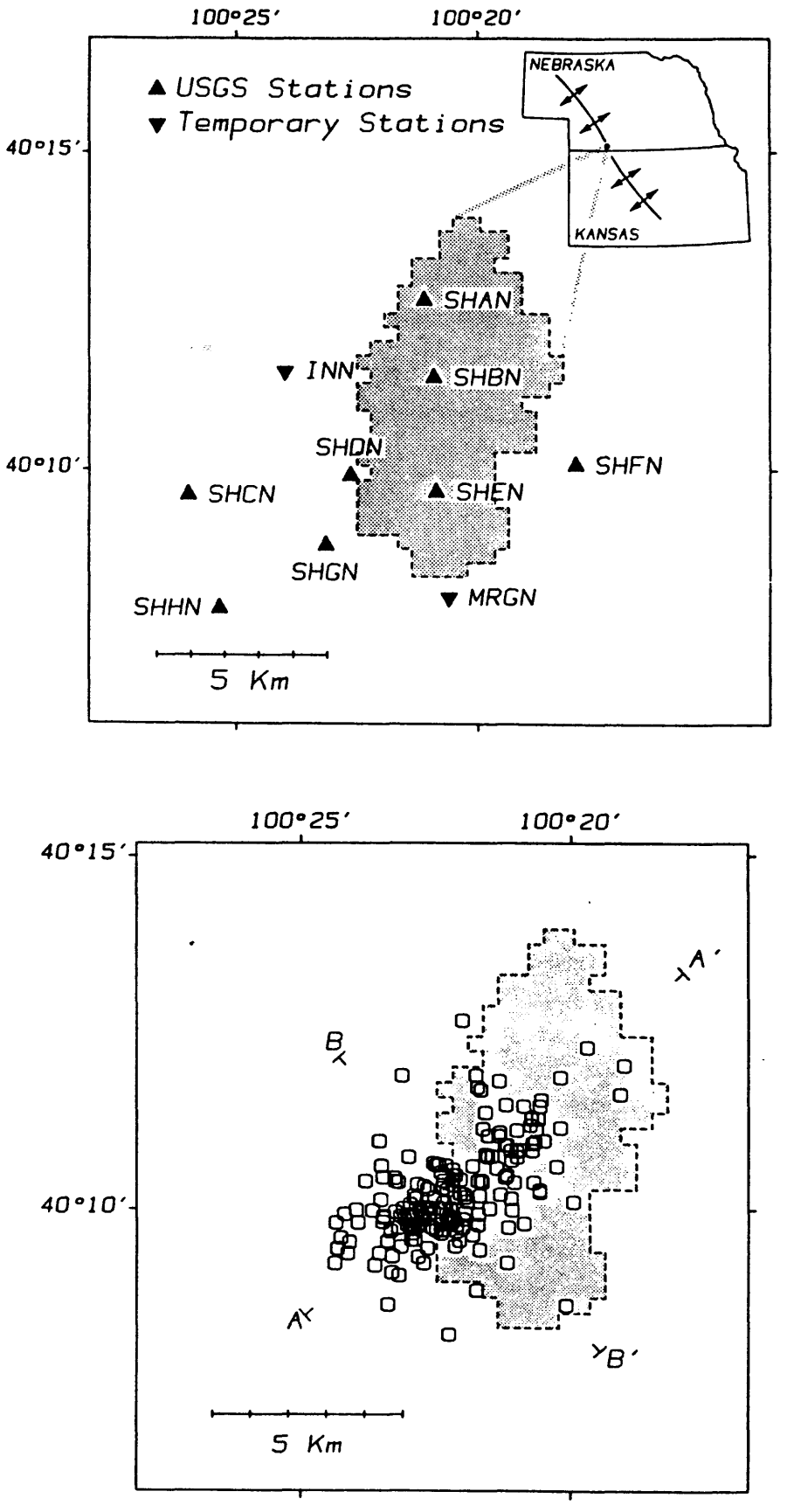
100°25'
100°20'
40°15'
40°10'
USGS Stations
Temporary Stations
NEBRASKA
KANSAS
SHAN
INN
SHBN
SHDN
SHFN
SHCN
SHEN
SHGN
SHHN
MRGN
5 Km
A
A'
B
B'
5 Km

FIGURE A11

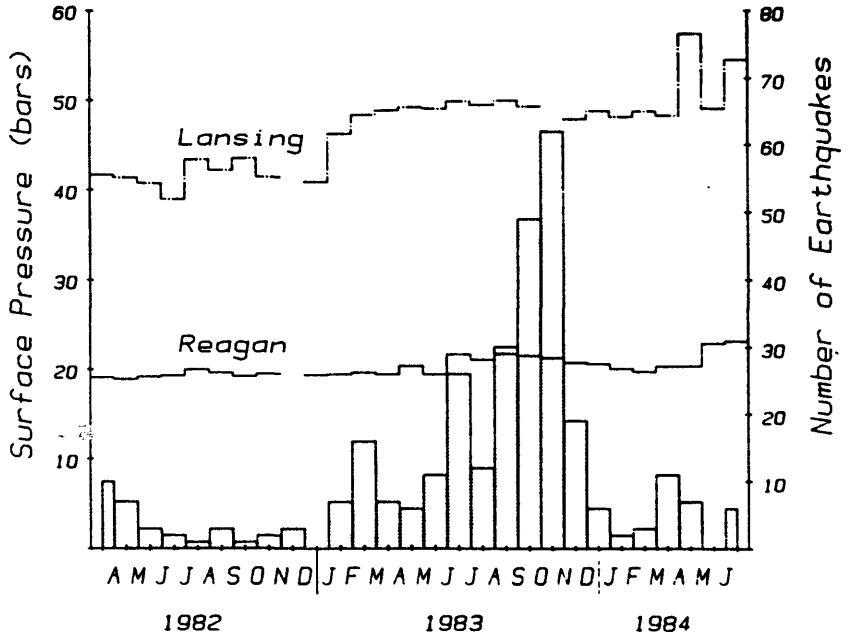
Surface Pressure (bars)
Number of Earthquakes
Lansing
Reagan
60
50
40
30
20
10
80
70
60
50
40
30
20
10
A M J J A S O N D J F M A M J J A S O N D J F M A M J
1982
1983
1984

FIGURE A12

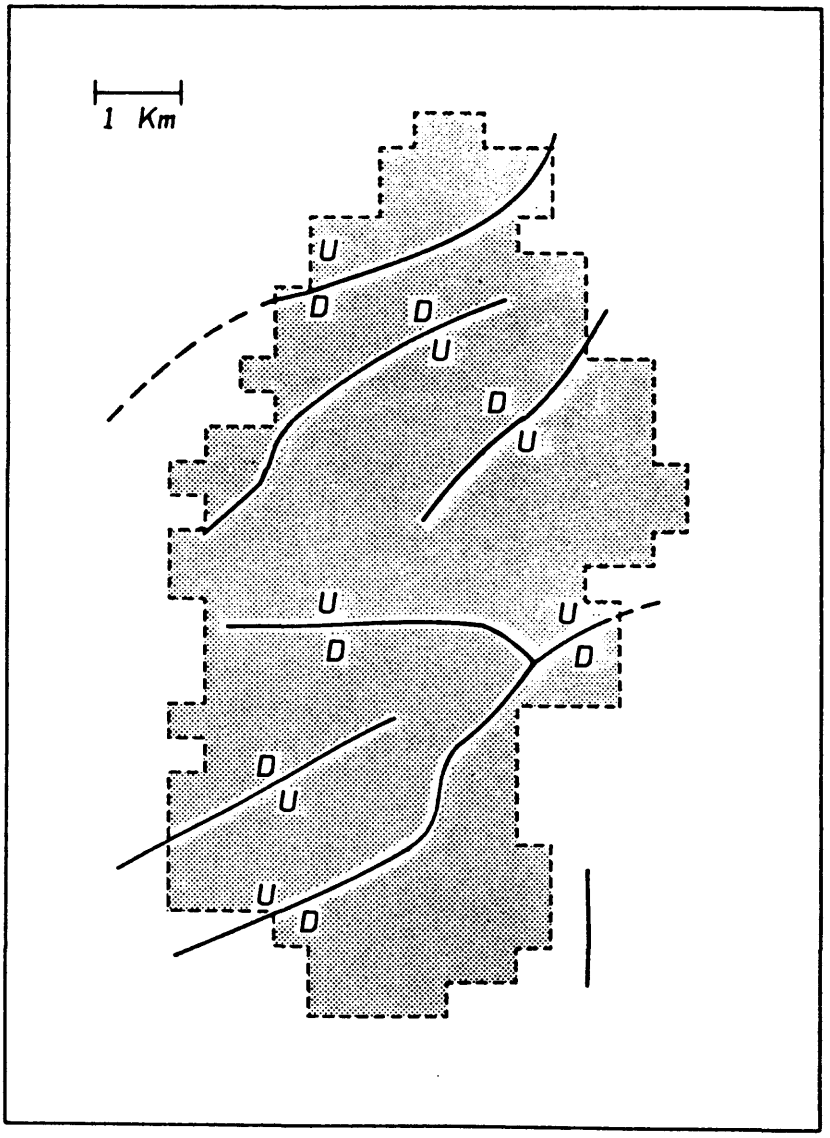
1 Km
U
D
D
U
D
U
U
U
D
D
D
U
U
D

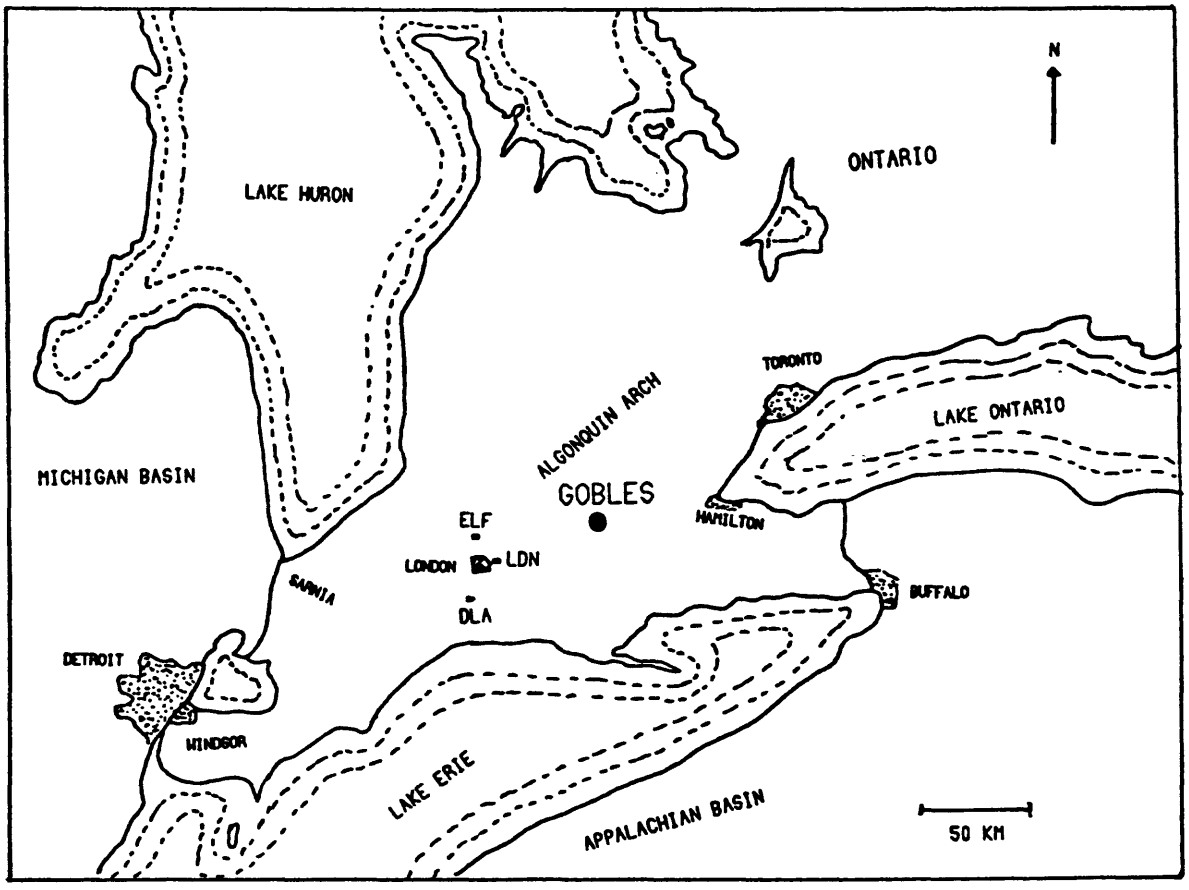

Location map of Gobles oil field in Southwestern Ontario. The oil trap occurs as a pinch-out of an Upper Cambrian Sandstone formation on the Appalachian side of the Algonquin arch. Seismic stations of the University of Western Ontario permanent seismic array are DLA, LDN, and ELF.

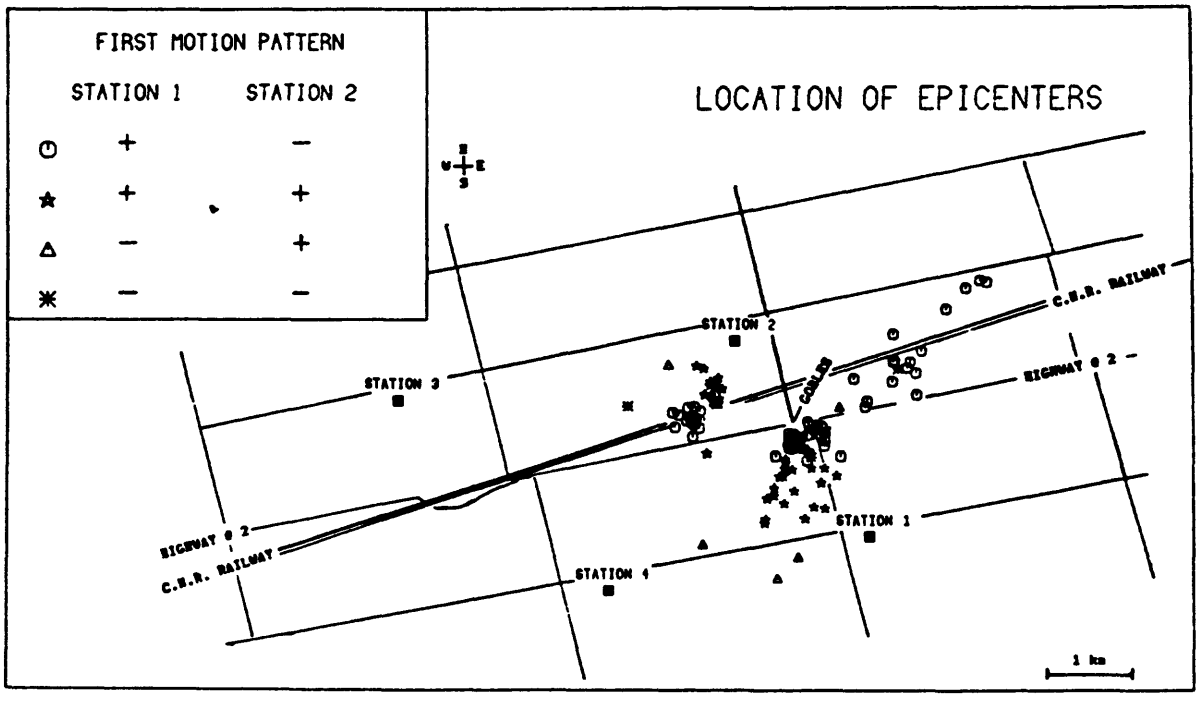

Gobles earthquake epicenter map.

FIGURE A13

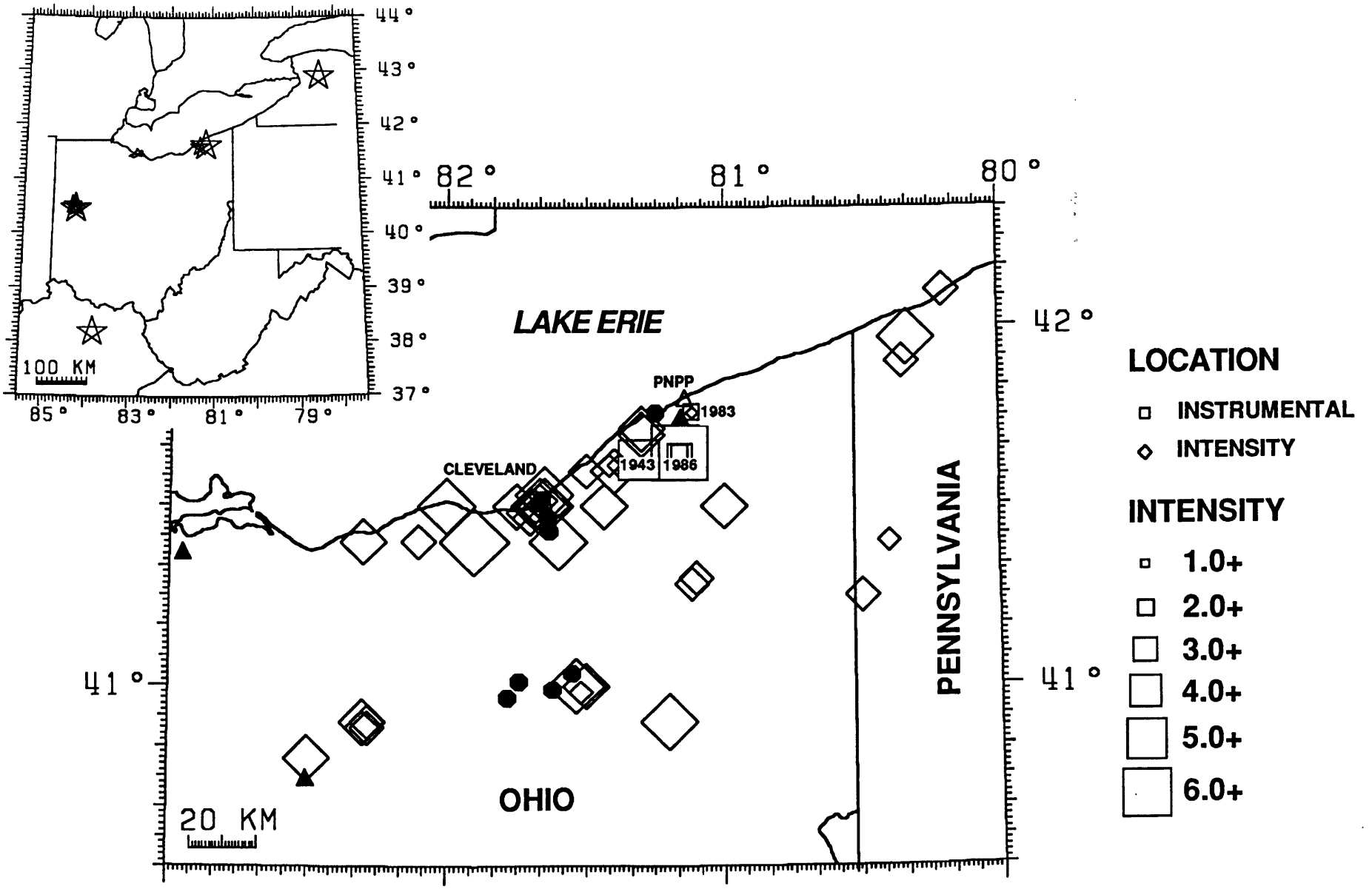
44°
43°
42°
41°
40°
39°
38°
37°
100 KM
85°
83°
81°
79°
82°
81°
80°
LAKE ERIE
42°
PNPP
1983
1943
1986
CLEVELAND
PENNSYLVANIA
41°
41°
OHIO
20 KM
LOCATION
INSTRUMENTAL
INTENSITY
INTENSITY
1.0+
2.0+
3.0+
4.0+
5.0+
6.0+

FIGURE A14

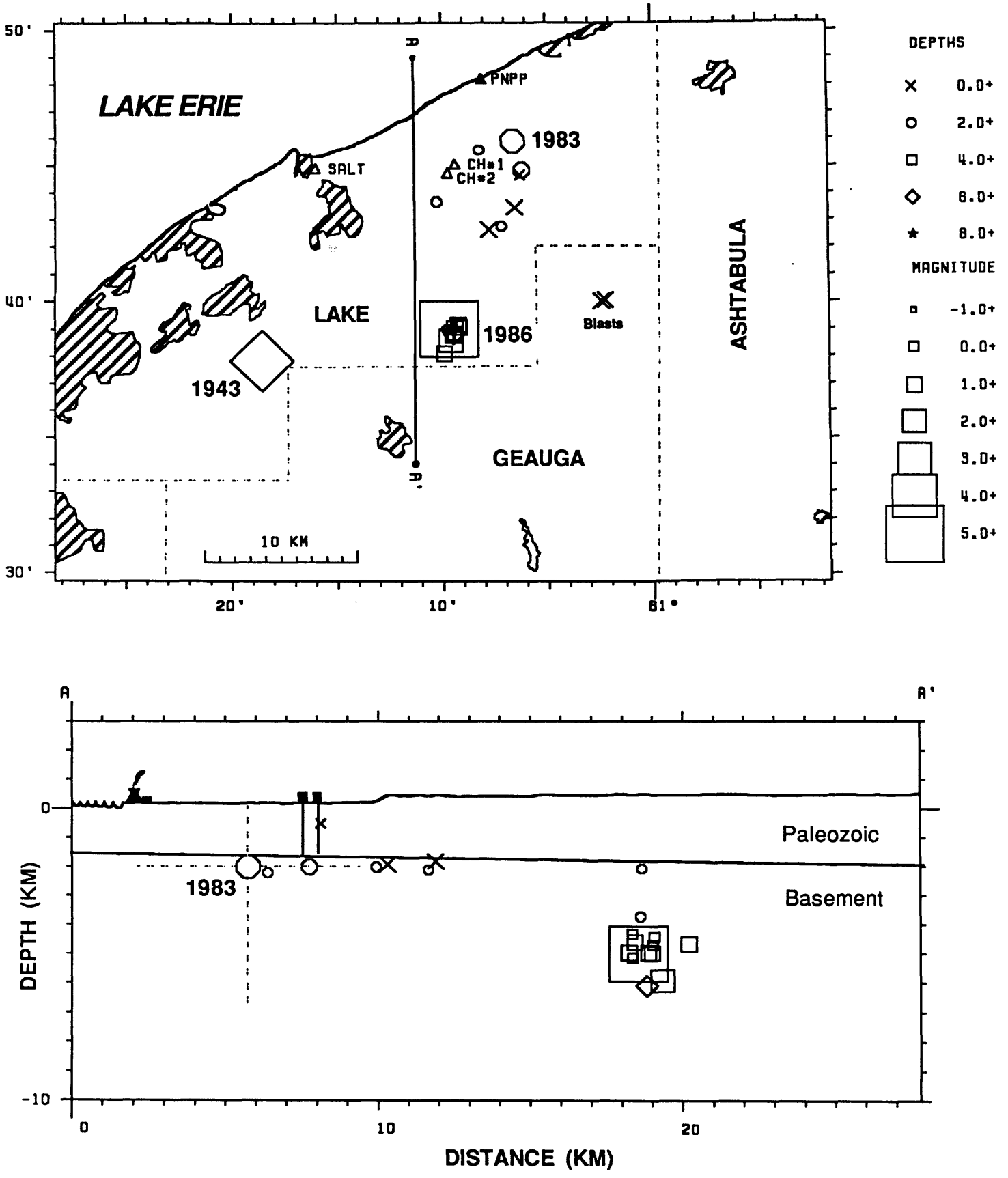
LAKE ERIE
PNPP
1983
SALT
CH#1
CH#2
LAKE
1986
Blasts
ASHTABULA
1943
GEAUGA
10 KM
50'
40'
30'
20'
10'
81°
A
A'
DEPTHS
0.0+
2.0+
4.0+
6.0+
8.0+
MAGNITUDE
-1.0+
0.0+
1.0+
2.0+
3.0+
4.0+
5.0+
Paleozoic
Basement
1983
DEPTH (KM)
DISTANCE (KM)
0
-10
10
20

FIGURE A15

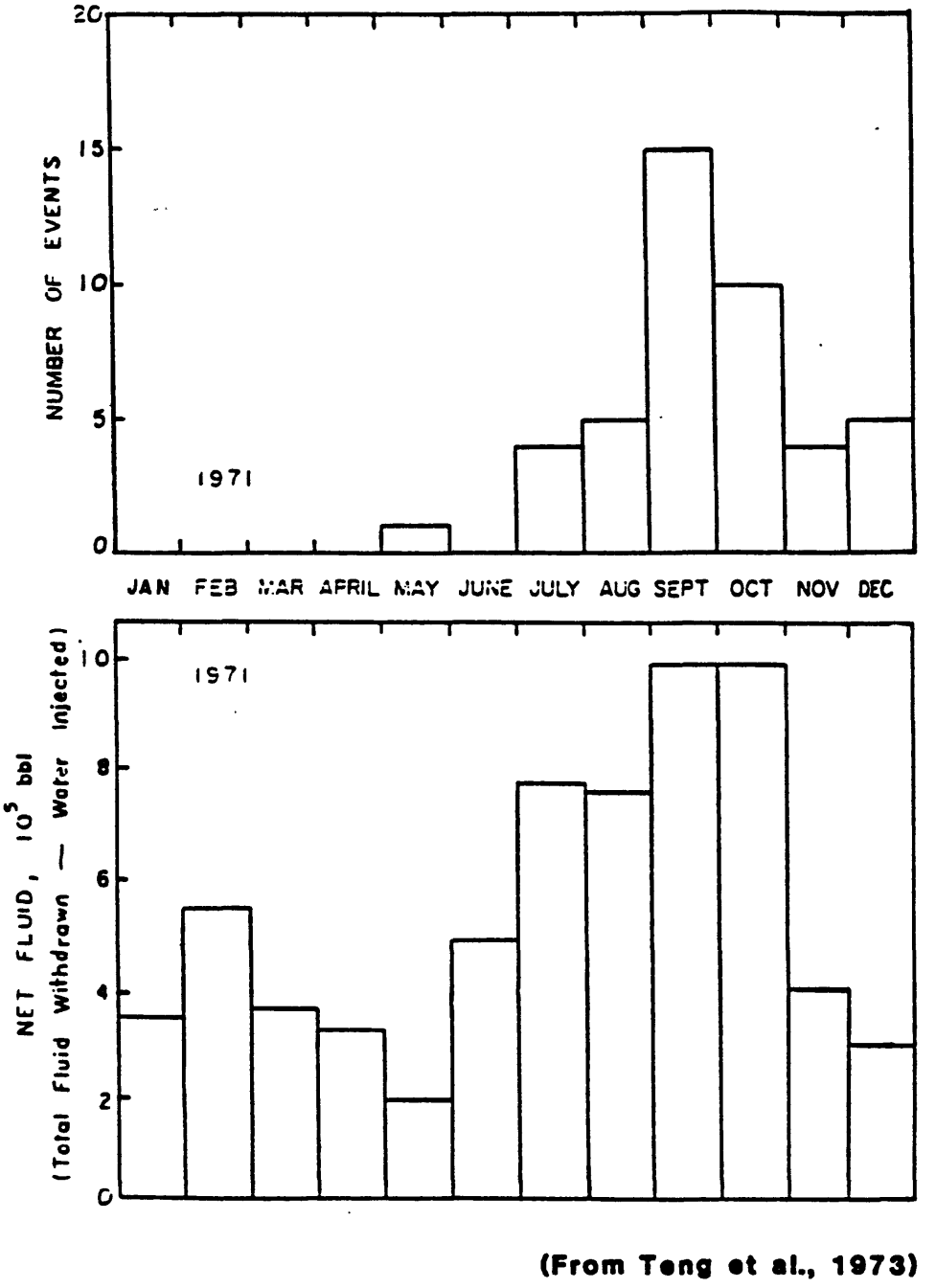

FIGURE A16 Correlation of seismic activity with net fluid injection at the Inglewood Oil Field, CA.

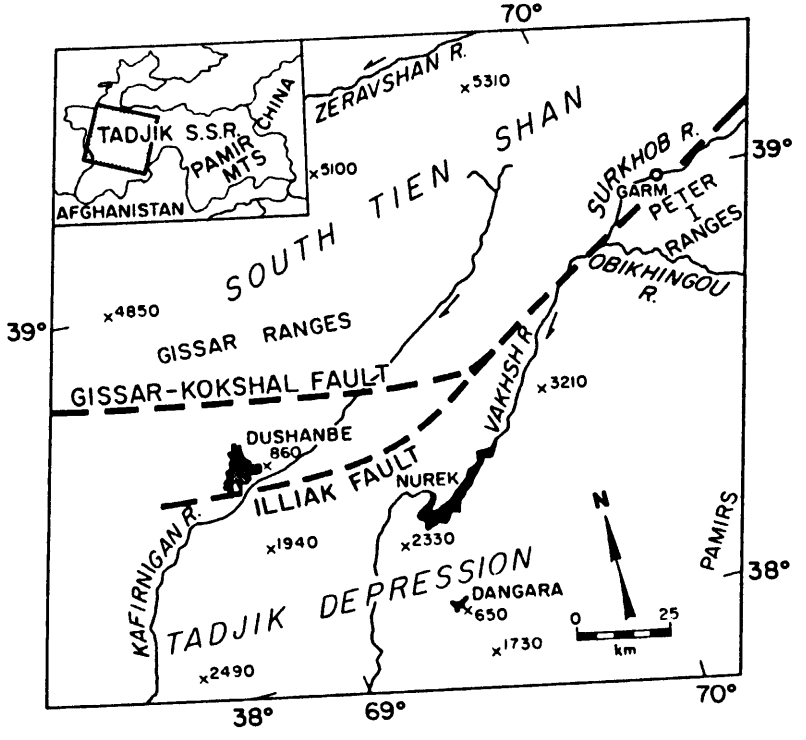
70°
TADJIK S.S.R.
PAMIR MTS
CHINA
AFGHANISTAN
ZERAVSHAN R.
×5310
×5100
SOUTH TIEN SHAN
SURKHOB R.
GARM
PETER I RANGES
39°
×4850
GISSAR RANGES
OBIKHINGOU R.
GISSAR-KOKSHAL FAULT
VAKHSH R.
×3210
DUSHANBE
860
ILLIAK FAULT
NUREK
KAFIRNIGAN R.
×1940
×2330
TADJIK DEPRESSION
DANGARA
×650
×1730
×2490
PAMIRS
N
0 25
km
38°
69°
70°

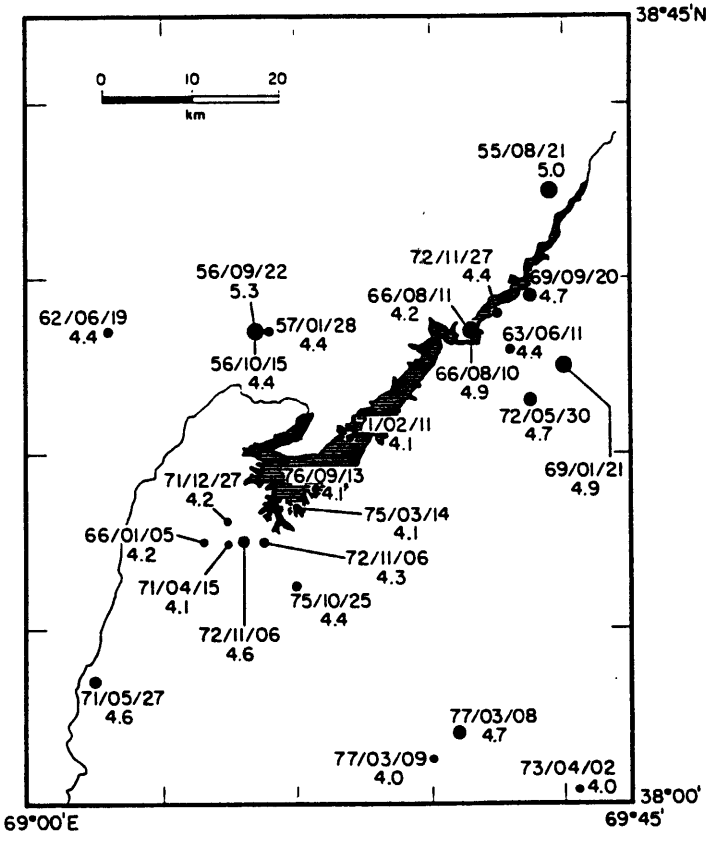
38°45'N
0 10 20
km
55/08/21
5.0
72/11/27
4.4
69/09/20
4.7
56/09/22
5.3
66/08/11
4.2
62/06/19
4.4
57/01/28
4.4
63/06/11
4.4
56/10/15
4.4
66/08/10
4.9
72/05/30
4.7
71/02/11
4.1
69/01/21
4.9
71/12/27
4.2
76/09/13
4.1
75/03/14
4.1
66/01/05
4.2
72/11/06
4.3
71/04/15
4.1
75/10/25
4.4
72/11/06
4.6
71/05/27
4.6
77/03/08
4.7
77/03/09
4.0
73/04/02
4.0
38°00'
69°00'E
69°45'

FIGURE B1

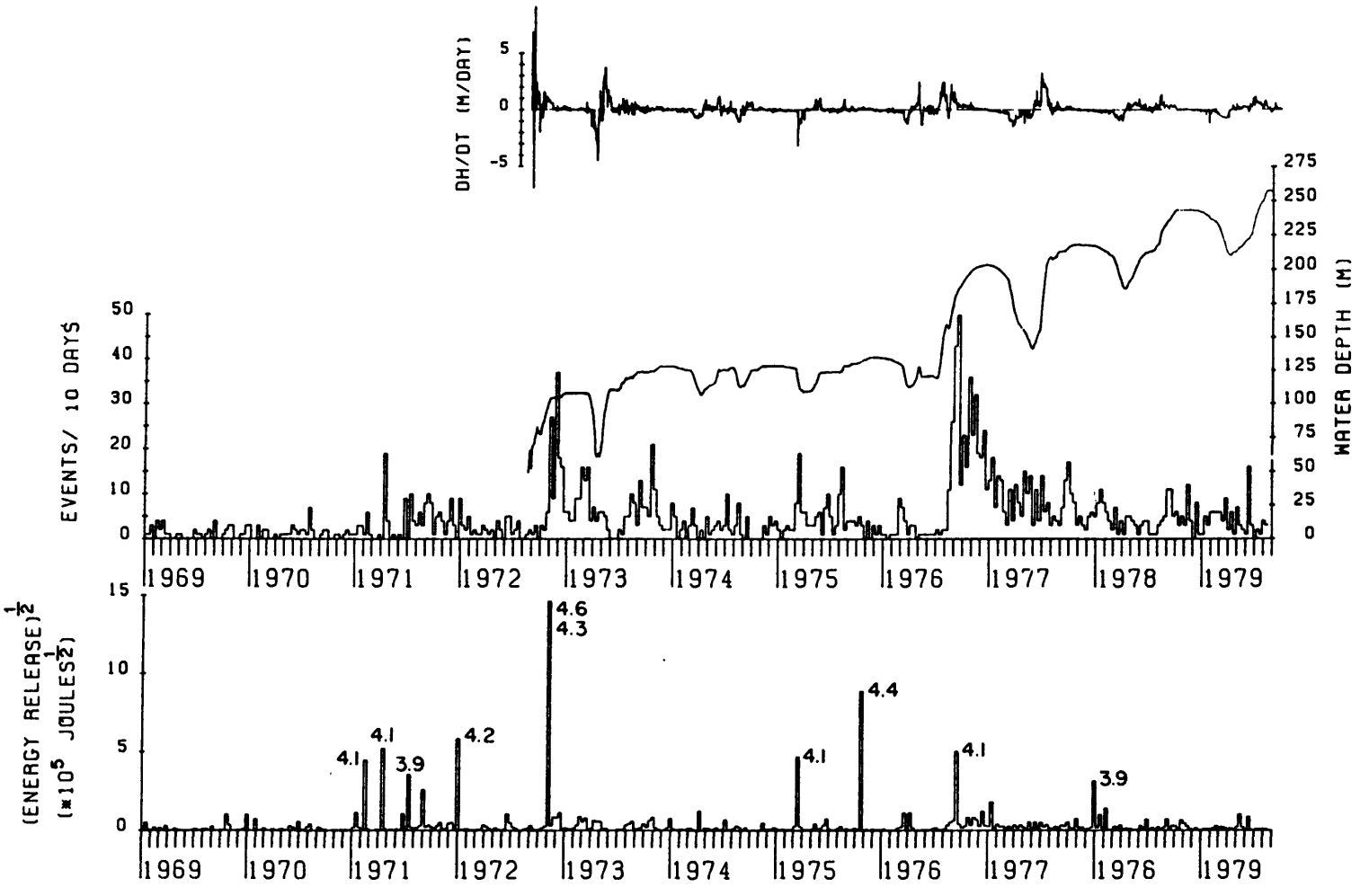

Temporal variations in seismicity within the reservoir area and daily water level at Nurek. The number of earthquakes and square root of energy release/10 days are given in the same manner as in Figure 5. Numbers in the *lower section* are the magnitudes of the larger earthquakes. Water level gradient (dH/dt) is the daily change in the water level, calculated from the water level data. Positive gradient represents filling, and negative gradient emptying, of the reservoir.

FIGURE B2